

THESIS  
2  
2008

LIBRARY  
Michigan State  
University

This is to certify that the  
dissertation entitled

Development and validation of novel molecular techniques to  
elucidate mechanisms of endocrine disruption

presented by

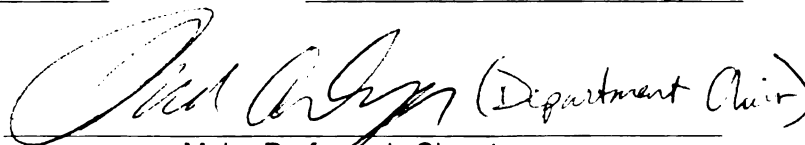
June-Woo Park

has been accepted towards fulfillment  
of the requirements for the

\_\_\_\_\_  
Doctoral

degree in

\_\_\_\_\_  
Department of Zoology-  
Environmental Toxicology

 (Department Chair)

\_\_\_\_\_  
Major Professor's Signature

4 - 2 - 08

Date

*MSU is an affirmative-action, equal-opportunity employer*

**PLACE IN RETURN BOX** to remove this checkout from your record.  
**TO AVOID FINES** return on or before date due.  
**MAY BE RECALLED** with earlier due date if requested.

DATE DUE	DATE DUE	DATE DUE

DEVELOPMENT AND VALIDATION OF NOVEL MOLECULAR TECHNIQUES  
TO ELUCIDATE MECHANISMS OF ENDOCRINE DISRUPTION

By

June-Woo Park

A DISSERTATION

Submitted to  
Michigan State University  
in partial fulfillment of the requirements  
for the degree of

DOCTOR OF PHILOSOPHY

Department of Zoology-Environmental Toxicology

2008



## ABSTRACT

### DEVELOPMENT AND VALIDATION OF NOVEL MOLECULAR TECHNIQUES TO ELUCIDATE MECHANISMS OF ENDOCRINE DISRUPTION

By

June-Woo Park

Understanding the effects of chemicals on the endocrine systems of vertebrates requires development of methods that enable the research of the specific molecular responses to these compounds. The overall objective of my dissertation research was to develop and validate novel sensitive and reliable histological and molecular techniques that can be used to elucidate modes of chemical action on the endocrine systems of vertebrates.

During the first phase of my research, I optimized a SYBR<sup>®</sup> Green I-based quantitative reverse transcription polymerase chain reaction (Q RT PCR) technique to be used as a sensitive means to research the effects of EDCs on aromatase gene expression in testicular tissue of male *Xenopus laevis*. This optimization included a comparison of different PCR quantification methods. The comparison revealed that the comparative C<sub>T</sub> method was optimal for the quantification of gene expression in *X. laevis* testis. The optimized Q RT PCR method was then validated by examining induction of *CYP19a* mRNA gene expression in ovary and testes after exposure to forskolin, a known aromatase inducer. There was little aromatase enzyme activity or *CYP19a* gene expression and the two parameters were not significantly correlated. The optimized Q RT PCR methodology was successfully used to demonstrate that the herbicide atrazine does not up-regulate *CYP19a* gene expression in gonads of male *X. laevis*.

In the second phase of my dissertation research, I optimized an *in situ* hybridization methodology using fluorescent labeling (FISH) for use in whole mounts of a small fish, the Japanese medaka (*Oryzias latipes*). The developed FISH methods allowed for the evaluation of gene expression profiles simultaneously in multiple target tissues in sections of Japanese medaka. The key issue that was addressed during the optimization studies was reduction of auto-fluorescence of tissues and components of the *in situ* hybridization (ISH) procedure, which is one of the major limitations in the application of FISH on tissue sections. This was done using a combination of chemical treatment (sodium borohydride) and an advanced confocal microscopy system. The optimized FISH system was validated in a test exposure with the aromatase inhibitor fadrozole by revealing tissue specific expression of the *CYP19a* gene. Moreover, the combination of FISH with histological analysis provided insights into the molecular changes at the cellular level, indicating that the observed changes were primarily due to a change in cell composition rather than an increase in gene expression per cell. Using the optimized FISH methodology, I further examined short-term effects of 17 $\alpha$ -ethinylestradiol (EE2) and 17 $\beta$ -trenbolone (TB) on changes of three key gene (*Vitellogenin II*, *androgen receptor*, and *CYP19a*) expressions in male and female Japanese medaka. Both chemicals affected fecundity and gonad histology of medaka. Expression of the *Vit II* gene was gender and tissue specific in medaka and was induced after exposure to EE2. The *AR* gene was observed in both ovary and liver, but TB significantly induced *AR* gene expression in ovary only. Expression of the aromatase gene (*CYP19a*) was associated primarily with early stage oocytes and was up-regulated by EE2 at lesser concentrations but down-regulated at greater concentrations.

논문을 마치기 까지 많은 사랑과 격려를 보내주신 어머니와 누나 동생 그리고  
사랑하는 아내 이정은 아들 박지안 그리고 하나님께 영광을 돌립니다.

## ACKNOWLEDGEMENT

First of all, I am deeply grateful to my academic advisor Dr. John P. Giesy for his guidance and encouragement which have allowed me to achieve academic goal, and my committee members, Dr. Patrick Muzzall, Dr. Steven Bursian, Dr. Jack Harkema, and Dr. Markus Hecker for their thoughtful and critical advices throughout my Ph.D. dissertation project. Most of all, I would like to give my special thank to Dr. Markus Hecker for his assistance and guidance for my Ph.D. project.

I would like to thank our Aquatic Toxicology lab colleagues, Hoon, Amber, Eric, and Howard for their fish husbandry and technical help, and Dr. Melinda Frame for her analytical help on fluorescence images.

I would also like to tell my sincere gratitude to my wife, Jung-Eun Lee who has always encouraged me during my time in Michigan, and I would like to share this joy with my mother, my brother and sister and with my lovely son Jonathan Park. Finally, I would like to give my special thank to the grace of God and believers in my church who have prayed for my studies at MSU.

This study was supported by a grant from the US Environmental Protection Agency Strategic to Achieve Results (STAR) to J.P. Giesy, M. Hecker, and P.D. Jones (Project no. R-831846), an Area of Excellence grant from the University Grants Committee of the Hong Kong Special Administrative Region, China (Project no. AoE/P-04/04) and a grant from the Hong Kong University Grants Council (Project no. 7002234) to D. Au and J.P. Giesy.

## TABLE OF CONTENTS

LIST OF TABLES.....	ix
LIST OF FIGURES .....	x
ABBREVIATIONS .....	xiv
INTRODUCTION	
Background .....	1
Approaches to examine EDC modes of action in vertebrate species.....	3
Model species .....	5
Study objectives .....	9
References .....	14
CHAPTER 1	
Abstract .....	19
Introduction .....	20
Materials and Methods .....	22
Animals.....	22
Isolation of total RNA and first-strand cDNA synthesis.....	23
Real-time PCR using SYBR Green I.....	24
Synthesis of plasmid DNA standards .....	25
Quantification of <i>CYP19</i> mRNA expression.....	26
Confirmation of test system using positive controls .....	28
CYP19 aromatase activity .....	29
Statistical analysis .....	30
Results .....	30
RT PCR amplification efficiencies, linearity and reproducibility.....	30
Comparison of different quantification methods for <i>CYP19</i> gene expression .....	34
Comparison of <i>CYP19</i> gene expression and aromatase activity .....	37
Gonadal <i>CYP19</i> gene expression after exposure to forskolin .....	38
Discussions.....	39

Development and optimization of Q-RT PCR system to quantify <i>CYP19</i> gene expression in male <i>X. laevis</i> .....	39
Comparison of different gene quantification methods .....	42
Comparison of <i>CYP19</i> gene expression with aromatase enzyme activity .....	44
Implications for toxicological assessment of environmental pollutants.....	45
Acknowledgement.....	47
References .....	48

## CHAPTER 2

Abstract .....	54
Introduction .....	55
Materials and Methods .....	59
Test chemical.....	59
Culture of Japanese medaka .....	59
Fadrozole exposure.....	59
ISH procedure.....	60
Q RT PCR procedure.....	67
Histology .....	67
Statistics.....	68
Results .....	70
Reduction of autofluorescence .....	70
Tissue and cell specificity of <i>CYP19a</i> gene expression .....	71
Fadrozole exposure.....	74
Discussions.....	78
Optimization of FISH .....	78
Validation of FISH method .....	80
Utilization of FISH .....	81
Comparison of FISH data to morphometric and histological results .....	83
Acknowledgement.....	85
References .....	86

## CHAPTER 3

Abstract .....	92
Introduction .....	93

Materials and Methods .....	97
Test chemicals .....	97
Culture of Japanese medaka ( <i>O. latipes</i> ) .....	97
Chemical exposures .....	97
ISH procedure .....	98
Histology .....	104
Statistics .....	105
Results .....	105
Weight, length, biological indices and fecundity .....	105
Histology of medaka exposed to EE2 or TB .....	108
Chemical-induced gene expression changes by ISH .....	111
Discussions .....	117
Optimization of <i>in situ</i> hybridization analysis .....	117
Fecundity, histology and gene expression of medaka exposed to EE2 .....	118
Fecundity, histology and gene expression of medaka exposed to TB .....	123
Acknowledgement .....	126
References .....	127
CONCLUSION .....	133

## LIST OF TABLES

Table 1.1 Reproducibility and precision of standard curve method for CYP19 and GAPDH plasmid DNA .....	34
Table 1.2 Diverse gene expression quantification methods and aromatase enzyme activities in individual male <i>X. laevis</i> .....	36
Table 1.3 Pearson correlation coefficient ( $r$ ) and probabilities ( $p$ ) between the different parameters measured.....	38
Table 2.1 Probes with primers, GenBank accession number, amplicon size, and cycling condition for conventional PCR.....	69
Table 2.2 Targeted genes with primers, GenBank accession number, amplicon size, and cycling conditions for Q RT PCR analysis .....	69
Table 3.1 Probes with primers, GenBank accession number, amplicon size, and cycling condition for conventional PCR.....	100
Table 3.2 Body weight (g) and length (mm) of Japanese medaka used in this study.....	106



## LIST OF FIGURES

Figure 1.1 *GAPDH* plasmid DNA standard curve. (A) Amplification curves of six dilutions of *GAPDH* plasmid DNA standard from  $1 \times 10^1$  to  $1 \times 10^6$  copies/ $\mu$ L. (B) *GAPDH* plasmid DNA standard curve plotting the log copies/ $\mu$ L (x) of *GAPDH* plasmid DNA against  $C_T$  (y), the equation was calculated by linear regression analysis ( $r^2=0.998$  and 105.7% of PCR efficiency). (C) Melting curve of PCR products, showing specificity of the reaction. (D) 1.5% agarose gel electrophoresis of the PCR products in the serially diluted samples.....32

Figure 1.2 *CYP19* plasmid DNA standard curve. (A) Amplification curves of six dilutions of *CYP19* plasmid DNA standard from  $1 \times 10^1$  to  $1 \times 10^6$  copies/ $\mu$ L. (B) *CYP19* plasmid DNA standard curve plotting the log copies/ $\mu$ L (x) of *CYP19* plasmid DNA against  $C_T$  (y), the equation was calculated by linear regression analysis ( $r^2=0.994$  and 96.7% of PCR efficiency). (C) Melting curve of PCR products, showing specificity of the reaction. (D) 1.5% agarose gel electrophoresis of the PCR products in the serially diluted samples .....33

Figure 1.3 Comparisons among quantification methods for measuring *CYP19* mRNA expression used in the Q-RT PCR system. ER and  $2^{\Delta\Delta C_T}$  were calculated from standard curve method and comparative  $C_T$  method, respectively.  $C_T$  ratio represents the ratio of  $C_T$  value of *CYP19* to  $C_T$  value of *GAPDH*. (A) Represents comparison of *CYP19* gene expression from standard curve method to that from comparative  $C_T$  method. (B) Represents comparison of *CYP19* gene expression from standard curve method to that from  $C_T$  ratio of *CYP19/GAPDH*. (C) Represents comparison of *CYP19* gene expression from  $C_T$  ratio of *CYP19/GAPDH* to that from comparative  $C_T$  method.....37

Figure 1.4 Fold-change (x-change, mean  $\pm$  S.D.) of *CYP19* mRNA in testicular (A) and ovarian (B) explants of *Xenopus laevis* after exposure to 100  $\mu$ M forskolin (100  $\mu$ M) for 20h, using the standard curve method for quantification of mRNA. SC = solvent control (0.1% DMSO).....39

Figure 2.1 Brief steps of mRNA in situ hybridization with fluorescence labeled riboprobe .....66

Figure 2.2 Autofluorescence images of juvenile medaka ovary and emission spectra of the sections obtained after excitation with a 488 laser (A, B, and C) of CLSM and

autofluorescence image of section after applying Linear spectral unmixing (D) of CLSM. (A). Section not subjected to ISH procedure; (B). section *in situ* hybridized without probe and without SB treatment; (C). Section *in situ* hybridized without probe and with SB treatment; (D). Section *in situ* hybridized without probe and SB treatment after application of linear unmixing; (E). Autofluorescence intensities of the sections. PO = previtellogenic oocytes. Scale bar = 100  $\mu$ m.....71

Figure 2.3 Expression of *CYP19a* mRNA in the ovary of juvenile Japanese medaka after hybridization of longitudinal whole mount sections with a fluorescence riboprobe. Expression of *CYP19a* mRNA was detected in the ovary hybridized with antisense probe (A); Very weak *CYP19a* detection was observed in the oocytes hybridized with sense probe (B); no signal in the ovary hybridized without probe (C). PO = previtellogenic oocytes. Scale bar = 100  $\mu$ m.....72

Figure 2.4 Fold-changes of *CYP19a* mRNA gene expression by Q RT PCR analysis in gonads of Japanese medaka exposed to fadrozole (1, 10, and 100  $\mu$ g/L), using comparative  $C_T$  method for quantification of mRNA.  *$\beta$  actin* served as the internal control gene. All data are expressed as the median  $\pm$  the interquartile range. One-way ANOVA was used to analyze data by treatment groups for each tissue and sex separately, followed by SNK test for multiple comparisons. Different letters indicate significant difference between treatment ( $p < 0.05$ ). .....73

Figure 2.5 Expression of *CYP19a* mRNA in the ovary of juvenile Japanese medaka using the optimized *in situ* hybridization. Strong signal detection of *CYP19a* mRNA in the early stage of oocytes was observed, while low *CYP19a* gene expression was localized in the outer layer of follicular cell layer of the vitellogenic and matured oocytes. PO = previtellogenic oocytes. Bar = 100  $\mu$ m.....73

Figure 2.6 Expression of *CYP19a* mRNA in the ovary of juvenile Japanese medaka using the optimized FISH technique in the control (A) and 100  $\mu$ g/L of fadrozole treatment group (B) for 7 days. Fluorescence signal intensity of *CYP19a* expression in randomly selected three early stage of oocytes in the ovary of Japanese medaka exposed to fadrozole (C) and each bar represents means  $\pm$  S.D. of 4 female fish. Significantly low signal of negative control (sense probe, right panel) and highly expressed *CYP19a* mRNA in the ovary exposed to 100  $\mu$ g/L of fadrozole was observed. Scale bar = 100  $\mu$ m .....76

Figure 2.7 Expression of *CYP19a* mRNA in the brain tissue of female Japanese medaka in the control (A), and brain tissue (B) and liver tissue (C) of 100  $\mu$ g/L of fadrozole

treatment group by the optimized *in situ* hybridization using fluorescence antisense riboprobe. No fluorescence signal detection was observed in brain and liver tissues. Bar = 100  $\mu$ m .....77

Figure 2.8 Gonadal somatic index (GSI) and liver somatic index (LSI) of male (A) and female (B) Japanese medaka exposed to fadrozole for 7 days. Bars represent mean and error bars are standard deviation.....77

Figure 3.1 Brief steps of mRNA in situ hybridization with fluorescence labeled riboprobe .....102

Figure 3.2 Mean values ( $\pm$  SEM) of liver somatic index (LSI) and gonado-somatic index (GSI) in Japanese medaka exposed to EE2 (A) or TB (B). Significant differences relative to the control are indicated with an asterisk ( $p < 0.05$ ,  $n = 4 \sim 6$ ) .....107

Figure 3.3 Cumulative numbers of viable fertilized eggs spawned by male and female Japanese medaka exposed to EE2 (A) or TB (B). Each treatment consisted of triplicate tanks, and each tank contained 6 pairs of medaka. Significant differences relative to the control are indicated with an asterisk ( $p < 0.05$ ).....107

Figure 3.4 H & E stained cross section of gonads of Japanese medaka. (A) testis of control (100X, bar = 20  $\mu$ m). SZ: spermatozoa, ST: spermatid, SC: spermatocyte, and SG: spermatogonia. (B) control ovary (40X, bar = 50  $\mu$ m). PR: primary oocyte, PO: previtellogenic oocyte, VO: vitellogenic oocyte, and MO: matured oocyte. (C) testis of male exposed to 500 ng/L of EE2 (200X, (40 and 400X in the boxes) bar = 10  $\mu$ m). Testis-ova observed in the form of perinuclear stage, degrading spermatozoa and greater proportion of connective tissue were observed. (D) ovary of female exposed to 500 ng/L of EE2 (40X, bar = 50  $\mu$ m). AO: atretic oocyte, and SST: somatic stromal tissue. There were fewer mature oocytes, more atretic oocytes, and larger volume of somatic stromal tissue. (E) testis of male exposed to 5,000 ng/L of TB (100X, bar = 20  $\mu$ m). Accelerated spermatozoa development and fewer spermatogonia were observed. (F) ovary of female exposed to 5,000 ng/L of TB (40X, bar = 50  $\mu$ m). Predominant matured oocytes and fewer previtellogenic oocytes were observed. ....110

Figure 3.5 H & E stained cross section of liver of Japanese medaka. (A) control male showing eosinophilia, (B) male liver of fish exposed to 500 ng/L of EE2 and (C) female liver of control Japanese medaka showing intense staining with hematoxylin. (D)

number of hematoxylin-stained stains (mean  $\pm$  SEM). Significant differences relative to the control are indicated with an asterisk ( $p < 0.05$ ). Bar = 50  $\mu\text{m}$  .....111

Figure 3.6 Expression of vitellogenin II mRNA in the gonads (A and B) and liver (C and D) of Japanese medaka after hybridization of longitudinal whole mount sections with a fluorescence riboprobes using optimized ISH. Expression of Vit II mRNA was detected in the testes (A, bar = 200  $\mu\text{m}$ ) exposed to EE2 and control ovary (B, bar = 100  $\mu\text{m}$ ) of fish with hybridization of antisense probe, especially strongly in the region of spermatogonia in testes and primary stage of oocytes in ovary, respectively. Very weak detected fluorescence signal in the section hybridized with sense probe. Vit II expression in the male liver (C, bar = 50  $\mu\text{m}$ ) of Japanese medaka exposed to EE2 (500 ng/L) was as high as that in the section of female liver (D, bar = 50  $\mu\text{m}$ ) hybridized with Vit II antisense probe. Display channel was set to green for antisense probe labeled with Alexa Fluor 488 and to red for autofluorescence .....113

Figure 3.7 Expression of CYP19a (A – D) and AR (E and F) in the ovary and liver of female Japanese medaka using the FISH. Expression of CYP19a was very lowly detected in the ovary hybridized with sense probe (A), while it was specifically detected in the cytoplasm of primary oocytes of control ovary (B, bar = 100  $\mu\text{m}$ ), ovary exposed to EE2 (C), and ovary exposed to TB (D, bar = 100  $\mu\text{m}$ ). AR mRNA expression was detected, but lowly, in the ovary (E, bar = 100  $\mu\text{m}$ ) and liver (F, bar = 50  $\mu\text{m}$ ) exposed to TB. Display channel was set to green for antisense probe labeled with Alexa Fluor 488 and to red for autofluorescence .....114

Figure 3.8 Fluorescence intensity of *Vit II* in testes (A), ovary (B), and liver (C) of Japanese medaka exposed to EE2. Each bar represents mean  $\pm$  SEM. Significant differences relative to the control are indicated with an asterisk ( $p < 0.05$ ) .....116

Figure 3.9 Fluorescence intensity of *AR* in ovary (A) and liver (B) of Japanese medaka exposed to TB. Each bar represents mean  $\pm$  SEM. Significant differences relative to the control are indicated with an asterisk ( $p < 0.05$ ) .....116

Figure 3.10 Fluorescence intensity of *CYP19a* in randomly selected three primary stage of oocytes in the ovary of Japanese medaka exposed to EE2 (A) and TB (B), and each bar represents mean  $\pm$  SEM. *CYP19a* mRNA expression was not significantly different among treatment in both EE2 and TB exposure ( $p > 0.05$ ) .....117

## ABBREVIATIONS

<b>AR <math>\alpha</math></b>	Androgen Receptor $\alpha$
<b>AR <math>\beta</math></b>	Androgen Receptor $\beta$
<b>CLSM</b>	Confocal Laser Scanning Microscopy
<b>C<sub>T</sub></b>	Threshold Cycle
<b>CV</b>	Coefficient of Variation
<b>CYP19</b>	Cytochrome P450 aromatase
<b>DEPC</b>	Diethyl Pyrocarbonate
<b>DIG</b>	Digoxigenin
<b>DMSO</b>	Dimethylsulfoxide
<b>DNA</b>	Deoxyribonucleic Acid
<b>DNAse</b>	Deoxyribonuclease
<b>dNTP</b>	Deoxyribonucleotide Triphosphate
<b>E2</b>	17- $\beta$ Estradiol
<b>EDC</b>	Endocrine Disrupting Compounds
<b>EE2</b>	17 $\alpha$ -Ethinyl Estradiol
<b>ER</b>	Estrogen Receptor
<b>ER</b>	Expression Ratio
<b>ERE</b>	Estrogen Responsive Element
<b>FISH</b>	Fluorescent In Situ Hybridization
<b>GAPDH</b>	Glyceraldehyde-3-phosphate Dehydrogenase
<b>GSI</b>	Gonadal Somatic Index
<b>GtH</b>	Gonadotropin Hormone

<b>H &amp; E</b>	Hematoxylin and Eosin
<b>HPG axis</b>	Hypothalamus Pituitary Gonadal Axis
<b>IACUC</b>	Instituted Animal Care and Use Committee
<b>IHC</b>	Immuno-Histochemistry
<b>ISH</b>	In Situ Hybridization
<b>LSI</b>	Liver Somatic Index
<b>MO</b>	Matured Oocytes
<b>mRNA</b>	messenger RNA
<b>PCR</b>	Polymerase Chain Reaction
<b>PO</b>	Previtellogenic Oocytes
<b>PR</b>	Primary Oocytes
<b>Q RT PCR</b>	Quantitative Reverse Transcription Polymerase Chain Reaction
<b>RNA</b>	Ribonucleic Acid
<b>RNAse</b>	Ribonuclease
<b>rRNA</b>	Ribosomal Ribonucleic Acid
<b>SB</b>	Sodium Borohydride
<b>SC</b>	Spermatocytes
<b>SD</b>	Standard Deviation
<b>SEM</b>	Standard Error of the Mean
<b>SG</b>	Spermatogonia
<b>ST</b>	Spermatids
<b>SZ</b>	Spermatozoa
<b>TB</b>	17 $\beta$ -Trenbolone

<b>US EPA</b>	United States of Environmental Protection Agency
<b>Vit II</b>	Vitellogenin II
<b>VO</b>	Vitellogenic Oocytes

## INTRODUCTION

### *1. Background*

During the past 20 years a significant amount of research has been conducted to characterize the potential of chemicals to interact with the endocrine system of vertebrate species, so called endocrine disruptors (EDCs). While some of these chemicals occur naturally in plants or fungi such as phytoestrogens, others are of anthropogenic origin and are represented by a wide variety of chemicals including fungicides, certain polychlorinated dibenzo-*p*-dioxins and polychlorinated biphenyls, organotins, and polycyclic aromatic hydrocarbons, plasticizers, and synthetic hormones (Norris, 2007). EDCs are of increasing concern in context with both human and environmental risk assessments due to their potential to adversely impact key functions of organisms such as reproduction, energetics, growth, and development. The US EPA has officially defined an EDC as an exogenous agent that interferes with the production, release, transport, metabolism, binding, action, or elimination of natural hormones in the body responsible for the maintenance of homeostasis, reproduction, development, and/or behavior (Kavlock et al., 1996). In Europe, an EDC is defined as an exogenous substance that causes adverse health effects in an intact organism, or its progeny, consequent to changes in endocrine function, while a potential endocrine disruptor is a substance that possesses properties that might be expected to lead to endocrine disruption in an intact organism (European Commission 1996). Of importance here is the concept that endocrine disruptors encompass more than just environmental hormones, such as xenoestrogens and -androgens, and include any agent that can adversely affect any aspect of the endocrine



system. Advances in biomarkers have allowed progress in assessing the association between chemical exposures and potential adverse effects in wildlife. Generally, a biomarker can be defined as a cellular, histological, biochemical, or molecular change that can be measured in the product of an interaction between chemical and target molecule, resulting in the prediction of a relationship between chemical exposure and its effect in an organism. Molecular biomarkers using genomics and proteomics can be useful tools for measurement of exposure to very small concentrations of chemicals in an organism.

To date, most studies employing biomarkers have involved the expression of one to a few gene products that are known to be related to exposure to specific chemical classes. While the expression of specific genes has proven useful in assessing exposure to specific chemicals, the limited number of gene products assessed does not make it possible to distinguish patterns of gene expression that may be used to differentiate exposure and effects of different chemicals or chemical classes. New techniques in molecular biology make it possible to detect alterations in the expression of many or all genes in an organism as a result of exposure to chemicals or other environmental stressors. Historically, studies have primarily focused on one tissue at one specific time in the development of an organism. Chemicals, to which humans and wildlife might be exposed, can result in a disruption of the endocrine system by direct and indirect mechanisms. For instance, some chemicals are direct acting agonists or antagonists while others act indirectly by modulating signal transduction or cybernetic systems. For example, the triazine herbicide atrazine does not bind to the estrogen receptor (ER), but *in vitro* in a mammalian cell system, atrazine has been found to up-regulate the

expression of aromatase (*CYP19*), the enzyme that transforms testosterone to estradiol. Although atrazine does not act like a typical estrogen via binding the ER, in mammalian cell systems it is likely to result in an estrogenic effect by increasing endogenous estradiol production (Sanderson et al., 2000). Thus, simple, targeted screening methods such as receptor binding assays or even receptor mediated functional assays may not identify these other types of effects. Also, expression of different neuro-endocrine systems and their specific components can vary greatly during development (Sanderson et al., 2001). Some genes are only expressed in certain tissues, while others are expressed in specific tissues at only certain times of development. Also, when using laboratory small animal model species, the small amounts of individual tissues available for study and the difficulty in excising them from small organisms has limited the efficacy of these techniques to determine effects during critical windows of time during ontogenesis.

Therefore, sensitive and flexible monitoring tools are needed that allow for the screening of multiple genes in multiple tissues simultaneously at any stage of development, without the need to dissect out the small critical tissues.

## ***2. Approaches to examine EDC modes of action in vertebrate species***

The recent advent of genomic sciences opened new perspectives to scientists researching modes of chemical action. There are four commonly used methods for detection and quantification of transcription, which are northern blotting, RNase protection assays, quantitative reverse transcription polymerase chain reaction (Q RT PCR) and *in situ* hybridization (ISH) (Bustin, 2000). Briefly, northern blotting can

provide information about mRNA size, alternative splicing, and the integrity of mRNA samples. The RNase protection assay is useful for mapping transcript initiation and termination sites and for discriminating between related mRNAs of similar size (Bustin, 2000). While these methods have proven useful in developing gene expression profiles that can be related to potential modes of action of EDCs, I focused on two methods, Q RT PCR and ISH because they are the most sensitive and allow for the detection of spatial changes of gene expression, respectively. Also, northern blotting and RNase protection assays require relatively large amounts of mRNA, and thus, do not provide the necessary sensitivity to detect low expression of genes such as *CYP19a* in gonads of male frogs which was the aim of Chapter 1.

Quantitative (real-time) reverse transcriptase polymerase chain reaction (Q RT PCR) is a sensitive and flexible technique that can detect small quantities of mRNA in small amounts of tissue (Bustin, 2000 and 2002) and has been applied successfully as a tool for the investigation of multiple functionally related genes in endocrine disrupter research (Rotchell and Ostrander, 2003). This technique, which amplifies the number of copies of mRNA many times, can theoretically measure as little as a single molecule of the target mRNA (Bej et al., 1991). However, there are some disadvantages of using RT PCR such as non-specific DNA amplification due to high sensitivity of *Taq* polymerase, mis-incorporation of nucleotides by lack of 3'-5' exonuclease capacity in *Taq* polymerase, and difficulty in PCR amplification of long transcripts (> 5k bp) (Bej et al., 1991). Most of all, based on empirical observation, it was difficult to extract large amount of RNA from individual small tissue such as brain and testis of fish without pooling them, and, in some cases extracted RNA was not purified and/or degraded. Enough input of non-

degraded RNA as template is critical for reverse transcription efficiency to synthesize cDNA and in turn will affect on the efficiency of target gene quantification. Therefore, additional methods such as *in situ* hybridization that allow for detection and quantification of intact mRNA directly in the tissue of interest without extraction or further treatments such as reverse transcription and amplification are needed.

*In situ* hybridization (ISH) involves the specific annealing of labeled probes to complementary sequences of interest in fixed tissues, followed by visualization of the labeled probes. The major advantage of this method is that it provides a sensitive means to localize and quantify the mRNA for specific genes in organs and tissues of interest in a manner that is consistent with other methods that are used to detect lesions including histopathology and immuno-histochemistry. ISH also provides a direct visualization of the spatial location of specific sequences, which is crucial for elucidation of the organization and function of genes. As a result, ISH has become an important tool in a number of fields, such as the research of chromosomal arrangement, viral infection, and analysis of gene function (Wilkinson, 1992; Jin and Lloyd, 1997).

### **3. *Model species***

There is increasing concern regarding the effects of EDCs on aquatic vertebrates such as amphibians and fish because they are continuously exposed and in direct contact with these compounds. Especially amphibians have been regarded as good indicator species for the exposure to environmental contaminants because they are subject to both aqueous and terrestrial exposure routes. Recently, there was an increasing concern about the potential of triazine herbicides to interact with the endocrine system of male frogs by

inducing aromatase which catalyzes the conversion of androgens to estrogens, resulting in an increase of endogenous estrogen production and subsequently causing feminization or demasculinization of males (Hayes et al., 2002). However, the investigation of this proposed mode of action failed to date due to limitations in the sensitivity of the applied tests systems, especially in males where the endpoints of interest (gonadal aromatase) were naturally very low, and typically below the method detection limits of the utilized assays (Hecker et al., 2004). Therefore, to increase our ability to determine possible changes in aromatase activity in the testis, a more sensitive test system such as an optimized Q RT PCR method was needed by examining subtle effects on the aromatase gene (*CYP19a*) expression.

In the first phase of my dissertation research, I developed a Q RT PCR method for detection and quantification of *CYP19a* gene expression in the testes of male African clawed frog (*Xenopus laevis*). This species has been used as one of the key models to assess the effects of atrazine on the endocrine system of frogs (Hayes et al., 2002; Carr et al., 2003; Coady et al., 2004; Hecker et al., 2004 and 2005a). The African clawed frog is a carnivorous frog native in Africa, and inhabits warm and stagnant grassland ponds. Tadpoles metamorphose within 2 or 3 mo of egg laying, and frogs reach sexual maturity within one or two years, depending on breeding conditions such as temperature and frequency of feeding. *X. laevis* is easily maintained in the laboratory, and has been commonly used as model species for developmental studies (Wu and Gerhart, 1991).

In general, four principal actions for how EDCs can affect reproduction include estrogenic, antiestrogenic, androgenic, and antiandrogenic effects that can lead to feminization, neutralization of sexual differentiation, masculinization, and feminizing

effects, respectively (Kloas, 2002). Generally sexual differentiation is primarily determined by on a sex-specific basis that leads to functional gonadal sex development and that in turn is responsible for secondary sexual differentiation. Sexual differentiation of frogs is regulated by the ratio of sex steroids, estrogens and androgens, in developing eggs and embryos and can be shifted by supplements of estrogens or androgens by changing the ratio. At the time of hatching, expression of estrogen and androgen receptor mRNAs are increased, indicating that early stage after hatching is sensitive for sexual differentiation. For example, *Xenopus* frog larvae develop into 50% males (ZZ) and 50% females (ZW) under normal physiological conditions, however, exposure to estrogen shift sex ratio to feminization, while treatments of methyltestosterone and dihydrotestosterone induced significant masculinization. Sexual differentiation also can be shifted by regulation of ER and AR mediated cellular responses. Antiandrogens, such as vinclozolin, caused feminization by suppressing the androgen receptor-mediated cellular processes, leading indirectly to alter the ratio resulting in feminization. Antiestrogens, such as tamoxifen, led to neutralization by blocking estrogen-induced developmental processes in genetic females and males, resulting in a general depression of gonadal development (Kloas, 2002). However there are still debates whether such general characterization of modes of action is applicable to all amphibians. Only estrogen always caused a clear feminization, while the effects of masculinization by testosterone are dependent on the species. Also antiestrogenic and antiandrogenic chemicals resulted in contradictory data (Rastogi and Chieffi, 1975).

In the second phase of my dissertation research, I developed and validated techniques for the research of spatial changes in gene expression using a whole animal

approach, the Japanese medaka (*Oryzias latipes*). The test system applied in these studies utilized whole mount sections, an approach requiring a small model fish. The medaka is a small oviparous (egg-laying) freshwater fish native to Asia. Its physiology, embryology, and genetics have been extensively studied for more than 100 years (Wittbrodt et al., 2002). The medaka represents an important test system for environmental research and is widely used for testing endocrine disruptors in ecotoxicology. Another advantage of the medaka is its rapid development and ease of breeding, producing eggs on a regular schedule under the appropriate conditions of lighting and temperature. Currently, several medaka genome projects are underway, and over 90% of the medaka genome has already been sequenced so that DNA sequences are already available for most of the genes of interest for this study. This strain exhibits sexual dimorphism with males being orange-red, while females are white, and based on their coloring the genetic sex can be determined. This was a great advantage for this study because the genetic sex of each individual could be determined prior to the initiation of the studies and at time of sampling. Furthermore, our research team had already developed some of the basic techniques required for my studies, including the sectioning and tissue fixing and preparation of ISH (Kong, et al., 2008; Tompsett et al., 2008).

Many environmental chemicals exhibit estrogenic or androgenic activity. Inappropriate induction of vitellogenin in juvenile or male fish has become one of the most notable biological responses of fish involved in EDC exposure, especially in estrogenic compounds. The most dramatic increase of vitellogenin levels appear to be in fish exposed to sewage discharges which contain sufficiently high concentration of

estrogenic compounds (Purdom et al., 1994). Vitellogenin induction was also exhibited in fish exposed to municipal sewage discharges which might have natural and/or synthetic estrogen (Folmar et al., 1996). Phytoestrogens in pulp and paper mill effluents, such as  $\beta$ -sitosterol also induced vitellogenin levels in male and juvenile female fish (Tremblay and Vad Der Kraak, 1999). Vitellogenin induction in male can cause reduced calcium concentration in scales and skeleton, enlarged livers, kidney damage and reduced testicular growth (Herman and Kincaid, 1988; Harries et al., 1997). Further male genotypes become apparently normal female phenotypes as a result of feminization effect during the sensitive part of gonadal development, such as development of testis-ova, and oviduct (Wester and Canton, 1986; Gimeno et al., 1996). Thus, these estrogenic effects will reduce male's reproductive fitness, such as reduced fertilization success by impairment in the sperm quality and abnormal reproductive behavior. Androgenic and antiandrogenic effects on fish have not been well documented as the estrogenic and antiestrogenic effects. Several studies have reported the masculinization of female exposed to kraft mill effluents containing stigmasterol degradation product which have androgenic properties. These masculinization features include development of gonopodium in female and hermaphroditic conditions in male (Howell and Denton, 1989; Bortone et al., 1989; Bortone and Cody, 1999).

#### ***4. Study Objectives***

The overall objective of my dissertation research was to develop and validate novel sensitive and reliable molecular techniques that can be used to elucidate the endocrine modes of chemical action in vertebrates. The techniques developed allow for



the determination of mechanisms of toxic action of single chemicals or complex mixtures. Specifically, using the developed and validated methods I examined potential effects of chemicals at the level of gene expression by measuring the amount of mRNA and evaluated how changes in gene expression relate to reproductive functioned in the test organism. The specific objectives of my research were:

- To develop and optimize Q RT PCR analysis to measure lowly expressed genes such as *CYP19* in testicular tissue of male *X. laevis*
- To develop and optimize an ISH protocol using fluorophore-labeled probes to detect specific mRNA sequences in whole animal sections of Japanese medaka (*O. latipes*).
- To validate the FISH methods developed in this study by examining *CYP19a* mRNA in medaka after exposure to the specific aromatase inhibitor fadrozole, and by comparing the gene expression data with that obtained during parallel Q RT PCR analysis using the techniques developed during the above studies with *X. laevis*
- To characterize the effects of 17 $\alpha$ -ethinylestradiol (EE2) and 17 $\beta$ -trenbolone (TB) on the tissue specific expression of *CYP19a*, *vitellogenin II* (Vit II), and *androgen receptor  $\alpha$*  (AR) in whole sections of medaka using the optimized FISH protocol.
- Compare the changes in gene expression with histological, physiological, and/or organismal responses to further our understanding of the molecular mechanisms of the tested EDCs.

Once the methods had been developed and validated, they could be adapted for use with other genes and/or species of interest and used to efficiently and completely screen for endocrine disruptor effects. Moreover, these methods have the potential to significantly improve molecular profiling approaches to better understand mechanisms of action of individual compounds or complex mixtures, improving risk assessment of the chemicals in general to both humans and wildlife. The testable hypotheses of my research were:

- Developed Q RT PCR analysis is sensitive to detect and quantify weakly expressed gene such as *CYP19a* in testicular tissues of male *X.laevis*.
- Developed Q RT PCR analysis can be applied as a tool for studying enzymes with low activity.
- ISH method is a proper tool to detect changes in target gene expression profiles along the HPG-axis.
- Gene expression profiles of key genes by means of ISH show sex-and tissue-specific patterns.
- There are specific effects on changes of target gene expression profiles in an organism after exposing to “model” compounds.
- Specific changes in gene expression profiles by means of ISH are related with histological relevant endpoints.

In Chapter 1, I optimized a Q RT PCR technique to be used as a sensitive mean to research the effects of EDCs on aromatase gene expression in amphibians (Park et al., 2006). Specifically, I developed an assay to measure mRNA for *CYP19a* (aromatase). I

then applied the technique to test the hypothesis that the common pesticide, atrazine, could up-regulate expression of gonadal aromatase in the African clawed frog (*Xenopus laevis*). Due to low detection limit in enzymatic assays to measure aromatase enzyme activity in testicular tissues, it had been difficult to test this hypothesis previously. Thus, I optimized a SYBR<sup>®</sup> Green I-based quantitative reverse transcription polymerase chain reaction (Q RT PCR) method to quantify *CYP19a* mRNA in testicular tissue of male *X. laevis*. This optimization included a comparison of different PCR quantification methods, which revealed that of the methods tested, the absolute standard curve and the comparative C<sub>T</sub> method were optimal for the quantification of gene expression in *X. laevis* testis. Due to the labor intensity of the standard curve method, however, it was decided to use the comparative C<sub>T</sub> method for future studies. The optimized Q RT PCR method was then validated by examining induction of *CYP19a* mRNA gene expression in ovary and testes after exposure to forskolin, a known aromatase inducer. Although both aromatase activity, determined by the tritium release assay, and *CYP19a* mRNA were detectable in testes of *X. laevis*, there was little aromatase enzyme activity, or *CYP19a* gene expression and the two parameters were not significantly correlated. The Q RT PCR methodology optimized in this phase was used to measure *CYP19a* gene expression changes in gonads of male *X. laevis* exposed to the herbicide atrazine and it was successfully used to demonstrate that the atrazine does not up-regulate *CYP19a* gene expression in the tissues (Hecker et al., 2005a, and b).

In Chapters 2 and 3, I optimized an *in situ* hybridization methodology using a fluorescent labeling (FISH) for use in whole mounts of a small fish, the Japanese medaka (*Oryzias latipes*) (Park et al., 2008a, b; Tompsett et al., 2008; Zhang et al., 2008a, b, c).

The FISH methods developed allowed for the evaluation of gene expression profiles simultaneously in multiple target tissues in sections of Japanese medaka. The key issue that was addressed during the optimization studies was reduction of auto-fluorescence of tissues and components of the ISH procedure, which is one of the major limitations in the application of FISH on tissue sections. This was done using a combination of chemical treatment (sodium borohydride) and an advanced confocal microscopy system. The optimized FISH system was validated in a test exposure with the aromatase inhibitor fadrozole by revealing tissue specific expression of the *CYP19a* gene. Fadrozole (100 µg/L) up-regulated *CYP19a* expression and this trend was comparable with that obtained from Q RT PCR analysis. Moreover, the combination of FISH with histological analysis provided insights into the molecular changes at the cellular level, indicating that the observed changes were primarily due to a change in cell composition rather than an increase in gene expression per cell. Using the optimized FISH methodology, I further examined short-term effects of 17α-ethinylestradiol (EE2) and 17β-trenbolone (TB) on changes of three key genes (*Vitellogenin II*, *androgen receptor*, and *CYP19a*) expressions in male and female Japanese medaka (*Oryzias latipes*) (Park et al., 2008b). Both chemicals affected fecundity and gonad histology of medaka. Expression of the *Vit II* gene was gender and tissue specific in medaka and was induced after exposure to EE2. The *AR* gene was observed in both ovary and liver, but TB significantly induced *AR* gene expression in only the ovary. Expression of the aromatase (*CYP19a*) gene was primarily associated with early stage oocyte and was up-regulated by EE2 at lesser concentrations but down-regulated at greater concentrations.

## References

- Bej, AK., Mahbubani, MH., Atlas, RM., 1991. Amplification of nucleic acids by polymerase chain reaction (PCR) and other methods and their applications. *Critical Reviews in Biochemistry and Molecular Biology*, 26: 301–334.
- Bortone, SA., and Cody, RP. 1999. Morphological masculinization in poeciliid females from a paper mill effluent receiving tributary of the St. Johns River, Florida, USA. *Bulletin of the Environmental Contamination and Toxicology*, 63: 150-156.
- Bortone, SA., Davis, WB., and Bundrick, CM. 1989. Morphological and behavioral characters in mosquito fish as potential bioindication of exposure to kraft mill effluent. *Bulletin of the Environmental Contamination and Toxicology*, 43: 370-377.
- Bustin, SA. 2000. Absolute quantification of mRNA using real-time reverse transcription polymerase chain reaction assays. *Journal of Molecular Endocrinology*, 25: 169-193.
- Bustin, SA. 2002. Quantification of mRNA using real-time reverse transcription PCR (RT-PCR): trends and problems. *Journal of Molecular Endocrinology*, 29: 23-39.
- Carr, JA., Gentles, A., Smith, EE., Goleman, WL., Urquidi, LJ., Thuett, K., Kendall, RJ., Giesy, JP., Gross, TS., Solomon, KR., and Van Der Kraak, G. 2003. Response of larval *Xenopus laevis* to atrazine: assessment of gonadal and laryngeal morphology, *Environmental Toxicology and Chemistry*, 22: 396-405.
- Coady, KK., Murphy, M., Villeneuve, DL., Hecker, M., Jones, PD., Carr, JA., Solomon, K., Smith, EE., Van Der Kraak, G., Kendall, RJ., and Giesy, JP. 2004. Effects of atrazine on metamorphosis, growth and gonadal development in the green frog (*Rana clamitans*). *Journal of Toxicology and Environmental Health, Part A*, 67: 941-957.
- European Commission. 1996. European workshop on the impact of endocrine disruptors on human health and wildlife. Weybridge, 2-4 Dec. 1996. Report EUR 17594, Environment and Climate Research Programme, DG XII, European Commission.
- Gimeno, S., Gerritsen, A., Bowmer, T., and Komen, H. 1996. Femization of male carp.

Nature, 384: 221-222.

Folmar, LC., Denslow, ND, Rao, V., Chow, M., Crain, DA., Enblom, J., Marcino, J., and Guillette, LJ. 1996. Vitellogenin induction and reduced wrum testosterone concentrations in feral male carp (*Cyprinus carpio*) captured near a major metropolitan sewage treatment plant. Environmental Health Perspectives, 104: 1096-1101.

Harries, JE., Sheahan, DA., Jobling, S., Matthiessen, P., Neall, P., Sumpter, JP., Tylor, T., and Zaman, N. 1997. Estrogenic activity in five United Kingdom rivers detected by measurement of vitellogenesis in caged male trout. Environmental Toxicology and Chemistry, 16: 534-542.

Hayes, TB., Collins, A., Lee, M., Mendoza, M., Noriega, N., Stuart, AA., Vonk, A., 2002. Hermaphroditic, demasculinized frogs after exposure to the herbicide atrazine at low ecologically relevant doses. Proc. Natl. Acad. Sci. U. S. A. 99, 5476–5480.

Hecker, M., Giesy, JP., Jones, PD., Jooste, AM., Carr, JA., Solomon, KR., Smith, EE., Van Der Kraak, G., Kendall, RJ., du Preez, L. 2004. Plasma sex steroid concentrations and gonadal aromatase activities in African clawed frogs (*Xenopus laevis*) from South Africa. Environmental Toxicology and Chemistry, 23: 1996-2007.

Hecker, M., Kim, WJ., Park, JW., Murphy, MB., Villeneuve, DL., Coady, KK., Jones, PD., Solomon, KR., Van Der Kraak, G., Carr, JA., Smith, L. EE., du Preez, L., Kendall, RJ., and Giesy, J P. 2005a. Effects of estradiol and atrazine on plasma sex steroid concentrations, gonadal aromatase activity and ultrastructure of the testis in *Xenopus laevis*. Aquatic Toxicology, 72: 383-396.

Hecker, M., Park, JW., Murphy, MB., Jones, PD., Solomon, KR., Van Der Kraak, G., Carr, J A., Smith, EE., du Preez, L., Kendall, RJ., and Giesy, JP. 2005b. Effects of atrazine on *CYP19a* gene expression and aromatase activity in testes and on sex steroid concentrations in plasma of male African clawed frogs (*Xenopus Laevis*). Toxicological Sciences, 86: 273-280.

Herman, RL., and Kincaid, HL. 1988. Pathological effects of orally administrated estradiol to rainbow trout. Aquacluture, 72: 165-172.

- Howelll, WM., and Denton, TE. 1989. Gonopodial morphogenesis in female mosquitofish, *Gambusia affinis affinis*, masculinized by exposure to degradation products from plant sterols. *Environmental Biology of Fishes*, 24: 43-51.
- Jin, L., and Lloyd, RV. 1997. In situ hybridization: Methods and applications. *Journal of Clinical Laboratory Analysis*, 11: 2-9.
- Kavlock, R., DAston, GP., DeRosa, C., Fenner-Crisp, P., Gray, LE., Kaatari, S., Lucier, G., Luster, L., Mac, MJ., Macza, C., Miller, R., Moore, J., Rolland, R., Scott, G., Sheehan, DM., Sinks, T., and Tilson, HA. 1996. Research needs for the risk assessment of health and environmental effects of endocrine disruptors: A report of the U.S. EPA-sponsored workshop. *Environmental Health Perspective*, 104 (Suppl): 715-740.
- Kong, RYC., Giesy, JP., Wu, RSS., Chen, EXH., Chiang, MWL., Lim, PL., Yuen, BBH., Yip, BWP., Mok, HOL., and Au, DWT. 2008. Development of a marine fish model for studying in vivo molecular responses in ecotoxicology. *Aquatic Toxicology*, 86:131-141.
- Kloas, W. 2002. Amphibians as a model for the study of endocrine disruption. *International Review of Cytology*, 216: 1-57
- Norris, DO. 2007. An overview of chemical bioregulation in vertebrates. In: Norris, D.O. (Ed), *Vertebrate endocrinology*, Elsevier Academic Press, Boston, MA, pp: 1-29
- Park, JW., Hecker, M., Murphy, MB., Jones, PD., Solomon, KR., Van Der Kraak, G., Carr, JA., Smith, EE., du Preez, L., Kendall, RJ., and Giesy, JP. 2006. Development and optimization of a Q-RT PCR method to quantify *CYP19* mRNA expression in testis of male adult *Xenopus laevis*: comparisons with aromatase enzyme activity. *Comparative Biochemistry and Physiology, Part B*, 144: 18-28.
- Park, JW., Tompsett, A., Newsted, JL., Jones, PD., Au, D., Kong, R., Wu, RSS., Giesy, JP., and Hecker, M. 2008a. Fluorescence in situ hybridization techniques (FISH) to detect changes in CYP19a gene expression of Japanese medaka (*Oryzias latipes*). *Toxicology and Applied Pharmacology*, (Submitted).
- Park, JW., Tompsett, A., Newsted, JL., Jones, PD., Au, D., Kong, R., Wu, RSS., Giesy, JP., and Hecker, M. 2008b. Effects of ethinylestradiol and trenbolone on

histology and gene expression of Japanese medaka (*Oryzias latipes*) using a combination of fluorescence in situ hybridization (FISH) and traditional histology. Toxicological Sciences (Submitted).

Purdum, CE., Hardiman, PA., Bye, VJ., Eno, NC., Tyler, CR., and Sumpter, JP. 1994. Estrogenic effects of effluents from sewage treatment works. Chemistry and Ecology, 8: 275-285.

Rastogi, PK., and Chieffi, G. 1975. The effects of antiestrogens and anitandrogens in nonmammalian vertebrates. General and Comparative Endocrinology, 26: 79-91.

Rotchell, JM., and Ostrander, GK. 2003. Molecular markers of endocrine disruption in aquatic organisms. Journal of Toxicology and Environmental Health, Part B: Critical Review, 6: 453-496.

Sanderson, JT., Letcher, RJ., Heneweer, M., Giesy, JP., and Van den Berg, M. 2001. Effects of Chloro-S-Triazine Herbicides and Metabolites on Aromatase (CYP19) Activity in Various Human Cell Lines and on Vitellogenin Production in Male Carp Hepatocytes. Environmental Health Perspectives, 109:1027-1031.

Sanderson. JT., Seinen, W., Giesy JP., and van den Berg, M. 2000. 2-chloro-S-Triazine Herbicides Induce Aromatase (CYP-19) Activity in H295R Human Adrenocortical Carcinoma Cells: A Novel Mechanism for Estrogenicity. Toxicological Sciences 54:121-127.

Tompsett, AR., Park, JW., Zhang, X., Jones, PD., Newsted, JL., Au, DTW., Chen, EHX., Yu, RMK., Wu, RSS., Kong, RYC., Giesy, JP., and Hecker, M. 2008. Development and validation of an *in situ* hybridization system to detect gene expression along the HPG-axis in Japanese medaka, *Oryzias latipes*. Achieves of Environmental Contamination and Toxicology, (Submitted).

Tremblay, L., and Van Der Kraak, G. 1999. Comparison between the effects of the phytosterol b-sitosterol and pulp and paper mill effluents on sexually immature rainbow trout. Environmental Toxicology and Chemistry, 18: 329-336.

Wester, PW., and Canton, JH. 1986. Histopathological study of *Oryzias latipes* (Medaka) after long-term  $\beta$ -hexachlorocyclohexane exposure. Aquatic Toxicology, 9: 21-45.



- Wilkinson, DG. 1992. The theory and practice of in situ hybridization. In: Wilkinson, D.G. (Ed), In situ hybridization: A practical approach, Oxford University Press, New York, NY, pp: 1-13.
- Wittbrodt, J., Shima, A., and Scharl, M. 2002. Medaka – a model organism from the Far East. *Natural Reviews Genetics*. 3: 53-64.
- Wu, M., and Gerhart, J. 1991. Raising *Xenopus* in the laboratory, In: Kay, BK., Peng, HB. (Eds.), *Xenopus laevis: Practical uses in cell and molecular biology*, Academic Press, Inc., San Diego, CA, pp: 3-17.
- Zhang, X., Hecker, M., Park, JW., Tompsett, AR., Newsted, JL., Nakayama, K., Jones, PD., Au, D., Kong, R., Wu, RSS., and Giesy, JP. 2008a. Real time PCR array to study effects of chemicals on the Hypothalamic-Pituitary-Gonadal axis of the Japanese medaka. *Aquatic Toxicology*, (Submitted).
- Zhang, X., Park, JW., Hecker, M., Tompsett, AR., Jones, PD., Newsted, JL., Au, D., Kong, R., Wu, RSS., and Giesy, JP. 2008b. Time-dependent transcriptional profiles of hypothalamic-pituitary-gonadal (HPG) axis in medaka (*O. latipes*) exposed to fadrozole and 17beta-trenbolone. *Aquatic Toxicology*, (Submitted).
- Zhang, W., Park, JW., Tompsett, AR., Jones, PD., Newsted, JL., Au, D., Wu, RSS., Giesy, JP., and Hecker, M. 2008c. Responses of the Medaka HPG axis PCR array and reproduction to prochloraz and ketoconazole. *Environmental Sciences and Technology*, (Submitted).

## CHAPTER 1

Development and optimization of a Q-RT PCR method to quantify *CYP19* mRNA expression in testis of male adult *Xenopus laevis*: Comparisons with aromatase enzyme activity

### Abstract

Due to limitations of the currently used enzymatic assays, it is difficult to determine aromatase activity in testicular tissue of amphibians. Quantitative reverse transcription polymerase chain reaction (Q-RT PCR) is a sensitive and reliable technique to detect low amounts of mRNA for specific genes. This study was designed to develop and optimize a SYBR Green I-based Q-RT PCR method to quantify *CYP19* mRNA in testicular tissue from male *Xenopus laevis*. Four quantification methods for measuring *CYP19* mRNA expression were compared. The established test system proved to be highly sensitive (detectable mRNA copies < 10), reproducible (interassay CV < 5.4%, intraassay CV < 0.9%), precise and specific for the *CYP19* gene. To confirm the validity of the applied test system, an ex vivo testicular and ovarian explant study with a known inducer of aromatase, forskolin, was conducted. Forskolin induced *CYP19* gene expression in both ovarian (3.7-fold) and testicular (2.6-fold) explants. Of the four quantification methods, the absolute standard curve and the comparative  $C_T$  method appear to be optimal as indicated by their highly significant correlation ( $r^2 = 0.998$ ,  $p < 0.001$ ). In conclusion, we recommend the comparative  $C_T$  method over the standard curve method because it is more economical in terms of both cost and labor. Although both aromatase activity and

*CYP19* mRNA were clearly detectable in testes of *X. laevis*, both aromatase enzyme activity and *CYP19* gene expression were very low. Also, no significant relationships were found between aromatase enzyme activity and gene expression. This is likely due the fact that the aromatase enzyme may have been dormant at the developmental stage the frogs were in during the experiment.

## **Introduction**

The cytochrome P450 enzyme aromatase is the key enzyme that catalyzes the conversion of androgens to estrogens and represents the rate-limiting step in estrogen biosynthesis. The protein that catalyzes the aromatization of steroid hormones is encoded by the *CYP19* gene (Thompson and Siiteri, 1974; Simpson et al., 1994). Estrogens, especially estradiol-17 $\beta$  (E2), have been shown to play a key role in ovarian development, reproductive function and sexual differentiation in various amphibian species (Miyashita et al., 2000; Miyata and Kubo, 2000; Kuntz et al., 2003a; Kato et al., 2004). Thus, disruption of either activity or production of this enzyme is likely to result in altered developmental or reproductive biology of organisms. Due to its key function in estrogen biosynthesis and associated reproductive processes, aromatase has been considered as an important endpoint to assess the exposure to compounds that may interact with reproductive endocrinology in vivo and in vitro (Sanderson et al., 2002; Hayes et al., 2002; Rotchell and Ostrander, 2003).

Recently, concern was raised about the potential of triazine herbicides to interact with the endocrine system of male frogs by inducing aromatase resulting in an increase of endogenous estrogen production and subsequently causing feminization or

demasculinization of males (Hayes et al., 2002). Although studies by Sanderson et al. (2002) and Roberge et al. (2004) have found that high concentrations of triazine herbicides can induce aromatase in mammalian cells in culture, to date there have been no reports of this mechanism of action being observed in vivo in amphibians. This may be due to the fact that testicular aromatase enzyme activities are often low and are thus difficult to detect because they are near the detection limits of the commonly used enzymatic assays (Hecker et al., 2004). Therefore, to increase our ability to determine possible changes in aromatase activity in the testis, a more sensitive test system is needed that allows for detecting even subtle changes. One way to examine the potential for such subtle effects on the expression of aromatase activity is by measuring the changes in the expression of *CYP19* mRNA. Quantitative (real-time) reverse transcriptase polymerase chain reaction (Q-RT PCR) is a sensitive and flexible technique that can detect small quantities of mRNA in small amounts of tissue (Bustin, 2000 and 2002). This technique, which amplifies the number of copies of mRNA many times, can theoretically measure as little as a single molecule of the target mRNA (Linz et al., 1990; Bej et al., 1991).

There have been few studies analyzing *CYP19* gene profiles in the African clawed frog (*Xenopus laevis*) or in amphibians in general (Miyashita et al., 2000; Akatsuka et al., 2004; Kuntz et al., 2004). None of above studies, however, have focused on adult males and, to our knowledge, Q-RT PCR methods using reliable quantification methods have not yet been applied to quantify the gene expression levels of *CYP19* in testes of *X. laevis*. It is known that *CYP19* is differentially expressed based on the sex or life-stage in most vertebrate species (Miyashita et al., 2000; Liu et al., 2004; Sakata et al., 2005; Forlano and Bass, 2004) and that one cannot simply extrapolate between sexes,

especially with regard to effects of chemical exposure. Therefore, the objective of this study was to develop and optimize a Q-RT PCR procedure to measure the expression level of *CYP19* in testicular tissue of male *X. laevis*. To facilitate accurate quantification, a cDNA standard was produced that could be used for the determination of absolute copy numbers of *CYP19* mRNA in addition to the relative quantification determined by comparison to the expression of housekeeping genes. Furthermore, comparison of *CYP19* gene expression in male with aromatase enzyme activities was conducted to establish a link between expression and function of gonadal aromatase in male *X. laevis*.

## **Materials and Methods**

### *Animals*

Adult male *X. laevis*, 30–50g, were purchased from Xenopus Express (Plant City, FL, USA). Each frog was treated with 0.06% NaCl upon their arrival at the laboratory to reduce the risk of possible infections. Frogs were acclimated for several weeks at the Michigan State University's Aquatic Toxicology Laboratory before the experiment was initiated. During acclimation, animals were held in 600-L fiberglass tanks under flow-through conditions. The photoperiod was 12:12-h light/dark. Frogs were fed Nasco frog brittle (Nasco, Fort Atkinson, WI, USA) three times per week *ad libitum*. Fourteen frogs were under static renewal conditions individually in 40 L aquarium for 36 days, with 50% of water renewal every 3 days. Feeding regimen, temperature, and photoperiod during the exposures were consistent with acclimatization conditions. All procedures used during all phases of this study were in accordance with protocols approved by the Michigan State University Instituted Animal Care and Use Committee (IACUC).

### *Isolation of total RNA and first-strand cDNA synthesis*

Frogs were sampled on exposure day 36 and were anesthetized by immersion in 250 mg/l MS-222 (tricaine methanesulfonate). Total RNA was isolated from testes of 14 male *X. laevis* using the SV Total RNA Isolation System (Promega, Madison, WI, USA) following the manufacturer's specifications with minor modifications to maximize the efficiency of total RNA isolation. Briefly, tissues were homogenized using a Kontes pestle and lysed in microcentrifuge tubes with guanidine thiocyanate and  $\beta$ -mercaptoethanol mixture. After centrifugation to remove precipitated proteins and cellular debris, nucleic acids were precipitated with ethanol and bound to a glass fiber membrane. All samples were treated with RNase-free DNase I at room temperature for 15min to remove the chromosomal DNA. RNA integrity was checked by denaturing agarose gel electrophoresis (not shown) and 260:280nm absorbance ratio ( $2.33 \pm 1.03$ ) using a DU530 UV/VIS spectrophotometer (Beckman Coulter, Inc., CA, USA). Concentrations of total RNA were determined using the RiboGreen™ RNA quantitation reagent (Molecular Probes, Inc., OR, USA) in a TD700 laboratory fluorometer (Turner BioSystems, Sunnyvale, CA, USA). Purified RNA was stored at  $-80^{\circ}\text{C}$  until further analysis.

A sample containing 500ng of total RNA was used to synthesize single-strand cDNA in accordance with the manufacturer's directions (SuperScript™ First-Strand Synthesis System for RT PCR, Invitrogen, CA, USA). Briefly, prior to reverse transcription, total RNA was treated with DNase I to remove potential chromosomal DNA. Then, 1.25 $\mu\text{L}$  of 12–18 Oligo(dT) (0.5 $\mu\text{g}/\mu\text{L}$ ) and 10mM dNTP mix were added

to the total RNA, and incubated at 65°C for 5min. The reaction was stopped by chilling the test solution on ice. Reaction mixture (10× RT buffer, 25mM MgCl<sub>2</sub>, 0.1M DTT and recombinant ribonuclease inhibitor) was added to the RNA/primer mixture and incubated at 42°C for 2min. SuperScript II reverse transcriptase (1.25μL of 50U M-MLV) was added and the reaction mixture was incubated at 42°C for 50min, followed by a second incubation at 70°C for 15min. To confirm complete removal of possible genomic contamination, a negative control (sample without reverse transcriptase) was run in parallel in the Q-RT PCR system, which resulted in no amplification of the PCR product (data not shown). To improve sensitivity of the PCR to amplify the *CYP19* mRNA from cDNA, the RNA template from the cDNA:RNA hybrid molecule was removed by digestion with *Escherichia coli* RNase H (2U/μL) after first-strand cDNA synthesis took place.

#### *Real-time PCR using SYBR Green I*

To determine the accumulation of the PCR product, SYBR Green I dye was used as a real-time reporter of the presence of double-stranded DNA. The expression level of *CYP19* mRNA was normalized to an internal control gene, glyceraldehyde-3-phosphate dehydrogenase (*GAPDH*). Both cDNA sequences were obtained from the public GenBank database of NCBI. The *X. laevis* *CYP19* gene primer [forward primer: 5'CGGTTCCATATCGTTACTTCC3', reverse primer: 5'GCATCTTCCTCTCAATGTCTG3', amplicon length (bp): 140] was designed in our laboratory based on consideration of GC content, length, secondary structure and melting temperature of the primer using the program Beacon Designer 2 (PREMIER Biosoft Intl.,

Palo Alto, CA, USA). Sequences for the *GAPDH* gene primer [forward primer: 5'GCT CCT CTC GCAAAG GTC AT3', reverse primer: 5'GGG CCA TCC ACT GTC TTC TG3', amplicon length (bp): 101] was obtained from the published literature (Wiechmann and Smith, 2001). Primer specificity was verified by a single distinct peak obtained during the melting curve analysis of the SYBR Green-based RT PCR system and by DNA sequencing of the PCR amplicons separated by gel electrophoresis. Best results were obtained at a dilution of the reverse-transcribed samples of 1/4 and 1/20 for *CYP19* and *GAPDH*, respectively. All PCR reactions were performed in a SmartCycler® II (Cepheid, Sunnyvale, CA, USA). PCR master mix was prepared on ice with 10× SYBR Green I buffer containing 3μL of MgCl<sub>2</sub> (25mM/1.5mL), 0.5μL of dNTP mix with dUTP (12.5mM/1 mL), proper primers (sense primer/antisense primer, 9.8 pM/μL:7.3 pM/μL for *CYP19* and sense primer/antisense primer, 9.3 pM/μL:11.3 pM/μL for *GAPDH*), 0.65 units of AmpliTaq Gold™ DNA polymerase (5U/μL) and 0.25 units of AmpErase (1U/μL). 5μL of diluted reverse-transcribed samples were added to 20μL of the PCR master mix. The PCR reaction mix was denatured at 95°C for 10min before the first PCR cycle. The thermal cycle profile was: (1) denaturation for 15s at 95°C, (2) annealing for 30s at 60°C and (3) extension for 30s at 72°C. A total of 50 PCR cycles was used for amplification due to the low *CYP19* copy numbers in many of the samples.

#### *Synthesis of plasmid DNA standards*

PCR products of *CYP19* and *GAPDH* were separately ligated into the pGEM T vector (Promega, Madison, WI, USA) following manufacturer's specifications. Sequence validity of the cloned amplicons was confirmed by automatic DNA sequencing and



followed by a BLAST2 analysis (National Center for Biotechnology Information, NCBI ([www.ncbi.nlm.nih.gov](http://www.ncbi.nlm.nih.gov)), Bethesda, MD, USA) with their corresponding sequences in GenBank. The concentrations of purified plasmids (*CYP19* plasmid DNA and *GAPDH* plasmid DNA) that spanned the target regions for forward and reverse primers were measured by using TD700 laboratory fluorometer (Turner design, CA, USA) with molecular probes' RiboGreen™ DNA quantitation reagent (Molecular Probes, Inc., OR, USA). These measured plasmids were converted to copy numbers/μL according to the formula below (Eq. (1)):

$$\text{Number of DNA molecules per } \mu\text{L} = (\text{ng}/\mu\text{L} \cdot 1.515 \div N_{\text{bp}}) \cdot 6.023 \cdot 10^{11} \quad (1)$$

where  $N_{\text{bp}}$  = size of dsDNA (plasmid size plus DNA insert size) expressed as bp.

To evaluate PCR efficiency, uniformity and linear dynamic range of each Q-RT PCR assay, standard curves for *CYP19* and *GAPDH* were constructed using serial dilution of PCR product-inserted plasmid DNA standards ( $1 \times 10^1$ – $1 \times 10^6$  copies/μL).

#### *Quantification of CYP19 mRNA expression*

There are two methods that are commonly used for the analysis of data obtained from the RT PCR system. These include relative measurements, where the change in expression of the mRNA of interest is compared to that of an internal housekeeping gene that is assumed to be unaffected by the study treatment(s) (comparative  $C_T$  method). This method does not require any standards and is generally sufficient to demonstrate changes in gene expression. The more accurate method is to develop standards of either mRNA or the appropriate cDNA so that a standard curve can be developed to which the results of

the PCR from a sample can be compared (absolute standard curve method). To assure the accuracy of measurements, both methods were applied and the results compared.

#### Comparative C<sub>T</sub> method

This method in which the expression of the *CYP19* target gene (cDNA made from mRNA) was normalized to that of *GAPDH* in each RT PCR reaction (referred to as C<sub>T</sub>) is the most commonly used method. Differences between median  $\Delta C_T$  of test group and  $\Delta C_T$  of each sample were expressed as  $\Delta\Delta C_T$ . The fold difference ( $2^{\Delta\Delta C_T}$ ) of gene expression in *CYP19* was calculated for each sample. While this method is accurate and generally gives reliable results, the absolute quantification method, which relies on a standard curve for each gene, is more accurate.

#### Absolute standard curve method

In addition to the comparative method, an absolute method, based on standard curves developed for each transcript was generated from a dilution series of synthesized plasmid cDNA standards and a linear regression model was applied to quantify the data (Eq. (2)).

$$Y = aX + b \quad (2)$$

where Y = C<sub>T</sub> value, a = the slope of the standard curve, X = logarithm of the total copy numbers and b = y-intercept.

The amount of mRNA present in the original RNA extract was determined using the Q-RT-PC method. Data were expressed as the C<sub>T</sub> value, which is the cycle number when a reaction reaches the threshold (level of detection of increasing fluorescence) (Girault et al., 2002). Determination of transcript abundance (mean of C<sub>T</sub> value) of the

*CYP19* and the *GAPDH* genes were conducted in triplicate. The copy numbers of *CYP19* and *GAPDH* cDNA were calculated (Eq. (2)). To compensate for variations in RNA amount and RT efficiency, the copy number of *CYP19* was normalized to that of the internal gene (*GAPDH*). *GAPDH* was selected as the internal control (housekeeping gene) because it has been reported to be expressed at lesser levels than other housekeeping genes, such as  $\beta$  *actin* and 18S rRNA (Wiechmann and Smith, 2001). *GAPDH* is a consistently expressed gene, making it suitable as an internal standard for Q RT PCR assays (Raaijmakers et al., 2002). Expression ratio (ER) of mRNA copy numbers between *CYP19* and *GAPDH* in the same sample was also calculated (Eq. (3)).

$$\text{ER} = \text{mRNA copy number of } CYP19 / \text{mRNA copy number of } GAPDH \quad (3)$$

Quantitative (real-time) RT PCR efficiencies were calculated as follows (Eq. (4)).

$$\text{Efficiency (\%)} = [(10^{(-1/a)}) - 1] \cdot 100 \quad (4)$$

where *a* is the slope of the standard curve derived from Eq. (3).

#### *Confirmation of test system using positive controls*

To confirm the validity of the developed methods, testicular and ovarian tissues from adult *X. laevis* were exposed to a model compound, forskolin (Sigma-Aldrich, St. Louis, MO), that is known to induce *CYP19* ovarian gene expression (Watanabe and Nakjin, 2004). Briefly, ovarian and testicular tissues were harvested and plated in Medium 199 (Hepes supplemented with 0.1mM IBMX and 1 $\mu$ g/mL 25-hydroxycholesterol) in 24-well plates (Corning, NY, USA) (testis: approx. 0.1 g/well, ovary: approx. 0.5 g/well). Prior to transferring tissue from male frogs to plates, each testis was dissected into eight pieces of equal size. Testicular fragments from all animals were then combined and four pieces

were randomly assigned to each well to minimize variation of *CYP19* gene expression due to inter-individual differences. Exposure concentrations were 0 and 100 $\mu$ M forskolin using DMSO as solvent carrier. A solvent control was run in the forskolin experiment to test for possible effects of DMSO on *CYP19* gene expression. Experiments were conducted over a time period of 20h at 25°C. After exposure, *CYP19* gene expression was measured in tissue using the methods described above. Due to limitations in the amount of tissue available, no measurements of aromatase activity could be conducted in parallel.

#### *CYP19 aromatase activity*

Aromatase activity was measured following the protocol of Lephart and Simpson (1991) with minor modifications. Less than 0.5g of gonadal tissue was homogenized in 600 $\mu$ L of ice-cold gonad buffer (50mM KPO<sub>4</sub>, 1mM EDTA, 10mM glucose-6-phosphate, pH 7.4). The homogenate was incubated with 300nM 3H-androst-4-ene-3,17-dione (25.9Ci/nmol; Lot No. 3467-067; Cat. No. NET-926; New England Nuclear, MA, USA), 0.5 IU/mL glucose-6-phosphate (Sigma Cat. # G6378) and 1mM NADP (Sigma Cat. # N-0505) at 37°C and 5% CO<sub>2</sub> for 90min. Tritiated water released from each sample was extracted and activity determined by liquid scintillation counting. Aromatase activity was expressed as pmol androstenedione converted/h/mg protein. The specificity of the reaction for the substrate was determined by use of a competitive test with non-labeled androstenedione and the use of the specific aromatase inhibitor fadrozole (Novartis Pharma AG, Basel, CH). Addition of large amounts of androstenedione reduced tritiated water formation to the concentrations found in the tissue blanks. Furthermore, addition

of fadrozole during the tritium-release assay reduced aromatase enzyme activity in a dose-dependent manner with concentrations of 5 $\mu$ M and greater resulting in complete inhibition of enzyme activity to the levels measured in the blanks. This demonstrated that the activity being measured was specific for aromatase. Protein concentrations were determined using the Bradford assay (Bradford, 1976) with bovine serum albumin as the protein standard (Sigma-Aldrich, St. Louis, MO, USA).

### *Statistical analysis*

Statistical analyses in this study were conducted using SYSTAT 10 (SPSS Inc., Chicago, IL, USA). Data sets were tested for normality using Kolmogorov–Smirnov's one sample test. The Pearson correlation analysis was used to evaluate the relationship between CYP19 enzyme activity and *CYP19* mRNA expression, and a linear regression model was used to quantitatively determine relationships among gene quantification methods in the Q-RT PCR system. The Student's t-test was used to examine differences in gene expression between *CYP19* and *GAPDH*. The criterion for significance in all statistical tests was  $p < 0.05$ .

## **Results**

### *RT PCR amplification efficiencies, linearity and reproducibility*

Specificity of the PCR reaction, accuracy of mRNA quantification and sensitivity and linearity of SYBR Green based Q-RT PCR for *CYP19* and *GAPDH* in adult male *X. laevis* were determined. Real-time PCR amplification curves for the two genes obtained with the SmartCycler<sup>®</sup> were very reproducible and indicated that primers were selective

and effective in producing the specific PCR products (Figs. 1.1A and 1.2A). The melting curves (Figs. 1.1C and 1.2C) generated at the end of the PCR reaction show that all amplicons of the *CYP19/GAPDH* plasmid DNA standard had the same melting temperature (81°C). This result indicates that no primer–dimers were formed during the reactions (Figs. 1.1C and 1.2C). To further validate the specificity of the assay, gel electrophoresis (1.5% agarose) was performed on the PCR products obtained from serially diluted plasmid DNA standards (Figs. 1.1D and 1.2D). The results from the gel electrophoreses demonstrate that the amplification was specific for the ~ 140bp and ~ 101bp products of *CYP19* and *GAPDH*, respectively.

The accuracy of mRNA quantification, and sensitivity and linearity of SYBR Green-based Q-RT PCR were examined using a 10-fold serial dilution of each plasmid DNA standard. Efficiencies during the exponential phase were 96.7% and 105.7% for *CYP19* and *GAPDH*, respectively. The relationship between threshold cycle ( $C_T$ ) and the log copy number of plasmid DNA standard was linear with  $r^2 > 0.99$  for both genes, indicating that the  $C_T$  values changed proportionally with serial dilution of the samples. The reproducibility of the techniques within and between assays was tested, using serial dilutions of *CYP19* and *GAPDH* plasmid cDNA standards. Intraassay variabilities were assessed by evaluating the coefficient of variation (CV) for three replicates in each dilution within one run (Table 1.1). Interassay variabilities were assessed by conducting three different assays performed in triplicate of each dilution over a period of 3 days (Table 1.1). Intraassay CVs of  $C_T$  for both genes were very small ( $< 1.2\%$ ), indicating that the assays were highly reproducible for determining expression of both genes.

Although greater than intraassay CVs, interassay  $C_T$  values were also small with CVs < 5.4% for both genes.

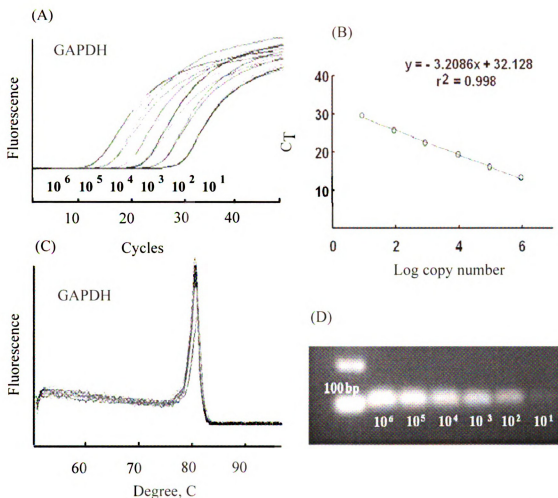


Figure 1.1 *GAPDH* plasmid DNA standard curve. (A) Amplification curves of six dilutions of *GAPDH* plasmid DNA standard from  $1 \times 10^1$  to  $1 \times 10^6$  copies/ $\mu$ L. (B) *GAPDH* plasmid DNA standard curve plotting the log copies/ $\mu$ L (x) of *GAPDH* plasmid DNA against  $C_T$  (y), the equation was calculated by linear regression analysis ( $r^2=0.998$  and 105.7% of PCR efficiency). (C) Melting curve of PCR products, showing specificity of the reaction. (D) 1.5% agarose gel electrophoresis of the PCR products in the serially diluted samples.

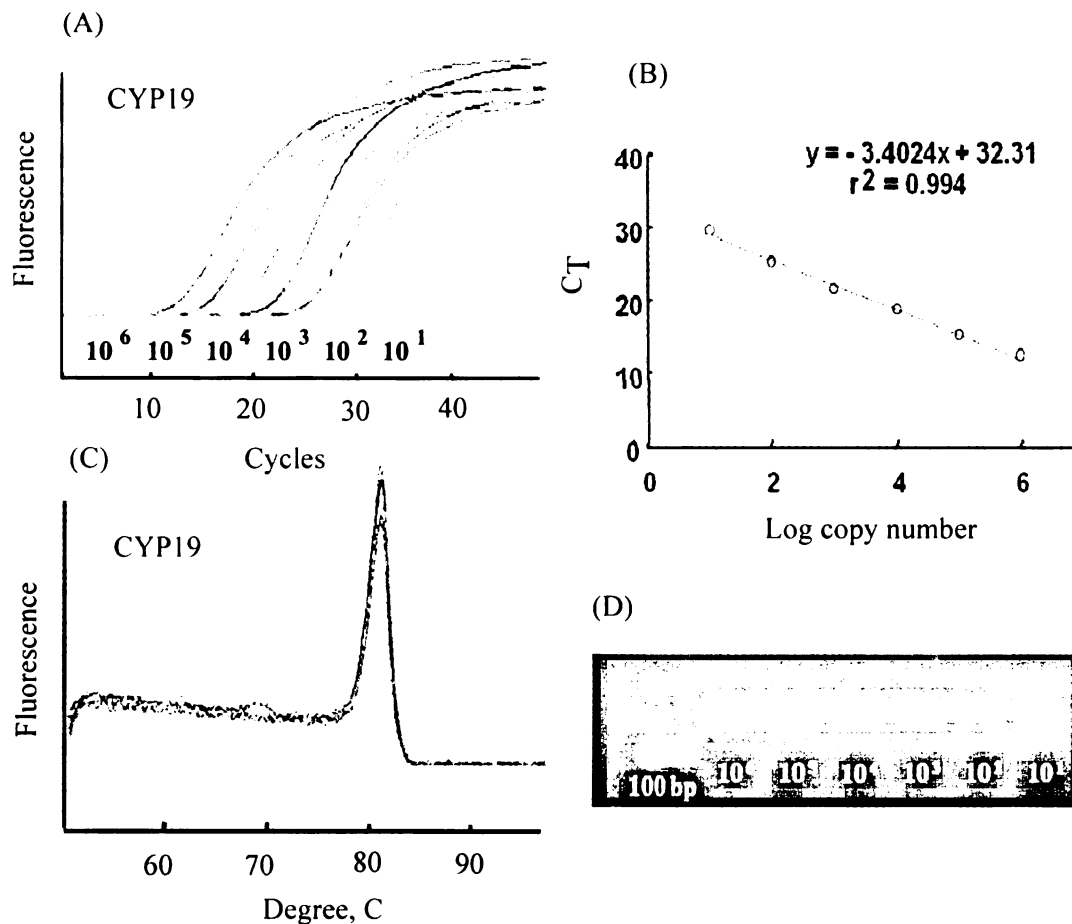


Figure 1.2 *CYP19* plasmid DNA standard curve. (A) Amplification curves of six dilutions of *CYP19* plasmid DNA standard from  $1 \times 10^1$  to  $1 \times 10^6$  copies/ $\mu$ L. (B) *CYP19* plasmid DNA standard curve plotting the log copies/ $\mu$ L (x) of *CYP19* plasmid DNA against  $C_T$  (y), the equation was calculated by linear regression analysis ( $r^2=0.994$  and 96.7% of PCR efficiency). (C) Melting curve of PCR products, showing specificity of the reaction. (D) 1.5% agarose gel electrophoresis of the PCR products in the serially diluted samples.



**Table 1.1 Reproducibility and precision of standard curve method for *CYP19* and *GAPDH* plasmid DNA.**

<i>CYP19</i> plasmid DNA (copies/ $\mu$ L)	a Intra assay			b Inter assay		
	<sup>c</sup> C <sub>T</sub> mean values	<sup>d</sup> SD	<sup>e</sup> CV	C <sub>T</sub> mean values	SD	CV
$1 \times 10^6$	12.37	0.04	0.31	12.57	0.23	1.79
$1 \times 10^5$	15.18	0.06	0.36	15.41	0.32	2.08
$1 \times 10^4$	18.56	0.16	0.84	18.62	0.15	0.83
$1 \times 10^3$	21.53	0.11	0.50	21.84	1.16	5.33
$1 \times 10^2$	25.18	0.11	0.44	25.65	0.72	2.80
$1 \times 10^1$	29.60	0.03	0.11	28.77	0.83	2.90
<i>GAPDH</i> plasmid DNA (copies/ $\mu$ L)	C <sub>T</sub> mean values	SD	CV	C <sub>T</sub> mean values	SD	CV
$1 \times 10^6$	13.11	0.12	0.95	13.20	0.08	0.61
$1 \times 10^5$	16.02	0.18	1.12	16.03	0.10	0.64
$1 \times 10^4$	19.23	0.10	0.54	19.32	0.10	0.50
$1 \times 10^3$	22.22	0.11	0.49	22.60	0.47	2.06
$1 \times 10^2$	25.52	0.04	0.15	25.81	0.35	1.34
$1 \times 10^1$	29.28	0.05	0.16	29.73	1.02	3.43

a; intra assay was assessed by evaluating the coefficient of variation (CV) for each dilution of the plasmid using three replicates within run

b; inter assay was assessed by evaluating the coefficient of variation (CV) for each dilution of the plasmid using three assays with three replicates over 3 different days

c; average of number of cycles when fluorescence crossed threshold

d; SD = standard deviation from the mean

e; CV = coefficient of variation (%)

### *Comparison of different quantification methods for CYP19 gene expression*

Serial dilutions ( $1 \times 10^1$  to  $1 \times 10^6$  copies/ $\mu$ L) of *CYP19* and *GAPDH* plasmid DNA

standards were used to quantify gene amplification rates for the genes of interest. The

results demonstrated that the SYBR Green-based Q-RT PCR assay allowed for the

quantification of small amounts of *CYP19* mRNA (10 copies/reaction) in all 14 adult

male *X. laevis*. Initial copy numbers for both genes in all 14 samples were determined by use of the standard curve method. *GAPDH* exhibited significantly greater abundances of the transcript with a mean  $C_T$  value of  $22.9 \pm 0.62$  (mean  $\pm$  S.D.) than *CYP19* with a mean  $C_T$  value of  $28.1 \pm 1.4$  ( $p < 0.001$ ). Mean copy numbers for all samples were  $25.2 \pm 23.4$  copies/ $\mu$ L and  $802.61 \pm 350.9$  copies/ $\mu$ L for *CYP19* and *GAPDH*, respectively.

Because of a number of factors such as varying amounts of mRNA in the samples, differences in reverse transcription efficiency and potential presence of PCR reaction inhibitors can influence the gene amplification reaction, the use of an internal control is necessary to normalize the measurements. The simplest way to quantify mRNA in RT PCR systems, the use of the  $C_T$  value ratio ( $C_T$  of target gene/ $C_T$  of internal gene), was also applied to quantify *CYP19* gene expression (Table 1.2). The similar efficiencies observed for the two genes in this PCR assay allow for the use of the comparative  $C_T$  method for quantifying *CYP19* gene expression after normalization to gene expression of the internal gene. The fold differences ( $2^{\Delta\Delta C_T}$ ) of *CYP19* gene expression of all 14 samples were calculated using the comparative  $C_T$  method. The average fold difference was not equal, but very close to 1.0. In addition to the calculations above, *CYP19* gene expression was measured using the standard curve method, where the expression was determined as copy numbers obtained from *CYP19* plasmid standard curve or as ER (Eq. (3)) normalized to the internal control (Table 1.2).

All four quantification methods were compared to each other using a linear regression ( $r^2$ ) model to determine the compatibility of different quantification approaches (Fig. 1.3). The comparative  $C_T$  method and the standard curve method were the most highly correlated in all comparisons ( $r^2 = 0.997$ ,  $p < 0.001$ ). The relationship

between  $C_T$  value ratio and comparative  $C_T$  method or  $C_T$  value ratio and standard curve method was less strong, with  $r^2 = 0.902$  and  $r^2 = 0.916$ , respectively. The coefficient for the correlation between the uncorrected *CYP19* copy number and the results from the comparative  $C_T$  method was the lowest overall ( $r^2 = 0.608$ ,  $p = 0.001$ ).

**Table 1.2** Diverse gene expression quantification methods and aromatase enzyme activities in individual male *X. laevis*.

Replicate	$C_T$ ratio <sup>a</sup>	$2^{-\Delta\Delta CT}$ <sup>b</sup>	ER <sup>c</sup>	<i>CYP19</i> copy <sup>d</sup>	Aromatase activity (fmol/h/mg protein)
1	1.260	0.443	0.014	9.961	3.095
2	1.293	0.267	0.008	6.301	5.063
3	1.259	0.442	0.014	9.436	2.760
4	1.194	1.057	0.034	9.184	4.886
5	1.207	1.045	0.031	24.781	9.454
6	1.211	1.000	0.030	24.669	3.210
7	1.260	0.421	0.013	7.565	1.779
8	1.200	1.214	0.036	34.603	21.144
9	1.195	1.437	0.041	63.769	13.057
10	1.313	0.182	0.006	3.497	11.907
11	1.164	1.950	0.059	30.842	8.621
12	1.168	1.807	0.055	27.991	19.842
13	1.255	0.526	0.016	16.070	15.669
14	1.171	2.042	0.058	84.733	9.362

a;  $C_T$  value of *CYP19* /  $C_T$  value of *GAPDH*

b; comparative  $C_T$  method

c; expression ratio calculated using standard curve method

d; number of mRNA copies (standard curve method)

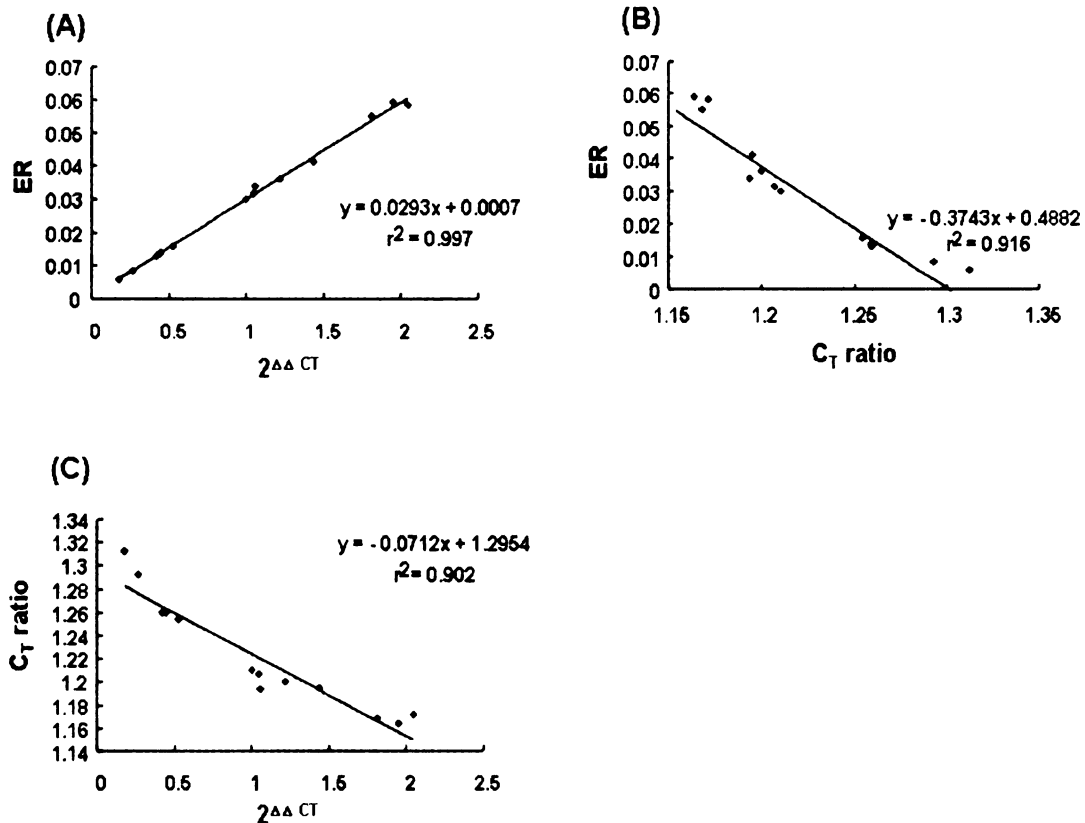


Figure 1.3 Comparisons among quantification methods for measuring *CYP19* mRNA expression used in the Q-RT PCR system. ER and  $2^{\Delta\Delta CT}$  were calculated from standard curve method and comparative  $C_T$  method, respectively.  $C_T$  ratio represents the ratio of  $C_T$  value of *CYP19* to  $C_T$  value of *GAPDH*. (A) Represents comparison of *CYP19* gene expression from standard curve method to that from comparative  $C_T$  method. (B) Represents comparison of *CYP19* gene expression from standard curve method to that from  $C_T$  ratio of *CYP19/GAPDH*. (C) Represents comparison of *CYP19* gene expression from  $C_T$  ratio of *CYP19/GAPDH* to that from comparative  $C_T$  method.

#### *Comparison of CYP19 gene expression and aromatase activity*

Aromatase activity was measurable in all frog testes analyzed with activities ranging from 1.78 to 21.14 fmol/h/mg protein. Variability among individuals was relatively great with a CV of 69%. This variability was similar to those observed for changes in gene expression: 63% for the standard curve method and 64% for the comparative  $C_T$  method.

However, when comparing aromatase enzyme activities with *CYP19* gene expression determined by either the comparative  $C_T$  method or the standard curve method in the same frogs, no significant correlations could be observed ( $r = 0.404$ ,  $p = 0.152$ ;  $r = 0.399$ ,  $p = 0.158$ , respectively) (Table 1.3).

Table 1.3 Pearson correlation coefficients ( $r$ ) and probabilities ( $p$ ) between the different parameters measured.

	<i>CYP19</i> copy	ER	$2^{-\Delta\Delta CT}$	$C_T$ ratio	Aromatase activity
<i>CYP19</i> copy	1				
ER	<b>0.743</b> (0.002)	1			
$2^{-\Delta\Delta CT}$	<b>0.780</b> (0.001)	<b>0.998</b> (<0.000)	1		
$C_T$ ratio	<b>-0.669</b> (0.009)	<b>-0.957</b> (<0.000)	<b>-0.950</b> (<0.000)	1	
Aromatase activity	0.339 (0.236)	0.399 (0.158)	0.404 (0.152)	-0.334 (0.243)	1

Bold numbers indicate significant correlation. Negative numbers indicated negative relationships.

Refer to Table 1.2 for explanations

#### *Gonadal CYP19 gene expression after exposure to forskolin*

Exposure of gonadal tissues to forskolin resulted in an increase of *CYP19* gene expression in both ovarian and testicular explants (Fig. 1.4). The greatest induction was observed in ovarian tissue with a 3.74-fold induction of *CYP19* gene expression compared to the solvent controls. In testicular tissue, *CYP19* mRNA copy numbers were increased 2.62-fold. The above results were achieved using the standard curve method. However, similar patterns were observed when applying other quantification methods such as  $C_T$  ratio method (data not shown).

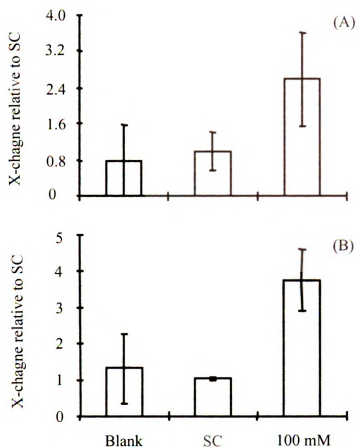


Figure 1.4 Fold-change (x-change, mean  $\pm$  S.D.) of *CYP19* mRNA in testicular (A) and ovarian (B) explants of *Xenopus laevis* after exposure to 100  $\mu$ M forskolin (100  $\mu$ M) for 20h, using the standard curve method for quantification of mRNA. SC = solvent control (0.1% DMSO).

## Discussion

### *Development and optimization of Q-RT PCR system to quantify CYP19 gene expression in male X. laevis*

The conditions of SYBR Green-Q-RT PCR analysis for detecting *CYP19* mRNA in testes from male *X. laevis* were established and optimized. The two-step Q-RT PCR method was selected over the one-step method due to its higher sensitivity, lesser risk of primer-

dimer formation during PCR reaction and lesser risk of contamination with genomic DNA (Vandesompele et al., 2002). It was possible to detect small quantities of *CYP19* mRNA (as few as 10 copies/reaction) in gonadal tissue (< 100mg) without prior cDNA amplification or a nested PCR approach, which requires a secondary amplification of the target gene using the PCR product from an initial gene amplification to improve sensitivity and specificity.

SYBR Green was chosen for the detection of amplicons during the PCR reaction because it is relatively inexpensive while its sensitivity, reproducibility and dynamic range were comparable to that of the fluorescent probe method (Lekanne Deprez et al., 2002). The melting curve analyses revealed that the obtained signal for both *CYP19* and housekeeping gene were specific, and did not result in the amplification of unwanted gene products. No primer–dimers were formed. The SYBR Green dye detection system proved to be highly sensitive with a method detection limit of as few as 10 copies of the target gene per reaction. The routine treatment of RNA samples with DNase I minimized co-amplification of pseudo-genes, which are genetically similar to the original gene but are not expressed, or non-specific DNA which the primer may have found (Kreuzer et al., 1999).

Quantitative analysis of gene expression is often achieved by normalization to the amplification of housekeeping genes as internal controls. Ideally, the internal control gene should be expressed at a constant level among different cell populations and individuals and should be unaffected by experimental conditions (Thellin et al., 1999). *GAPDH* is a gene that has these characteristics, which make it a useful and effective housekeeping gene to control for these types of variations (Wiechmann and Smith, 2001).

The use of the *GAPDH* as an internal control provides more accurate results since it not only compensates for sample-to-sample variations but also circumvents technical problems such as total RNA extraction efficiency and reverse transcription efficiency. However, there are studies that suggested that, in some cases, *GAPDH* might not be appropriate as an internal control for every RT PCR system. Some mammalian species showed unstable gene expression of *GAPDH* during the cell cycle (Mansur et al., 1993) and during different developmental stages (Calvo et al., 1997). A different study with humans found that *GAPDH* mRNA transcription levels can also vary widely among individuals (Bustin et al., 1999). In contrast, in our study, little variation in the expression of *GAPDH* was observed among individuals. This observation indicates that *GAPDH* is a suitable housekeeping gene for determining changes in *CYP19* expression in testes of *X. laevis* that are of similar developmental stage. However, this study was not designed to address effects of different developmental stages on the expression of *GAPDH* and, therefore, when conducting a developmental study the appropriateness of the *GAPDH* as a housekeeping gene would need to be further validated.

In order to obtain accurate and reproducible results, the PCR reaction should have efficiency as close to 100% as possible. At this efficiency, the template doubles after each cycle. Efficiencies of the PCR reactions were very close to the desired efficiency of 100% for both *CYP19* and *GAPDH*, indicating that the increase in gene expression is directly proportional to the number amplification cycles. Furthermore, the small interassay variabilities among experiments conducted on 3 different days and the low CVs for the calculated  $C_T$  values for all experiments demonstrate the reproducibility and precision of the established test system.



In conclusion, the Q-RT PCR method developed to quantify *CYP19* gene expression in male *X. laevis* in this study is sufficiently sensitive to allow the measurement of single digit copies of total RNA. This sensitive and precise assay is a useful tool that allows for quantifying specific types of mRNA that are expressed at low levels in certain tissues such as *CYP19* in testes of male frogs and that allows for direct comparison of gene expression levels between samples.

#### *Comparison of different gene quantification methods*

In this study, four quantification methods were applied to quantify *CYP19* gene expression and were then compared to identify the optimal method for quantification. In the first method, *CYP19* mRNA copy numbers were calculated from the absolute standard curve obtained by serial 10-fold dilutions of a cloned plasmid standard without referring to the housekeeping gene. This method allowed estimation of the number of copies of *CYP19* mRNA present in the unknown samples. However, estimates of copy numbers of *CYP19* mRNA calculated from the linear equation derived from the absolute standard curve method did not appear to give an accurate estimate of the actual expression of *CYP19* mRNA molecules present in the sample. The inaccuracy of the estimate was indicated by the low correlation of these copy numbers with the housekeeping gene-corrected copy numbers or the calculated ratio from the comparative  $C_T$  method. This correlation was improved once the copy numbers were normalized to the internal control (expressed as ER). This demonstrates that the use of an internal control such as *GAPDH* is critical to accurately quantify *CYP19* gene expression profile in male *X. laevis* when using Q-RT PCR. The significant correlations among all three

quantification methods using *GAPDH* as the housekeeping gene demonstrate the applicability of all of these methods to quantify *CYP19* gene expression in *X. laevis* testes. However, compared to the very strong relationship between the standard curve and the comparative  $C_T$  method ( $r^2 = 0.997$ ,  $p < 0.001$ ), the  $C_T$  value ratio was less predictive for the standard curve method ( $r^2 = 0.916$ ,  $p < 0.001$ ) or the comparative  $C_T$  method ( $r^2 = 0.902$ ,  $p < 0.001$ ). Thus, we conclude that both the comparative  $C_T$  method and the standard curve method are optimal quantification methods to estimate low levels of *CYP19* gene expression in testicular tissue of *X. laevis*. There have been few studies using Q-RT PCR to measure aromatase mRNA expression in male African clawed frogs (Miyashita et al., 2000; Kuntz et al., 2004). These studies reported gene expression of *CYP19* without normalization (Miyashita et al., 2000), or simply by the ratio of *CYP19/Sf* *l* (Kuntz et al., 2004) and, to date, and to the best of our knowledge, no study has been conducted to measure *CYP19* mRNA level in male *X. laevis* using more accurate RT PCR quantification methods. The results from our study confirm that the simple ratio between housekeeping and *CYP19* gene is not as accurate and sensitive as more sophisticated methods such as the standard curve or comparative  $C_T$  method.

The advantage of the comparative  $C_T$  method over the absolute standard curve method is that this method eliminates the need to construct a standard curve, which is a time consuming and laborious process, allowing simple quantification of the relative gene expression of paired samples. Therefore, use of the economical and efficient comparative  $C_T$  method is recommended as the preferable method to quantify *CYP19* gene expression in testicular tissue of *X. laevis*.

### *Comparison of CYP19 gene expression with aromatase enzyme activity*

While mRNA quantification of *CYP19* provides important information on the regulation of protein synthesis, it may not directly reflect aromatase enzyme activity due to posttranscriptional control of enzyme activity. An earlier study reported that differences in *CYP19* gene expression between males and females were not proportional to aromatase enzyme activity in another amphibian species, the newt, *Pleurodeles waltl* (Kuntz et al., 2004). These authors hypothesized that this lack in correlation might be due to differences in the posttranscriptional regulation of aromatase. Posttranscriptional factors that can influence the net activity of the enzyme aromatase can be either due to modifications of the mRNA that lead to differential translation within a tissue or can be due to posttranslational modifications that alter the stability of functionality of the protein (Balthazart, et al., 2001; Genissel, et al., 2001).

Even though there is evidence that estrogens, which are catalyzed by aromatase, play a stimulatory role in germ cell development including spermatogonial division, germ cell viability and differentiation, acrosome biogenesis and function of the spermatozoa in rodents (O'Donnell et al., 2001), at present little is known of aromatase expression and the role of estrogens in the testis of amphibians. It appears that estrogens are involved in multiple actions of male reproductive system of amphibians during certain developmental stages (Fasano et al., 1989; Cobellis et al., 2002). The fact that aromatase enzyme activities in our study were very low and not correlated with *CYP19* gene expression indicates that this enzyme may have been dormant or at basal levels in non-active breeding conditions of frogs applied in this research. However, the confirmation experiments using an inducer of aromatase, forskolin, have demonstrated that *CYP19*

gene expression can be modulated (increased) both in ovarian and testicular tissue of *Xenopus*, indicating that stimulation of the enzyme results in a specific response at the gene expression level. This result indicates that the established Q-RT PCR system represents a valid method to determine alterations in the expression of *CYP19* in male testis.

#### *Implications for toxicological assessment of environmental pollutants*

Aromatase regulation and activity play a pivotal role in sexual development and in communicating reproductive processes in vertebrates. While in ovarian tissues the formation of estrogens from androgens via the enzyme aromatase is an essential process for gonadal maturation in males both expression and activity of aromatase are low in the testis during the maturation phase, which mainly depends on androgens. Accurate transcriptional regulation of the genes encoding steroidogenic enzymes such as aromatase is critical for the regulation of sex steroid homeostasis that is essential for ordinary sexual development processes in animals (Yamada et al., 1995). Thus, improper and untimely changes in *CYP19* gene expression may affect reproductive success in animals (Trant et al., 2001; Kuntz et al., 2003b). Therefore, the quantitative analysis of *CYP19* mRNA expression can be an important marker for detection of developmental and reproductive disruption by EDCs in animals of both sexes. In fact, a series of chemicals have been reported to have the potential to directly or indirectly disturb steroidogenesis simply by interfering with the regulation of *CYP19* gene expression either *in vivo* or *in vitro* (Connor et al., 1996; Sanderson et al., 2000; Miyata and Kubo, 2000; Kazeto et al., 2004). In the recent controversy about possible effects of pesticides and/or other environmental

contaminants on reproduction and development in amphibian species, it was hypothesized that abnormal sexual development such as compromised reproductive functions and/or characteristics may be due to the induction of aromatase by these chemicals causing a decrease of endogenous androgens in males (Hayes et al., 2002). However, although a series of studies has been conducted to identify effects of the exposure to triazine herbicides on aromatase activity or *CYP19* gene expression in fish or amphibians (Hayes et al., 2002; Kazeto et al., 2004; Lavado et al., 2004; Hecker et al., 2004), it has proved to be difficult to establish a direct link between exposure to these chemicals and changes in gonadal aromatase. As outlined previously, this is likely due to the fact that aromatase enzyme activities are low in adult testicular tissue, often being below or just above the method detection limits of enzymatic assays. The Q-RT PCR technique established in this study represents a method that can help to overcome this difficulty as it is capable of identifying very small amounts of *CYP19* mRNA and has been successfully used to determine gene expression in the testis of *X. laevis*.

In conclusion, the Q-RT PCR system established and optimized in this study represents a highly sensitive, rapid and reliable method to detect and measure very small quantities of *CYP19* mRNA in small amounts of tissue. Although *CYP19* mRNA expression does not seem to directly reflect aromatase enzyme activity in testicular tissue, the developed Q-RT PCR method is a powerful tool due to determine changes in the regulation of protein synthesis of aromatase that will be helpful in researching general regulatory mechanisms in the reproductive endocrinology of *X. laevis*. Furthermore, this method can be used as a highly sensitive marker in toxicological studies to identify effects of environmental contaminants at the pretranslational level of aromatase.

Currently, a parallel study is underway that uses this Q-RT PCR method to determine the effects of atrazine on testicular aromatase in *X. laevis*.

### **Acknowledgement**

We thank A. Hosmer for many helpful comments on experimental design. We also thank C. Bens, R. Bruce and S. Williamson. This research was facilitated by the Atrazine Endocrine Ecological Risk Assessment Panel, Ecorisk, Inc., Ferndale, WA and sponsored by Syngenta Crop Protection, Inc.

## References

- Akatsuka, N., Kobayashi, H., Watanabe, E., Iino, T., Miyashita, K., Miyata, S., 2004. Analysis of genes related to expression of aromatase and estradiol regulated genes during sex differentiation in *Xenopus* embryos. *Gen. Comp. Endocrinol.* 136, 382–388.
- Balthazart, J., Baillien, M., Ball, G.F., 2001. Phosphorylation processes mediate rapid changes of brain aromatase activity. *J. Steroid Biochem. Mol. Biol.* 79, 261–277.
- Bej, A.K., Mahbubani, M.H., Atlas, R.M., 1991. Amplification of nucleic acids by polymerase chain reaction (PCR) and other methods and their applications. *Crit. Rev. Biochem. Mol. Biol.* 26, 301–334.
- Bradford, M., 1976. A rapid and sensitive method for quantitation of microgram quantities of protein utilizing the principle of protein-dye binding. *Anal. Biochem.* 72, 248–254.
- Bustin, S.A., 2000. Absolute quantification of mRNA using real-time reverse transcription polymerase chain reaction assays. *J. Mol. Endocrinol.* 25, 169–193.
- Bustin, S.A., 2002. Quantification of mRNA using real-time reverse transcription PCR (RT-PCR): trends and problems. *J. Mol. Endocrinol.* 29.
- Bustin, S.A., Gyselman, V.G., Williams, N.S., Dorudi, S., 1999. Detection of cytokeratins 19/20 and guanylyl cyclase C in peripheral blood of colorectal cancer patients. *Br. J. Cancer* 79, 1813–1820.
- Calvo, E.L., Boucher, C., Coulombe, Z., Morisset, J., 1997. Pancreatic GAPDH gene expression during ontogeny and acute pancreatitis induced by caerulein. *Biochem. Biophys. Res. Commun.* 235, 636–640.
- Cobellis, G., Meccariello, R., Fienga, G., Pierantoni, R., Fasano, S., 2002. Cytoplasmic and nuclear Fos protein forms regulate resumption of spermatogenesis in the frog, *Rana esculenta*. *Endocrinology* 143, 163–170.

- Connor, K., Howell, J., Chen, I., Liu, H., Berhane, K., Sciarretta, C., Safe, S., Zacharewski, T., 1996. Failure of chloro-S-triazine-derived compounds to induce estrogen receptor-mediated responses in vivo and in vitro. *Fundam. Appl. Toxicol.* 30, 93–101.
- Fasano, S., Minnucci, S., DiMatteo, L., D'Antonio, M., Pierantonio, R., 1989. Intraatesticular feedback mechanisms in the regulation of steroid profiles in the frog, *Rana esculenta*. *Gen. Comp. Endocrinol.* 75, 335–342.
- Forlano, P.M., Bass, A.H., 2004. Seasonal plasticity of brain aromatase mRNA expression in Gila: divergence across sex and vocal phenotype. *J. Neurobiol.* 65, 37–49.
- Genissel, C., Levallet, J., Carreau, S., 2001. Regulation of cytochrome P450 aromatase gene expression in adult rat Leydig cells: comparison with estradiol production. *J. Endocrinol.* 168, 95–105.
- Girault, I., Lerebours, F., Tozlu, S., Spyrtos, F., Tubiana-Hulin, M., Lidereau, R., Bieche, I., 2002. Real-time reverse transcription PCR assay of *CYP19* expression: application to a well-defined series of post-menopausal breast carcinomas. *J. Steroid Biochem. Mol. Biol.* 82, 323–332.
- Hayes, T.B., Collins, A., Lee, M., Mendoza, M., Noriega, N., Stuart, A.A., Vonk, A., 2002. Hermaphroditic, demasculinized frogs after exposure to the herbicide atrazine at low ecologically relevant doses. *Proc. Natl. Acad. Sci. U. S. A.* 99, 5476–5480.
- Hecker, M., Giesy, J.P., Jones, P.D., Jooste, A.M., Carr, J.A., Solomon, K.R., Smith, E.E., Van der Kraak, G., Kendall, R.J., Du Preez, L., 2004. Plasma sex steroid concentrations and gonadal aromatase activities in African clawed frogs (*Xenopus laevis*) from South Africa. *Environ. Toxicol. Chem.* 23, 1996–2007.
- Kato, T., Matsui, K., Takase, M., Kobayashi, M., Nakamura, M., 2004. Expression of P450 aromatase protein in developing and in sex-reversed gonads of the XX/XY type of the frog *Rana rugosa*. *Gen. Comp. Endocrinol.* 137, 227–236.



- Kazeto, Y., Place, A.R., Trant, J.M., 2004. Effects of endocrine disrupting chemicals on the expression of *CYP19* genes in zebrafish (*Danio rerio*) juveniles. *Aquat. Toxicol.* 69, 25–34.
- Kreuzer, K.A., Lass, U., Landt, O., Nitsche, A., Laser, J., Ellerbrok, H., Pauli, G., Huhn, D., Schmidt, C.A., 1999. Highly sensitive and specific fluorescence reverse transcription–PCR assay for the pseudogene-free detection of beta-actin transcripts as quantitative reference. *Clin. Chem.* 45, 297–300.
- Kuntz, S., Chardard, D., Chesnel, A., Grillier-Vuissoz, I., Flament, S., 2003a. Steroids, aromatase and sex differentiation of the newt *Pleurodeles waltl*. *Cytogenet. Genome Res.* 101, 283–288.
- Kuntz, S., Chesnel, A., Duterque-Coquillaud, M., Grillier-Vuissoz, I., Callier, M., Dournon, C., Flament, S., Chardard, D., 2003b. Differential expression of P450 aromatase during gonadal sex differentiation and sex reversal of the newt *Pleurodeles waltl*. *J. Steroid Biochem. Mol. Biol.* 84, 89–100.
- Kuntz, S., Chardard, D., Chesnel, A., Ducatez, M., Callier, M., Flament, S., 2004. Expression of aromatase and steroidogenic factor 1 in the lung of the urodele amphibian *Pleurodeles waltl*. *Endocrinology* 145, 3111–3114.
- Lavado, R., Thibaut, R., Raldua, D., Martin, R., Porte, C., 2004. First evidence of endocrine disruption in feral carp from the Ebro River. *Toxicol. Appl. Pharmacol.* 196, 247–257.
- Lekanne Deprez, R.H., Fijnvandraat, A.C., Ruijter, J.M., Moorman, A.F., 2002. Sensitivity and accuracy of quantitative real-time polymerase chain reaction using SYBR green I depends on cDNA synthesis conditions. *Anal. Biochem.* 307, 63–69.
- Lephart, E.D., Simpson, E.R., 1991. Assay of aromatase-activity. *Methods Enzymol.* 206, 477–483.
- Linz, U., Delling, U., Rubsamenwaigmann, H., 1990. Systematic studies on parameters influencing the performance of the polymerase chain-reaction. *J. Clin. Chem. Clin. Biochem.* 28, 5–13.

- Liu, X., Liang, B., Zhang, S., 2004. Sequence and expression of cytochrome P450 aromatase and FTZ-F1 genes in the protandrous black porgy (*Acanthopagrus schlegeli*). *Gen. Comp. Endocrinol.* 138, 247–254.
- Mansur, N.R., Meyer-Siegler, K., Wurzer, J.C., Sirover, M.A., 1993. Cell cycle regulation of the glyceraldehyde-3-phosphate dehydrogenase/uracil DNA glycosylase gene in normal human cells. *Nucleic Acids Res.* 21, 993–998.
- Miyashita, K., Shimizu, N., Osanai, S., Miyata, S., 2000. Sequence analysis and expression of the P450 aromatase and estrogen receptor genes in the *Xenopus* ovary. *J. Steroid Biochem. Mol. Biol.* 75, 101–107.
- Miyata, S., Kubo, T., 2000. In vitro effects of estradiol and aromatase inhibitor treatment on sex differentiation in *Xenopus laevis* gonads. *Gen. Comp. Endocrinol.* 119, 105–110.
- O'Donnell, L., Robertson, K.M., Jones, M.E., Simpson, E.R., 2001. Estrogen and spermatogenesis. *Endocr. Rev.* 22, 289–318.
- Raaijmakers, M.H., van Emst, L., de Witte, T., Mensink, E., Raymakers, R.A., 2002. Quantitative assessment of gene expression in highly purified hematopoietic cells using real-time reverse transcriptase polymerase chain reaction. *Exp. Hematol.* 30, 481–487.
- Roberge, M., Hakk, H., Larsen, G., 2004. Atrazine is a competitive inhibitor of phosphodiesterase but does not affect the estrogen receptor. *Toxicol. Lett.* 154, 61–68.
- Rotchell, J.M., Ostrander, G.K., 2003. Molecular markers of endocrine disruption in aquatic organisms. *J. Toxicol. Environ. Health, Part B Crit. Rev.* 6, 453–495.
- Sakata, N., Tamori, Y., Wakahara, M., 2005. P450 aromatase expression in the temperature-sensitive sexual differentiation of salamander (*Hynobius retardatus*) gonads. *Int. J. Dev. Biol.* 49, 417–425.

- Sanderson, J.T., Seinen, W., Giesy, J.P., van den Berg, M., 2000. 2-Chloro-Striazine herbicides induce aromatase (CYP19) activity in H295R human adrenocortical carcinoma cells: a novel mechanism for estrogenicity? *Toxicol. Sci.* 54, 121–127.
- Sanderson, J.T., Boerma, J., Lansbergen, G.W.A., van den Berg, M., 2002. Induction and inhibition of aromatase (CYP19) activity by various classes of pesticides in H295R human adrenocortical carcinoma cells. *Toxicol. Appl. Pharmacol.* 182, 44–54.
- Simpson, E.R., Mahendroo, M.S., Means, G.D., Kilgore, M.W., Hinshelwood, M.M., Grahamlarence, S., Amarneh, B., Ito, Y.J., Fisher, C.R., Michael, M. D., Mendelson, C.R., Bulun, S.E., 1994. Aromatase cytochrome-P450, the enzyme responsible for estrogen biosynthesis. *Endocr. Rev.* 15, 342–355.
- Thellin, O., Zorzi, W., Lakaye, B., De Borman, B., Coumans, B., Hennen, G., Grisar, T., Igout, A., Heinen, E., 1999. Housekeeping genes as internal standards: use and limits. *J. Biotechnol.* 75, 291–295.
- Thompson, E.A., Siiteri, P.K., 1974. Involvement of human placental microsomal cytochrome-P-450 in aromatization. *J. Biol. Chem.* 249, 5373–5378.
- Trant, J.M., Gavasso, S., Ackers, J., Chung, B.C., Place, A.R., 2001. Developmental expression of cytochrome P450 aromatase genes (CYP19a and CYP19b) in zebrafish fry (*Danio rerio*). *J. Exp. Zool.* 290, 475–483.
- Vandesompele, J., De, P.A., Speleman, F., 2002. Elimination of primer–dimer artifacts and genomic coamplification using a two-step SYBR green I realtime RT-PCR. *Anal. Biochem.* 303, 95–98.
- Watanabe, M., Nakjin, S., 2004. Forskolin up-regulates aromatase (CYP19) activity and gene transcripts in the human adrenocortical carcinoma cell line H295R. *J. Endocrinol.* 180, 125–133.
- Wiechmann, A.F., Smith, A.R., 2001. Melatonin receptor RNA is expressed in photoreceptors and displays a diurnal rhythm in *Xenopus retina*. *Brain Res. Mol. Brain Res.* 91, 104–111.

Yamada, K., Harada, N., Honda, S., Takagi, Y., 1995. Regulation of placenta specific expression of the aromatase cytochrome-P-450 gene-involvement of the trophoblast-specific element-binding protein. *J. Biol. Chem.* 270, 25064–25069.

## CHAPTER 2

Fluorescence *in situ* hybridization techniques (FISH) to detect changes in *CYP19a* gene expression of Japanese medaka (*Oryzias latipes*)

### Abstract

The aim of this study was to develop a sensitive *in situ* hybridization methodology using fluorescence labeled riboprobes (FISH) that allows for the evaluation of gene expression profiles simultaneously in multiple target tissues of whole fish sections of Japanese medaka (*Oryzias latipes*). To date FISH methods have been limited in their application due to auto-fluorescence of tissues, fixatives or other components of the hybridization procedure. An optimized FISH method, based on confocal fluorescence microscopy was developed to reduce the auto-fluorescence signal. Because of its tissue- and gender-specific expression and relevance in studies of endocrine disruption, gonadal aromatase (*CYP19a*) was used as a model gene. The *in situ* hybridization (ISH) system was validated in a test exposure with the aromatase inhibitor fadrozole. The optimized FISH method revealed tissue specific expression of the *CYP19a* gene. Furthermore, the assay could differentiate the abundance of *CYP19a* mRNA among cell types. Expression of *CYP19a* was primarily associated with early stage oocytes, and expression gradually decreased with increasing maturation. No expression of *CYP19a* mRNA was observed in other tissues such as brain, liver, or testes. Fadrozole (100 µg/L) caused up-regulation of *CYP19a* expression, a trend that was confirmed by RT-PCR analysis. In a combination approach with gonad histology, it could be shown that the increase in *CYP19a* expression

as measured by RT-PCR on a whole tissue basis was due to a combination of both increases in numbers of *CYP19a*-containing cells and an increase in the amount of *CYP19a* mRNA present in the cells.

## **Introduction**

In recent years, an increasing number of genomic and/or proteomic techniques have been developed to identify mechanisms of toxic action in organisms exposed to environmental contaminants. Most of the methods that were developed to meet these objectives such as RT-PCR, Northern blotting, and RNase protection assays rely on high yields of RNA extracted from whole tissues. However, the limitations of these techniques are that they often fail to detect gene expression of low-abundance mRNA in small tissues, or they do not allow localizing changes within certain tissues or cell types. Some genes are only expressed in certain tissues, while others are expressed in specific tissues at only certain times of development (Sanderson et al., 2001). Especially when using small laboratory animal model species, the limited amount of individual tissues available for study and the difficulty in excising them from the organisms has limited the efficacy of these techniques to determine effects during critical windows of time during ontogenesis.

Many of the efforts in endocrine disruptor research have focused on individual endpoints such as receptor-mediated effects (Otsuka, 2002). However, such targeted screening methods may not be sufficient when disruptions are induced through indirect mechanisms. Some chemicals can act as direct agonists or antagonists to certain receptors while others act indirectly by modulating signal transduction, or affecting gene expression or substrate concentrations. For example, the triazine herbicide atrazine does

not bind to the estrogen receptor (ER), but *in vitro* in a mammalian cell system, atrazine has been found to up-regulate the expression of aromatase (CYP19), the enzyme that transforms testosterone to estradiol. Although atrazine does not act like a typical estrogen via binding the ER, in mammalian cell systems it can, under some situations, at relatively great concentrations result in estrogenic effects by increasing endogenous estradiol production (Sanderson et al., 2000). As a result, it is not only important to develop methodologies that allow for evaluation of chemical-induced effects in multiple target tissues simultaneously, but also to determine subtle effects on multiple endpoints simultaneously within these tissues.

Whole-animal *in situ* hybridization (ISH) is a promising method for determining spatial changes in gene expression (Tompsett et al., 2008; Zhang et al., 2008a and b). This methodology allows determination of effects on expression of multiple genes in multiple tissues simultaneously, and it can be used simultaneously with standard histology (Peterson and McCrone, 1993; Lichter, 1997; Hrabovszky et al., 2004; Jezzini et al., 2005; Ijiri et al., 2006). One of the major advantages of ISH is that it allows detection of changes in expression of mRNA for specific genes in organs, tissues, and/or cells of interest in a manner that is consistent with other methods that are used to detect lesions, including histopathology and immuno-histochemistry (IHC) (Streit and Stern, 2001). The principle underlying ISH is the hybridization of specifically-labeled probes to the complimentary mRNA sequences in tissue or cells. A number of different visualization techniques can be applied to detect an ISH signal including radionucleotides, enzyme linked systems (e.g. biotin, digoxigenin), and fluorophores. Each label type has strengths and weaknesses depending on application. Radiolabelled probes have been

widely used to detect specific mRNA sequence in tissues or embryos since the detection of mRNA in invertebrates and vertebrates was originally developed using the radiolabelled probe systems (Simeone, 1999). ISH utilizing radiolabelled probes have been found to be more sensitive and reliable than some other methods such as enzyme linked or fluorophore-based systems. However, radioisotope-based techniques have a number of disadvantages such as a relatively poor resolution, relatively long exposure times for auto-radiographic visualization, and they are expensive and require special certifications in many institutions and extra precautions in the laboratory (Braissant and Wahli, 1998; Simeone, 1999; Pernthaler and Amann, 2004; Tompsett et al., 2008). In contrast, enzymatic detection systems such as digoxigenin are very sensitive but tend to be variable. More recently, the application of fluorescent labeling techniques has considerably improved ISH due to the advantage of using different fluorescent tags to simultaneously detect different gene sequences (Wilkinson, 1999). However, application of fluorescent *in situ* hybridization (FISH) methods to detect specific mRNA in tissue sections has not been explored to the same extent as radioisotope or enzyme based methods due to issues with sensitivity and/or auto-fluorescence of tissues (Dirks, 1990; Wilkinson, 1999; Andreeff and Pinkel, 1999). Recent improvements in fluorescence labeling techniques render FISH techniques an increasingly useful tool. To effectively utilize FISH, however, a number of technical limitations needed to be overcome. Key issues include probe penetration of sections, auto-fluorescence of tissues, non-specific binding of probe, type of target tissues and species, and sample preparation (Wilkinson, 1999). Hence, there was need for the development and optimization of FISH methods to overcome these issues.



The main objective of this study was to develop and optimize an ISH protocol that uses fluorophore-labeled probes to detect specific mRNA sequences in whole animal sections of Japanese medaka (*Oryzias latipes*). Specific goals of this study were: (1) develop and optimize methods to design fluorescent riboprobes for use in ISH; (2) develop and optimize methods to reduce auto- and background fluorescence in fish tissue sections by using a combination of chemical treatment and advanced confocal microscopy techniques; (3) validate the FISH methods developed in this study using Q RT PCR; and (4) use the optimized FISH methods to examine changes in gonadal *CYP19a* gene expression in Japanese medaka exposed to a competitive pharmaceutical inhibitor of the aromatase enzyme, fadrozole. The physiology, embryology, and genetics of the Japanese medaka have been extensively studied in the past, and more recently, this species has been used as a model in endocrine disrupter research (Wittbrodt et al., 2002). The Japanese medaka has clearly defined sex chromosomes and sex determination (summarized in Wittbrodt et al., 2002). Cytochrome P450 aromatase, encoded by the *CYP19* gene, is the key enzyme in estrogen biosynthesis from androgens (Simpson et al., 1994), and it has been extensively used as an endpoint to assess the exposure of endocrine disrupting compounds (EDCs) due to its relation with reproductive processes (Sanderson et al., 2000; Hayes et al., 2002; Rotchell and Ostrander, 2003; Hecker et al., 2006). Fadrozole has been reported to affect *CYP19a* gene expression (Villeneuve et al., 2006) but was also shown to result in series of other physiological effects in fish including plasma estradiol concentrations, gonadal pathologies, and fecundity (Afonso et al., 1999; Ankley et al., 2002; Fenske and Segner, 2004).

## **Materials and Methods**

### *Test chemical*

The fadrozole (CGS016949A; MW: 259.74g) used in this research was provided by Novartis Pharma AG (Basel, CH).

### *Culture of Japanese medaka*

Japanese medaka were obtained from the aquatic culture at the US EPA Mid-Continent Ecology Division (Duluth, MN, USA). Medaka were held in flow through systems under conditions facilitating breeding (23-24 °C, 16:8 light/dark). All procedures used during all phases of this study were in accordance with protocols approved by the Michigan State University Instituted Animal Care and Use Committee (IACUC).

### *Fadrozole exposure*

Prior to initiation of exposure experiments, 12-14 wk old medaka were placed into 10 L tanks with 6 L of carbon filtered tap water and acclimated for 12 d under the same conditions as in the subsequent exposure of fadrozole. One fish died during acclimation. Each treatment group consisted of replicate tanks, and each tank contained 5 male and 5 female fish. After the acclimation period, fish were exposed to 1, 10, or 100 µg fadrozole /L or carbon filtered tap water as a control in a 7 d static renewal exposure. Every day one half of the water in each tank (3 L) was replaced with fresh carbon filtered water dosed with the appropriate amount of an aqueous fadrozole stock (5 mg/L). Fish were fed Aquatox flake food (Aquatic Ecosystems, Apopka, FL, USA) *ad libidum* once daily and held at 24 °C with a 16:8 light/dark cycle. Water quality parameters were measured

daily and values were within a normal range for water quality, as follows in all tanks: temperature (24 °C), pH (7.89-8.13), ammonia nitrogen (<0.02-0.04 mg/L), nitrate nitrogen (<0.02-0.3 mg/L), dissolved oxygen (4.3-6.9 mg/L), and hardness (370-480 mg CaCO<sub>3</sub>/L).

After 7 d of exposure medaka were euthanized in Tricaine S (50 mg/mL) (Western Chemical, Ferndale, WA, USA). Weight and snout length were recorded. Fish were separated into two groups, one group was for ISH and consisted of 2 fish per sex per tank, and a second group that was to be used for Q RT PCR procedures and included three fish per sex and treatment group. Fish from the ISH group were fixed for ISH and histological investigations as described below. For the Q RT PCR group, the brain, liver, and gonads were dissected from the fish and weighted individually. The liver somatic index (LSI) and gonadal somatic index (GSI) were calculated as follows (Equations 1 and 2):

$$LSI = (\text{liver weight/body weight}) * 100 \quad (1)$$

$$GSI = (\text{gonad weight/body weight}) * 100 \quad (2)$$

The organs were then placed into cryovials and stored in liquid nitrogen for later RNA extraction.

### *ISH procedure*

#### Preparation of sections

For ISH, fish were processed using methods adapted from Kong et al. (2008). Briefly, fish were gross dissected to remove fins, tail, skull roof, otoliths, and opercula. The body cavity was opened to improve the penetration of fixative (80% Histochoice MB (EMS,

Hatfield, PA, USA), 2% paraformaldehyde, and 0.05% glutaraldehyde) for better internal organ fixation. Fish were then immersed in individual vials containing the fixative, and allowed to fix overnight at room temperature. After approximately 22 h, fish samples were removed from the fixative, and were washed with 70% methanol and dehydrated through a graded methanol series (80%, 95%, and 100%), and then cleared in chloroform at 4 °C. Fixed and cleared samples were infiltrated with melted Paraplast Plus paraffin (McCormick Scientific, St. Louis, MO, USA) at 60 °C. The paraffin was allowed to harden overnight at room temperature, and paraffin blocks were stored under RNase free conditions at 4 °C until sectioning.

Fish samples were sectioned on a rotary AO-820 microtome (American Optical, Buffalo, NY, USA) that had been cleaned and decontaminated with absolute ethanol and RNase-Zap (Sigma-Aldrich, St. Louis, MO, USA). Serial sections were cut at 7µm. The sections were floated out onto a 40 °C water bath, and placed on Superfrost Plus slides (Erie Scientific, Portsmouth, NH, USA), followed by drying at 40 °C overnight. Slides were stored in RNase-free containers at room temperature until used for ISH.

#### Fluorescence labeled riboprobe synthesis

In this study, RNA probes (riboprobes) were used for the detection of target mRNA. All sequences used to design RNA probes were obtained from the NCBI database ([www.ncbi.nlm.nih.gov](http://www.ncbi.nlm.nih.gov)). To synthesize riboprobes, reverse-transcribed first-strand cDNA was used as a template in a conventional PCR with appropriate primers to amplify PCR products (Table 2.1). The probes were designed to be approximately 500 bp long using Beacon Designer 2 software (PREMIER Biosoft Int., Palo Alto, CA, USA). Probe

length was chosen based on a review of Wilkinson (1999) that reported that either too short or too long probes may give weaker signals possibly due to either low specificity to target transcript or low penetration efficiency into tissue, respectively. The sequence of the riboprobe to detect *CYP19a* mRNA was compared with all sequences of known genes in Japanese medaka using Blast2 analysis (NCBI, Bethesda, MD, USA), and no sequence homogeneity was found except for the target gene.

The PCR products were cloned into a pGEM T-Easy vector (Promega, Madison, MI, USA) following manufacturer's direction so that it was flanked by two different RNA polymerase initiation sites (T7 and SP6). Sequence validity of cloned amplicons was confirmed by automatic DNA sequencing and followed by a BLAST2 analysis with their corresponding sequences in GenBank. In order to synthesize sense and antisense probes for *CYP19a*, cloned plasmids were digested with *SalI* and *NcoI* (Invitrogen, Carlsbad, CA, USA), respectively. Complete digestion was confirmed with electrophoresis on agarose gel (data not shown).

Sense and antisense riboprobes for *CYP19a* mRNA were synthesized using *in vitro* transcription. Briefly, the sense riboprobes were transcribed with T7 polymerase with their respective plasmids, while the antisense probes were transcribed with SP6 polymerase using manufacturer's direction (Roche, Indianapolis, IN, USA). Sizes of synthesized riboprobes were confirmed by MOPS-formaldehyde gel electrophoresis (data not shown), followed by purification using lithium chloride precipitation (Ambion, Foster City, CA, USA).

Synthesized riboprobes were labeled with ULYSIS Nucleic Acid Labeling Kits (Alexa Fluor 488, Molecular Probes, Eugene, OR, USA). After labeling, the riboprobes

were purified with a gel filtration based spin column, Micro Bio-Spin 30 Columns in RNase-Free Tris (Bio-Rad, Hercules, CA, USA) to remove excess, unincorporated fluorescent dyes. The quality of fluorescence labeled riboprobes was confirmed by MOPS-formaldehyde gel electrophoresis without ethidium bromide (data not shown). The quantity of the riboprobes was measured using a spectrophotometer (260 nm). Riboprobes were separated into aliquots and stored at -80 °C. Probes were used within few days after synthesis to minimize degradation of RNA degradation.

#### Fluorescent *in situ* hybridization

Slides on which whole histological sections of medaka had been placed were incubated at 60 °C for 1 h to allow paraffin to melt and to fuse the sections to the slide (Fig. 2.1). The slides were then de-paraffinized and rehydrated as follows; washing with (a) xylene 3 times for 3 minutes, (b) 100% ethanol 2 times for 3 min, (c) PBS for 5 minutes, and (e) diethyl pyrocarbonate (DEPC)-treated water for 1 min. In order to reduce auto-fluorescence signal originating either from the tissues or from the fixative, slides were then treated 3 times for 20 min with 10 mg/mL sodium borohydride (SB) (Sigma-Aldrich, Saint-Louis, MO, USA) in PBS (Billinton and Knight, 2001). Slides were then rinsed with PBS and DEPC treated water and the sections were permeabilized for 20 min with 0.2N HCl. To increase specificity of probes to target mRNA, slides were treated with 0.1 U/mL of RNase-free DNase I (Roche, Indianapolis, IN, USA), followed by inactivation of DNase I with DNase stop solution (10mM Tris-HCl, 150mM NaCl and 20mM EDTA). Sections were acetylated in triethanolamine-HCl buffer plus 0.25% acetic anhydride (2 times) (Sigma-Aldrich, Saint-Louis, MO, USA), and then pre-hybridized with

hybridization buffer (2X SSC, 50% deionized formamide, 1X Denhardt's solution, 0.4  $\mu\text{g/mL}$  of sonicated salmon sperm DNA, 1% SDS, 20% dextran sulfate, and DEPC-treated water to make 31.25 mL) without probes for 1 h in a humid box at 43°C to reduce non-specific binding of probes. Probes were denatured at 90 °C for 10 min and chilled on ice. Sections were hybridized with the riboprobe (2 ng/ $\mu\text{L}$ ) at 43 °C for 16 h. The negative control consisted of sections that were hybridized with equal amounts of sense probe under the same ISH conditions as described above. Following hybridization, the slides were washed in a SSC gradient (4X at room temperature (5 min), 2X at 37 °C (10 min), 2X at RT (5 min), and 0.2X at room temperature (5 min)). Following washing, slides were air dried, mounted with fluoromount G (EMS, Hatfield, PA, USA), and left in a dark chamber until the mounting medium was completely dry. Thereafter, slides were kept in the slide box to prevent photo-bleaching and photo-activation of fluorescent molecules until analysis by confocal microscopy. The optimum concentration of SB to quench auto- and background fluorescence signals was determined during preliminary studies with SB at 10 or 20 mg/mL, copper (II) sulfate at 10 or 100 mM, and a combination of SB and copper (II) sulfate.

#### Confocal laser scanning microscopy (CLSM) image analysis

Spectral distributions of fluorescence were determined with a Zeiss LSM 510 Meta confocal system (Carl Zeiss, Jena, Germany). Images were collected with a Zeiss EC Plan NEOFLUAR 10X (Carl Zeiss, Jena, Germany). Using the 458-nm line of an argon laser for excitation, 16 spectrally resolved images were recorded at 10.7  $\mu\text{m}$  intervals

from 475.5  $\mu\text{m}$  – 646.7  $\mu\text{m}$ . Sections of ovary were imaged with a pinhole aperture corresponding to an optical thickness of  $< 2.0 \mu\text{m}$ .

Several endogenous and/or fixative-induced fluorophores have broad band emission spectra that make separation from emission spectra related to riboprobe fluorophores particularly difficult. In this study, the effort focused on the separation of the individual spectral components associated with auto-fluorescence, background, and Alexa Fluor 488 dye. Auto-fluorescence and background spectral components were obtained from ovary sections (early stage oocytes) and other tissues, respectively, on slides hybridized without probe to account for these variables in the overall fluorescence associated with these sections. The specific spectrum of Alexa Fluor 488 dye was obtained directly from the dye reagent. Once the number of significant and independent sources of the specific spectral components was defined by means of CLSM, the linear spectral unmixing was applied to separate the individual components, to remove autofluorescence signal in the recorded images (Fig. 2.2) and to isolate the specific fluorescence signal of the Alexa Fluor 488 dye. With each set of ISH experiments, a section with no probe added was included to control for alterations in the autofluorescence spectral shape by photo-bleaching that can result from consecutive laser scans.

Each set of ISH slides had at least one ISH section with sense probe that served as a negative control. Images of the ovary were collected at 10X magnification. For quantification, 3 different portions were randomly selected in the ovary of each section hybridized with *CYP19a* antisense probe and then 3 early stage of oocytes in each portion were randomly selected (less than 100  $\mu\text{m}$  in diameter). Based on morphological criteria



developed by Iwamatsu et al. (1988), those oocytes are classified into the previtellogenic stage. Then we applied the above described spectral unmixing method to quantify the intensities of the true Alexa Fluor signal in these oocytes. Due to the detection of low quantities of Alexa Fluor dye in the section hybridized with sense probe, we normalized the *CYP19a* antisense signal to the *CYP19a* sense signal in each set of ISH.

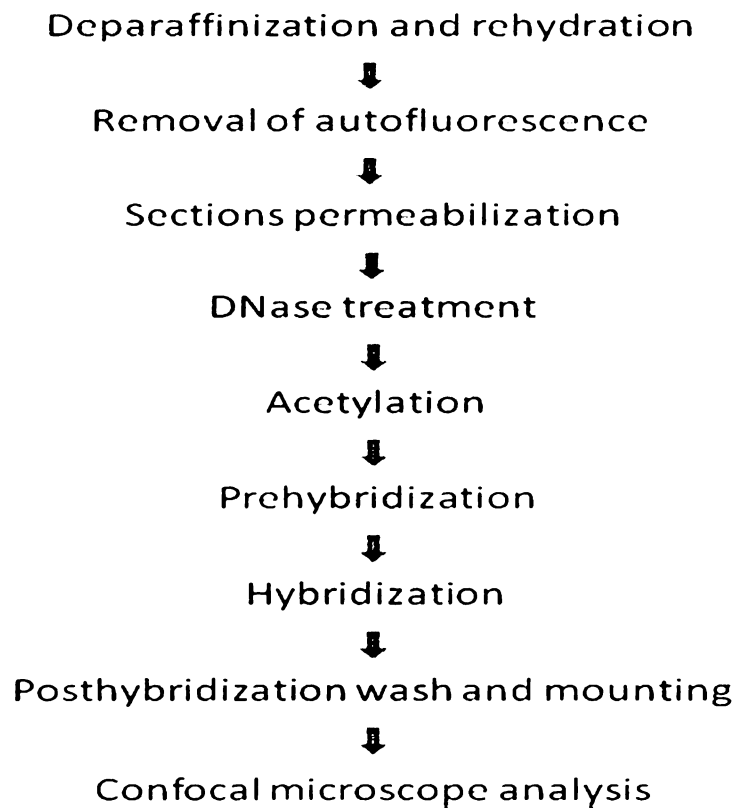


Figure 2.1. Brief steps of mRNA *in situ* hybridization with fluorescence labeled riboprobe.

### *Q RT PCR procedure*

Total RNA isolation, cDNA synthesis, and RT PCR were conducted as described by Park et al. (2006). To confirm complete removal of possible genomic contamination, a negative control (sample without reverse transcriptase) was run in parallel with each PCR experiment, and which resulted in no amplification of the PCR product (data not shown). To improve sensitivity of PCR amplification, the cDNA:RNA hybrid molecules were removed by digestion with *E. coli* RNase H after first-strand cDNA synthesis. The expression level of CYP19 mRNA was normalized to an internal control gene,  *$\beta$  actin*.

To determine the accumulation of the PCR product, SYBR Green I dye (bioMérieux, Marcy l'Etoile, France) was used as a real-time reporter of the presence of double-stranded DNA. All cDNA sequences were obtained from the public GenBank database of NCBI. The primers were obtained using Beacon Designer 2 (Premier Biosoft International, Palo Alto, CA, USA). Primer sequences and conditions used for Q RT PCR analysis are given (Table 2.2). Primer specificity was verified by a single distinct peak obtained during the melting curve analysis of the SYBR Green I based real time PCR system and by DNA sequencing of the PCR amplicons separated by gel electrophoresis (data not shown).

### *Histology*

Histological changes in medaka ovaries were evaluated using H & E stained sections (Tompsett et al., 2008). Briefly, slides were de-paraffinized in xylene and rehydrated through a descending ethanol series (100, 95, and 70%). Slides were then stained in Harris' hematoxylin (EMS, Hatfield, PA, USA) for 3 min, processed through acid alcohol,

ammonia, and ethanol washes, and then stained in 1% Eosin Y (EMS, Hatfield, PA, USA) in 80% ethanol for 1 min. Slides were then dehydrated through an ethanol series (70, 95, and 100%) and cleared in xylene. Slides were preserved under glass cover slips using Entellan mounting medium (EMS, Hatfield, PA, USA) and allowed to dry. Images of the gonad on each slide were recorded using a Camedia C-3040 ZOOM digital camera (Olympus, Center Valley, PA, USA) attached to an Olympus BX41 microscope (Optical Analysis Corporation, Nashua, NH, USA).

### *Statistics*

Statistical analyses in this study were conducted using SAS (SAS Institute Inc. Cary, NC, USA). Prior to analysis, data sets were tested for normality using the Shapiro Wilk's test. One way ANOVA test was applied to test for differences of *CYP19a* gene expression across all treatment groups in both Q RT PCR and ISH, followed by the Student-Newman-Keul's test for multiple comparisons. The 2-tailed Spearman rank correlation analysis was used to evaluate the relationship between *CYP19a* gene expression levels by means of Q RT PCR analysis and ISH analysis. The criterion for significance in all statistical tests was  $p < 0.05$ .

Table 2.1 Probes with primers, GenBank accession number, amplicon size, and cycling condition for conventional PCR.

Probes	Primers (sense/antisense, 5'-3')	Accession number	Amplicon size	Cycling condition		
				Denaturation (°C /time,s)	Annealing (°C /time,s)	Extension (°C /time,s)
<i>CYP19a</i>	CCTGTTAATGGTCTGGAGTCAC/ GAAGAGCCTGTTGGAGATGTC	D82968	496	94/45	55/30	72/90

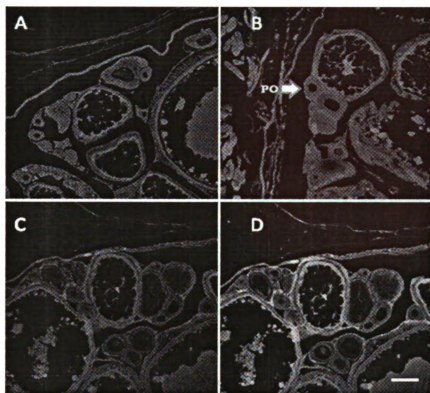
Table 2.2 Targeted genes with primers, GenBank accession number, amplicon size, and cycling conditions for Q RT PCR analysis.

Targeted genes	Primers (sense/antisense, 5'-3')	Accession number	Amplicon size	Cycling condition		
				Denaturation (°C /time,s)	Annealing (°C /time,s)	Extension (°C /time,s)
<i>CYP19a</i>	GCCCGCTTATGTCCTATTTGAG/ CCTCTCCGTTGATCCACACTC	D82968	108	95/15	59/50	72/30
<i>Beta actin</i>	GAGGTTCCGTTGCCCAGAG/ TGATGCTGTTGAGGTGGTCTC	S74868	89	95/15	61/50	72/30

## Results

### *Reduction of autofluorescence*

Initial experiments revealed strong auto-fluorescence in non-treated sections (Figs. 2.2A-B). Of the treatments tested, only sodium borohydride (SB) and SB + copper (II) sulfate significantly decreased autofluorescence, but there were no significant difference in the signal intensity between the two treatments (data not shown). Therefore, SB was used in all further experiments. However, complete removal of autofluorescence to levels observed in the negative controls was not possible (Figs. 2.2C and 2.2E). When SB-treated sections were subjected to linear spectral unmixing of CLSM the background fluorescence signal previously observed in medaka ovaries was reduced or eliminated (Fig. 2.2D) relative to traditional excitation/emission filter system laser microscopy (Fig. 2.2C). Thus, for further analysis it was decided to treat all samples with 10mg/mL SB to reduce and/or minimize the signal of autofluorescence, and then to subject each image to the above described spectral unmixing method.



E

Emission wavelength (nm)	Intensity		
	A	B	C
513	1356.1	869.3	733.2
524	1035.6	979.6	769.9
534	1131.0	1087.1	818.7

Figure 2.2 Autofluorescence images of juvenile medaka ovary and emission spectra of the sections obtained after excitation with a 488 laser (A, B, and C) of CLSM and autofluorescence image of section after applying Linear spectral unmixing (D) of CLSM. (A). Section not subjected to ISH procedure; (B). section *in situ* hybridized without probe and without SB treatment; (C). Section *in situ* hybridized without probe and with SB treatment; (D). Section *in situ* hybridized without probe and SB treatment after application of linear unmixing; (E). Autofluorescence intensities of the sections. PO = previtellogenic oocytes. Scale bar = 100  $\mu$ m.

#### *Tissue and cell specificity of CYP19a gene expression*

Longitudinally sectioned whole medaka hybridized with *CYP19a* antisense probe

exhibited a fluorescence signal that was specific to ovary (Fig. 2.3A). The specificity of

hybridization was demonstrated with negative controls using sense probe, which gave a very weak fluorescence signal (Fig. 2.3B). Sections hybridized in the absence of probe showed no signal (Fig. 2.3C). The greatest fluorescence was found in thecal cells, granulosa cells, and premature early stage pre-vitellogenic oocytes. *CYP19a* expression in vitellogenic oocytes was much less and matured oocytes cells exhibited little fluorescence (Fig. 2.3). If present, *CYP19a* expression was found only in the outer layers of matured oocytes (Fig. 2.5). Furthermore, fluorescence specific for positive *CYP19a* staining was observed only in ovary and no *CYP19a* mRNA could be detected by ISH in other tissues such as the brain or liver (Fig. 2.7). When measured by RT-PCR, *CYP19a* gene expression was greatest in ovary, while both brain and liver tissues expressed little *CYP19a* mRNA (data not shown).

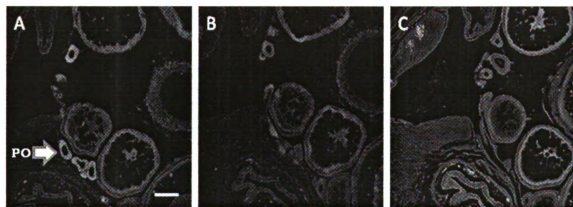


Figure 2.3 Expression of *CYP19a* mRNA in the ovary of juvenile Japanese medaka after hybridization of longitudinal whole mount sections with a fluorescence riboprobe. Expression of *CYP19a* mRNA was detected in the ovary hybridized with antisense probe (A); Very weak *CYP19a* detection was observed in the oocytes hybridized with sense probe (B); no signal in the ovary hybridized without probe (C). PO = previtellogenic oocytes. Scale bar = 100  $\mu$ m.

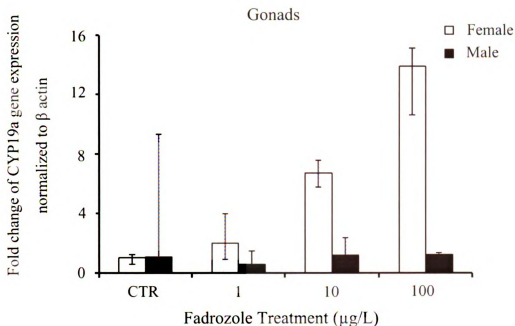


Figure 2.4 Fold-changes of *CYP19a* mRNA gene expression by Q RT PCR analysis in gonads of Japanese medaka exposed to fadrozole (1, 10, and 100 µg/L), using comparative  $C_T$  method for quantification of mRNA.  $\beta$  actin served as the internal control gene. All data are expressed as the median  $\pm$  the interquartile range. One-way ANOVA was used to analyze data by treatment groups for each tissue and sex separately, followed by SNK test for multiple comparisons. Different letters indicate significant difference between treatment ( $p < 0.05$ ).

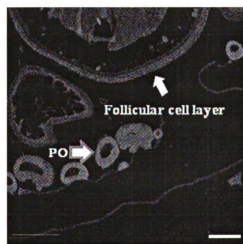


Figure 2.5 Expression of *CYP19a* mRNA in the ovary of juvenile Japanese medaka using the optimized *in situ* hybridization. Strong signal detection of *CYP19a* mRNA in the early stage of oocytes was observed, while low *CYP19a* gene expression was localized in the outer layer of follicular cell layer of the vitellogenic and matured oocytes. PO = previtellogenic oocytes. Bar = 100 µm.



### *Fadrozole exposure*

#### Gene expression

Expression of *CYP19a* in ovaries of medaka exposed to fadrozole, as measured by both RT PCR and ISH, was greatest in medaka exposed to 100 µg fadrozole /L. RT PCR analyses showed that there was a significant, dose-dependent up-regulation of *CYP19a* gene expression in ovary of fadrozole-exposed females (Fig. 2.4). Exposure to 100 µg fadrozole/L caused a 14-fold up-regulation of *CYP19a* expression in ovaries, relative to that of controls. While there was also greater *CYP19a* expression measured by ISH, due to the relative great variation and the semi-quantitative nature of the analyses these differences were not statistically significant. Furthermore, the 1.4 fold change observed by use of ISH was less than that demonstrated by use of RT-PCR (Fig. 2.6). While the up-regulation of *CYP19a* expression caused by 100 µg fadrozole /L showed the same increasing trend than that determined by RT-PCR, ISH was unable to demonstrate effects for lesser concentrations of fadrozole. Although trends in *CYP19a* expression were similar between quantification between ISH and Q RT PCR, no statistically significant correlation was observed ( $r^2 = 0.015$ ,  $n = 16$ ,  $p = 0.957$ ).

#### Fadrozole exposure - Mortality, morpho-metric and histological endpoints

No mortality was observed in any of the exposure groups or the controls during the course of the experiment. Fadrozole caused no statistically significant changes in liver somatic (LSI) and gonadal somatic (GSI) indices of Japanese medaka ( $p > 0.05$ ) (Fig. 2.8). However, in a parallel study exposure to 100 µg/L fadrozole caused histological

effects. While female medaka fish from the control, 1.0, and 10 µg fadrozole /L treatments had oocytes in all stages of development, oocytes of females exposed to 100 µg fadrozole /L were predominantly in later vitellogenic stages, similar in size, and lacked a distinct yolk globule (stage VII and VIII of development as classified by Iwamatsu et al. (1988)). None of the ovaries in fish from this treatment group had stage IX or mature (with a pink-staining yolk globule) oocytes.

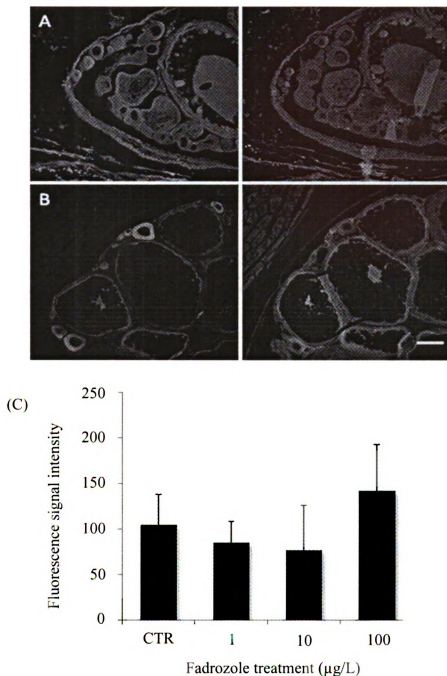


Figure 2.6 Expression of *CYP19a* mRNA in the ovary of juvenile Japanese medaka using the optimized FISH technique in the control (A) and 100  $\mu\text{g/L}$  of fadrozole treatment group (B) for 7 days. Fluorescence signal intensity of *CYP19a* expression in randomly selected three early stage of oocytes in the ovary of Japanese medaka exposed to fadrozole (C) and each bar represents means  $\pm$  S.D. of 4 female fish. Significantly low signal of negative control (sense probe, right panel) and highly expressed *CYP19a* mRNA in the ovary exposed to 100  $\mu\text{g/L}$  of fadrozole was observed. Scale bar = 100  $\mu\text{m}$ .

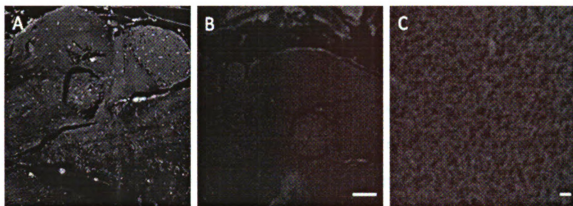


Figure 2.7 Expression of *CYP19a* mRNA in the brain tissue of female Japanese medaka in the control (A), and brain tissue (B) and liver tissue (C) of 100 µg/L of fadrozole treatment group by the optimized *in situ* hybridization using fluorescence antisense riboprobe. No fluorescence signal detection was observed in brain and liver tissues. Bar = 100 µm.

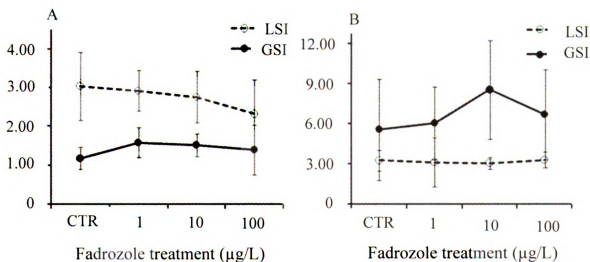


Figure 2.8 Gonadal somatic index (GSI) and liver somatic index (LSI) of male (A) and female (B) Japanese medaka exposed to fadrozole for 7 days. Bars represent mean and error bars are standard deviation.

## **Discussion**

### *Optimization of FISH*

Optimization of fluorescence ISH protocols, as described in this study, resulted in the development of a test system that allows for the identification of gene expression in paraffin embedded whole mount sections of small fish with relatively great sensitivity and spatial specificity. To date, the application of fluorescence microscopy techniques in ISH has been limited by the relatively great auto-fluorescence of many tissue types or components (e.g. fixative) used in the assay (Szöllösi et al., 1995). Typically, the emission spectrum of auto-fluorescence is very broad compared to the spectra of exogenous source such as a fluorescently labeled probe, complicating the use of fluorescent probes further because auto-fluorescence cannot be avoided by simply choosing dyes with excitation and emission spectra out of the range of the spectra of autofluorescent molecules. Sodium borohydride (SB) is a known blocker of aldehyde groups that are generated after reactions of amines and protein molecules with aldehyde fixatives, and eventually these aldehyde groups combine covalently to any amino groups, resulting in aldehyde-induced fluorescence (Beisker et al., 1987). However, the capacity of SB to reduce auto-fluorescence seems to be species and/or tissue specific. For example, attempts to reduce the auto-fluorescence in the aldehyde fixed-human bone marrow paraffin sections failed, and even resulted in an increase of fluorescence (Baschong et al., 2001). Other studies have reported that SB quenched the fixative induced auto-fluorescence in brain tissue of mammals (Tagliaferro et al., 1997; Clancy and Cauller, 1998). While in our study treatment with SB significantly reduced auto-fluorescence, the specific signal of Alexa Fluor 488 dye was still obscured by the

relatively strong autofluorescence signal when using traditional fluorescent microscopy techniques, which indicates that aldehyde-induced fluorescence was only one contributor to the observed auto-fluorescence. Furthermore, the small difference in the strength of the auto-fluorescence signal of sections that did and did not undergo ISH implies that the components of the ISH procedures used in this study did not significantly contribute to auto-fluorescence. The true dye signal could be detected after complete removal auto-fluorescence signal by use of linear spectral unmixing with CLSM to isolate the Alexa Fluor 488 dye signal from the remaining auto-fluorescence. The linear spectral unmixing technique is able to identify and separate specific spectral components in fluorescence images (Chorvat et al., 2005). The application of this procedure allowed isolation of the dye-specific signal that allowed clearly discerning between background and gene probe signal. The significantly greater fluorescence intensity in sections hybridized with antisense probe compared to those hybridized with the sense probe indicated the specificity of the developed ISH protocol. However, the optimization techniques applied did not completely reduce the fluorescence signals in samples processed with sense probe. Possible reasons for this could be that probes were not completely removed from the tissue during post-hybridization washing steps, or that some of the tissue autofluorescence signal corresponded to the specific spectrum of Alexa Fluor 488 dye. Regardless of these artifacts, the FISH system developed in this study allowed for spatial determination of specific gene signals in medaka with high resolution and sensitivity, which represents a significant improvement compared to most of the previous FISH approaches.

### *Validation of FISH method*

The Q RT PCR analysis revealed differential expression of *CYP19a* mRNA in brain and ovary of juvenile female medaka (data not shown). Average  $C_T$  values for ovary and brain were 21 and 35, indicating a  $2 \times 10^{14}$  difference in abundance of *CYP19a* transcript between these tissues. Significant greater induction of *CYP19a* mRNA in ovary compared to brain is in accordance with findings of other studies with teleost fish (Callard et al., 2001; Kishida and Callard, 2001 (zebrafish); Villeneuve et al., 2006 (fathead); Liu et al., 2007 (catfish)). The results of the ISH revealed a clear signal for *CYP19a* mRNA only in ovary. However, while no expression of *CYP19a* in brain could be observed with ISH, expression was detectable at very low levels by use of Q RT PCR. This result indicates that ISH on whole animal sections is relatively less sensitive than use of Q-RT-PCR with excised tissue. This difference in sensitivity is likely due to the fact that *CYP19a* was amplified during the PCR process while the ISH signal is proportional to the absolute amount of mRNA present in the tissue. Furthermore, the RT PCR method applied here utilized mRNA extracted from an entire gonad while the ISH procedure is limited to the visualization of a small section of a tissue. Now that the utility of the ISH method has been demonstrated for whole tissue mounts, future work could increase tissue-specific sensitivity by use of in situ PCR.

While qualitative determinations of up-regulation of *CYP19a* expression by fadrozole could be detected both by the ISH on whole fish sections and RT-PCR with excised tissues the correlation between the magnitude of change measured by the two methods was poor ( $r^2 = 0.015$ ). This result is in accordance with a parallel study that investigated the effects of fadrozole on *CYP19a* gene expression in the same fish using

radionucleotide based ISH (Tompsett et al., 2008). The increase in ovarian *CYP19a* expression after exposure to fadrozole compares well to findings of Villeneuve et al. (2006) in juvenile female fathead minnow. It has been hypothesized that this increase in gene expression, which is opposite to that of enzyme activity, is most likely due to a compensatory response through increased GtH from pituitary in response to decreased levels of E2 (Kime, 1998; Tompsett et al., 2008). However, these findings indicate that the developed fluorescent ISH method is indicative of changes at the gene expression level that were previously reported in the same experiment using different analytical (RT-PCR) or detection (radionucleotide ISH) systems.

#### *Utilization of FISH*

The high resolution and integration into classical histological analysis suggests that FISH is a useful technique for use in studies aiming to elucidate mechanisms of effects of chemicals. However, while FISH allows the localization of mRNA in a number of tissues simultaneously with comparison to histological responses, FISH is less sensitive and more variable than Q RT PCR. Thus, currently the results of FISH in whole animals sections are semi-quantitative. This is in accordance with a parallel study using radionuclide based ISH, and which also reported relatively great variation between replicate slides and difficulties to quantify the ISH signal (Tompsett et al., 2008).

Utilization of ISH for localization and expression of mRNA in tissues or whole organisms are not novel, but the improvement made by reduction in auto-fluorescence has made it more useful. Specifically, the expression of the *CYP19a* gene has been studied in various teleost fish species previously (Goto-Kazeto et al., 2004; Kobayashi et



al., 2004; Dong and Willett, 2008; Wang and Orban, 2007; Tompsett et al., 2008). However, these studies have employed non-fluorescent visualization systems such as enzyme or radionucleotide labeled probes. While such systems represent useful approaches to identify the spatial and tissue specific expression of genes, they are associated with a series of issues that limit their applicability. Enzyme based detection systems such as digoxigenin and biotin require immunochemical steps that are time and sometimes cost intensive. Furthermore, while more sensitive than fluorescence based systems, enzymatic or immunological amplification steps for probe visualization typically show a poor correlation between signal intensity and the abundance of mRNA (Day et al., 2007). One of the limitations of the use of radionucleotide detection methods is the limited resolution and sensitivity by which tissue specific changes in gene expression can be determined (Day et al., 2007; Tompsett et al., 2008). While there are alternative detection methods such as silver-grain based techniques that are highly sensitive and provide good resolution (Hrabovzky et al., 2004), these techniques are labor intensive and very expensive.

The FISH approach applied in this study allowed specific, high resolution detection of *CYP19a* in whole mount female medaka sections. *CYP19a* was specific to the ooplasm of early stage oocytes that were less than 100  $\mu\text{m}$  in diameter and possessed high expression of *CYP19a*, and the follicle cell layer of previtellogenic and vitellogenic stage of oocytes, albeit less expressed, which is consistent with the results of other studies with teleost fishes, such as killifish (Dong and Willett, 2008), zebrafish (Goto-Kazeto et al., 2004; Wang and Orban, 2007), and Atlantic croaker (Nunez and Applebaum, 2006). Overall, *CYP19a* mRNA gene expression gradually lessened with maturation of oocytes:

early stage of oocytes >> pre- and vitellogenic oocytes > mature oocytes. Expression of *CYP19a* has been reported to be primarily localized in the ooplasm of primary growth staged oocytes of developing killifish (*Fundulus heteroclitus*) and gradually declined from stage I oocytes (previtellogenic follicle) to non-detectable levels at stage IV oocytes (matured follicles) (Dong and Willett, 2008). Expression of *CYP19a* mRNA was also observed in the follicular layer of developing oocytes in the medaka (Suzuki et al., 2004). In Atlantic croaker, *CYP19a* mRNA transcripts were most expressed in previtellogenic ovary (Nunez and Applebaum, 2006). In zebrafish, a greater abundance of *CYP19a* mRNA was observed in the mid-vitellogenic oocytes than in the primary stage of oocytes, which were embedded in connective tissue (Goto-Kazeto et al., 2004). This may be indicative of differences in synthesis of E2 and associated vitellogenesis among species. Overall, these findings indicate the validity of the FISH system used in our study as it reproduced the findings of other studies with teleost fish species. The utilization of the FISH could be further confirmed by the tissue specificity of *CYP19a* hybridization that was limited to the ovary.

#### *Comparison of FISH data to morphometric and histological results*

No significant effects on morphometric parameters, such as organ or body sizes, were observed to be caused by exposure to fadrozole, which is likely due to the relatively short duration of exposure. The histological analysis indicated that an effect on development of the ovary in response to fadrozole exposure occurred. This supports the hypothesis that aromatase is important in sexual development and gonadal maturation in medaka. This conclusion is supported by the results of studies that have shown that inhibition of

aromatase by specific inhibitors caused a decrease in plasma E2 and vitellogenin levels, and ultimately inhibited oocyte growth in teleost fishes (Ankley et al., 2002; Suzuki et al., 2004; Sun et al., 2007).

One of the major advantages of FISH is that it allows the localization of a specific gene at the tissue and/or cellular level. This tissue or cell specific response provides a clue for understanding relationships between molecular and histological processes. While both molecular approaches utilized in this study revealed an increase in *CYP19a* gene expression at the greatest dose tested, the magnitude of the effect was very different, and based on this results the ISH data would have not allowed predicting the great increase measured by RT-PCR. By combining the ISH with standard histology, however, it was possible to demonstrate that there was a change in the number of earlier stage oocytes, the types of cells that are characterized by increased *CYP19a* expression. Given the relatively small change in *CYP19a* gene expression measured by ISH when compared to RT-PCR, therefore, it can be concluded that the change in tissue composition - increase in the number of cells that have increased *CYP19a* expression – is likely to be the main factor resulting in the increase in gonadal aromatase expression in response to fadrozole exposure.

In summary, the optimized FISH method developed in this study allowed to detect *CYP19a* mRNA expression in the ovary of medaka. The method not only can provide useful information relative to temporal and spatial changes in gene expression, but also can aid in explaining molecular changes at the level of histological observation with the ultimate goal of being able to link histological changes to potential pathologies.

Furthermore, FISH has the potential to be further optimized using multiple riboprobes with different emission spectrums simultaneously with the same section.

### **Acknowledgement**

This study was supported by a grant from the US. EPA Strategic to Achieve Results (STAR) to J.P. Giesy, M. Hecker and P.D. Jones (Project no. R-831846). Prof. Giesy was supported by an at large Chair Professorship at the Department of Biology and Chemistry and Research Centre for Coastal Pollution and Conservation, City University of Hong Kong and by a grant from the University Grants Committee of the Hong Kong Special Administrative Region, China (Project no. AoE/P-04/04) to D. Au and J.P. Giesy and a grant from the City University of Hong Kong (Project no. 7002117).

## References

- Afonso, L.O.B., Iwama, G.K., Smity, J., Donaldson, E.M., 1999. Effects of the aromatase inhibitor fadrozole on plasma sex steroid secretion and ovulation rate in female coho salmon, *Oncorhynchus kisutch*, close to final maturation. Gen. Comp. Endocrinol. 113, 221-229.
- Andreeff, M., Pinkel, D., 1999. Introduction to fluorescence in situ hybridization: principles and clinical applications. John Wiley & Sons, New York, p 455
- Ankley, G.T., Kahl, M.D., Jensen, K.M., Hornung, M.W., Korte, J.J., Makynen, E.A., Leino, R.L., 2002. Evaluation of the aromatase inhibitor fadrozole in a short-term reproduction assay with the fathead minnow (*Pimephales promelas*). Toxicol. Sci. 67, 121-130.
- Baschong, W., Suetterlin, R., Laeng R.H., 2001. Control of autofluorescence of archival formaldehyde-fixed, paraffin-embedded tissue in confocal laser scanning microscopy (CLSM). J. Histochem. Cytochem. 49, 1565-1671.
- Beisker, W., Dlobeare, F., Gray, J.W., 1987. An improved immunocytochemical procedure for high-sensitivity detection of incorporated bromodeoxyuridine. Cytometry 8, 235-239.
- Billinton, N., Knight, A.W., 2001. Seeing the wood through the trees: A review of techniques for distinguishing green fluorescent proteins from endogenous autofluorescence. Anal. Biochem. 291, 175-197.
- Braissant O., Wahli W., 1998. A simplified in situ hybridization protocol using non-radioactively labeled probes to detect abundant and rare mRNAs on tissue sections. Biochemica 1, 10-16.
- Callard, G.V., Tchoudakova, A.V., Kishida, M., Wood, E., 2001. Differential tissue distribution, developmental programming, estrogen regulation and promoter characteristics of CYP19 genes in teleost fish. J. Steroid Biochem. Mol. Biol. 79, 305-314.

- Chorvat, D.Jr., Kirchnerova, J., Cagalinec, M., Smolka, J., Mateasik, A., Chorvatova, A., 2005. Spectral unmixing of flavin autofluorescence components in cardiac myocytes. *Biophys. J.* 89, L55–L57.
- Clancy, B., Cauller, L.J., 1998. Reduction of background autofluorescence in brain sections following immersion in sodium borohydrate. *J. Neurosci. Methods.* 83, 97-102.
- Day, D.J., Mrkusich, E.M., Miller, J.H., 2007. Comparative quantitation of mRNA expression in the central nervous system using fluorescence in situ hybridization. *Methods Mol. Biol.* 353,125-142.
- Dirks, R.W., 1990. Simultaneous detection of different mRNA sequences coding for neuropeptide hormones by in situ hybridization using FITC and biotin labeled oligonucleotides. *J. Histochem. Cytochem.* 38, 467-473.
- Dong, W., Willet, K.L., 2008. Local expression of CYP19A1 and CYP19A2 in developing and adult killifish (*Fundulus heteroclitus*), *Gen. Comp. Endocrinol.* 155, 307-317.
- Fenske, M., Segner, H., 2004. Aromatase modulation alters gonadal differentiation in developing zebrafish (*Danio rerio*). *Aquat. Toxicol.* 67, 105-126.
- Goto-Kazeto, R., Kight, K.E., Zohar, Y., Place, A.R., Trant, J.M., 2004. Localization and expression of aromatase mRNA in adult zebrafish. *Gen. Comp. Endocrinol.* 139, 72-84.
- Hayes, T.B., Collins, A., Lee, M., Mendoza, M., Noriega, N., Stuart A.A., Vonk, A., 2002. Hermaphroditic, demasculinized frogs after exposure to the herbicide atrazine at low ecologically relevant doses. *Proc. Natl. Acad. Sci. U. S. A.* 99, 5476-5480.
- Hecker, M., Sanderson, J., Karbe, L., 2006. Supression of aromatase activity in populations of bream (*Abramis brama*) from the river Elbe, Germany. *Chemosphere* 66, 542-552.

- Hrabovszky, E., Kallo, I., Steinhäuser, A., Merchenthaler, I., Coen, C., Peterson, S., Liposits, Z., 2004. Estrogen receptor-beta in oxytocin and vasopressin neurons of the rat and human hypothalamus: Immunocytochemical and *in situ* hybridization studies. *J. Comp. Neurol.* 473, 315-333.
- Ijiri, S., Takei, N., Kazeto, Y., Todo, T., Adachi, S., Yamauchi, K., 2006. Changes in localization of cytochrome P450 cholesterol side-chain cleavage (P450<sub>scc</sub>) in Japanese eel testis and ovary during gonadal development. *Gen. Comp. Endocrinol.* 145, 75-83.
- Iwamatsu, T., Ohta, T., Oshima, E., Sakai, N., 1988. Oogenesis in the medaka *Oryzias latipes*-stages of oocytes development. *Zool. Sci.* 5, 353-373.
- Jezzini, S., Bodnarova, M., Moroz, L., 2005. Two-color *in situ* hybridization in the CNS of *Aplysia californica*. *J. Neurosci. Methods.* 149, 15-25.
- Kime, D.E., 1998. Introduction to fish reproduction. In: Kime, D.E. (Ed.), *Endocrine disruption in fish*. Kluwer Academic Publishers, Massachusetts, p. 81-101.
- Kishida, M., Callard, G.V., 2001. Distinct cytochrome P450 aromatase isoforms in zebrafish (*Danio rerio*) brain and ovary are differentially programmed and estrogen regulated during early development. *Endocrinology* 142, 740-750.
- Kobayashi, Y., Kobayashi, T., Nakamura, M., Sunobe, T., Morrey, C.E., Suzuki, N., Nagahama, Y., 2004. Characterization of two types of cytochrome P450 aromatase in the serial-sex changing gobiid fish, *Trimma okinawae*. *Zool. Sci.* 21, 417-425.
- Kong, R., Giesy, J.P., Wu, R., Chen, E., Chiang, M., Lim, P., Yuen, B., Yip, B., Mok, H., Au, D., 2008. Development of a marine fish model for studying *in vivo* molecular responses in ecotoxicology. *Aquat. Toxicol.* 86, 131-141.
- Lichter, P., 1997. Multicolor fishing: What's the catch? *Trends Genet.* 13, 475-480.
- Liu, Z., Wu, F., Jiao, B., Zhang, X., Hu, C., Huang, B., Zhou, L., Huang, X., Wang, Z., Zhang, Y., Nagahama, Y., Cheng, C.H.K., Wang D., 2007. Molecular cloning of doublesex and mab-3-related transcription factor 1, forkhead transcription factor

- gene 2, and two types of cytochrome P450 aromatase in southern catfish and their possible roles in sex differentiation. *J. Endocrinol.* 194, 223-341.
- Nunez, B.S., Applebaum, S.L., 2006. Tissue- and sex-specific regulation of CYP19a1 expression in the Atlantic croaker (*Micropogonias undulates*). *Gen. Comp. Endocrinol.* 149, 205-216.
- Otsuka, F., 2002. Gene expression assay for hazard assessment of chemicals. *Ind. Health.* 40, 113-120.
- Park, J.W., Hecker, M., Murphy M.B., Jones P.D., Solomon, K.R., Van Der Kraak, G., Carr, J.A., Smith, E.E., du Preez, L., Kendall, R.J., Giesy, J.P., 2006., Development and optimization of a Q-RT-PCR method to quantify CYP19a mRNA expression in testis of male adult *Xenopus laevis*: Comparison with aromatase enzyme activity. *Comp. Biochem. Physiol., Part B: Biochem. Mol. Biol.* 144, 18-28.
- Pernthaler, A., Amann R., 2004. Simultaneous fluorescence in situ hybridization of mRNA and rRNA in environmental bacteria. *Appl. Environ. Microbiol.* 70, 5426-5433.
- Peterson, S., McCrone, S., 1993. Use of dual-label *in situ* hybridization histochemistry to determine the receptor complement of specific neurons. In: Valentino, K.L., Eberwine, J.J., Barchas, J.D. (Eds.), *In situ* hybridization applications to neurobiology. Oxford University Press, New York, pp. 78.
- Rotchell, J.M., Ostrander, G.K., 2003. Molecular markers of endocrine disruption in aquatic organisms. *J. Toxicol. Environ. Health, Part B.* 6, 453-495.
- Sanderson, J.T., Letcher, R.J., Heneweer, M., Giesy, J.P., van den Berg, M., 2001. Effects of chloro-S-triazine herbicides and metabolites on aromatase (CYP19) activity in various human cell lines and on vitellogenin production in male carp hepatocytes. *Environ. Health Perspect.* 109, 1027-1031.
- Sanderson, J.T., Seinen, W., Giesy, J.P., van den Berg, M., 2000. 2-chloro-S-triazine herbicides induce aromatase (CYP-19) activity in H295R human adrenocortical carcinoma cells: A novel mechanism for estrogenicity. *Toxicol. Sci.* 54, 121-127.



- Simeone, A., 1999. Detection of mRNA in tissue sections with radiolabelled riboprobe. In: Wilkinson, D.G. (ed.), *In situ hybridization: A practical approach* (2<sup>nd</sup> Ed). IRL Press, Oxford, pp. 69-84.
- Simpson, E.R., Mahendroo, M.S., Means, G.D., Kilgore, M.W., Hinshelwood, M.M., Grahamlence, S., Amarnah, B., Ito, Y.J., Fisher, C.R., Michael, M.D., Mendelson, C.R., Bulun, S.E., 1994. Aromatase cytochrome-P450, the enzyme responsible for estrogen biosynthesis. *Endocr. Rev.* 15, 342-355.
- Streit, A., Stern, C., 2001. Combined whole-mount in-situ hybridization and immunohistochemistry in avian embryos. *Methods* 23, 339-344.
- Sun, L., Zha, J., Spear, P.A., Wang, Z., 2007. Toxicity of the aromatase inhibitor letrozole to Japanese medaka (*Oryzias latipes*) eggs, larvae and breeding adults. *Comp. Biochem. Physiol., Part C: Toxicol. Pharmacol.* 145, 533-541.
- Suzuki, A., Tanaka, M., Shibata, N., 2004. Expression of aromatase mRNA and effects of aromatase inhibitor during ovarian development in the medaka, *Oryzias latipes*. *J. Exp. Zool.* 301A, 266-273.
- Szöllösi, J., Lockett, S.J., Balázs, M., Waldman, F.M., 1995. Autofluorescence correction for fluorescence in situ hybridization. *Cytometry* 20, 356-361.
- Tagliaferro, P., Tandler, C.J., Ramos, A.J., Pecci Saavedra, J., Brusco, A., 1997. Immunofluorescence and glutaraldehyde fixation. A new procedure based on the Schiff-quenching method. *J. Neurosci. Methods.* 77, 191-197.
- Tompsett, A.R., Park, J.W., Zhang, X., Jone, P.D., Newsted, J.L., Au, D.W.T., Chen, E.X.H., Yu, R., Wu, R.S.S., Kong, R.Y.C., Giesy, J.P., Hecker, M., 2008. Development and validation of an in situ hybridization system to detect gene expression along the HPG-axis in Japanese medaka, *Oryzias latipes*. *Aquat. Toxicol.* (Submitted).
- Villeneuve, D.L., Knoebel, I., Kahl, M., Jensen, K., Hammermeister, D., Greene, K., Blake, L., Ankely, G., 2006. Relationship between brain and ovary aromatase activity and isoform-specific aromatase mRNA expression in the fathead minnow (*Pimephales promelas*). *Aquat. Toxicol.* 76, 353-368.

- Wang, X.G., Orban, L., 2007. Anti-mullerian hormone and 11 beta-hydroxylase show reciprocal expression to that of aromatase in the transforming gonad of zebrafish males. *Dev. Dyn.* 236, 1329-1338.
- Wilkinson, D.G., 1999. The theory and practice of in situ hybridization. In: Wilkinson, D.G. (ed.), *In situ hybridization: A practical approach* (2<sup>nd</sup> Ed). IRL Press, Oxford, pp. 1-21.
- Wittbrodt, T., Shima, A., Schartl, M., 2002. Medaka-a model organism from the Far East. *Nat. Rev. Genet.* 3, 53-64.
- Zhang, X., Hecker, M., Park, J.W., Tompsett, A.R., Newsted, J.L., Nakayama, K., Jones, P.D., Au, D., Kong, R., Wu, R.S.S., Giesy, J.P., 2008a. Real time PCR array to study effects of chemicals on the Hypothalamic-Pituitary-Gonadal axis of the Japanese medaka. *Aquat. Toxicol.* (Submitted).
- Zhang, X., Park, J.W., Hecker, M., Tompsett, A.R., Jones, P.D., Newsted, J.L., Au, D., Kong, R., Wu, R.S.S., Giesy, J.P., 2008b. Time-dependent transcriptional profiles of hypothalamic-pituitary-gonadal (HPG) axis in medaka (*O. latipes*) exposed to fadrozole and 17beta-trenbolone. *Aquat. Toxicol.* (Submitted).

### CHAPTER 3

Effects of ethinylestradiol and trenbolone on histology and gene expression of Japanese medaka (*Oryzias latipes*) using a combination of fluorescence in situ hybridization (FISH) and traditional histology

#### **Abstract**

Short-term effects of 17 $\alpha$ -ethinylestradiol (EE2) and 17 $\beta$ -trenbolone (TB) on the hypothalamus pituitary gonadal (HPG) axis of male and female Japanese medaka (*Oryzias latipes*) were determined by use of a combination of traditional histology (H&E staining), and fluorescence in situ hybridization (FISH). Four-month-old medaka were exposed to EE2 at 5, 50, or 500 ng/L or to TB at 50, 500, or 5,000 ng/L for 7 d in static renewal exposure system and effects on expression of vitellogenin II (*Vit II*), androgen receptor (*AR*), and gonadal aromatase (*CYP19a*) were determined. Exposure to either 500 ng EE2/L or 5000 ng TB/L resulted in significantly less fecundity relative to the controls as well as histological changes in ovary and testis. Greater intensity of staining of hepatocytes with hematoxylin was observed in males exposed to EE2 and was correlated with expression of the *Vit II* gene. This result suggests that greater staining of cells, which is related to greater amounts of genetic material, suggesting that the degree of staining with hematoxylin in hepatocytes can be used to examine the mechanisms of action for EE2 in fish. FISH used in conjunction with whole fish sections not only allowed for simultaneous determination of gene expression in multiple target tissues, but also revealed tissue-and/or gender-specific differences in the abundance of target mRNAs.

Expression of the *Vit II* gene was typically detected in liver and ovary of unexposed females, but little expression was observed in liver and testis of unexposed males. However, in male fish exposed to EE2, expression of the *Vit II* gene was up-regulated in both testis and liver relative to that of controls. There was little expression of the *AR* gene observed in ovary or liver of control females. Exposure of females to TB significantly up-regulated *AR* gene expression in ovary but did not alter the *AR* gene expression in liver. In ovary, expression of aromatase (*CYP19a*) was primarily associated with early stage oocytes. The synthetic estrogen (EE2) caused up-regulation of expression of *CYP19a* at concentrations less than 50 ng EE2/L, but exposure to 500 ng EE2/L caused down-regulation. FISH was able to localize changes in gene expression at the cellular/tissue level and provided useful spatial information on changes in these genes in a whole fish model.

## **Introduction**

To identify the molecular mechanisms of toxic action of a chemical, it is necessary to detect and quantify the expression of mRNAs that encode for proteins involved in key processes of the pathway of interest. Most of the techniques utilized have been based on reverse transcription-polymerase chain reaction (RT-PCR), Northern blotting, or RNase protection assays. These methods rely on either high yields of RNA extraction from bulk tissues or only focus on a few genes in one tissue at one specific time in the development of an organism. However, these methods are limited when used with small animal model species such as Japanese medaka (*Oryzias latipes*) or zebrafish (*Danio rerio*) that are commonly used in the assessment of effects and risks resulting from the exposure to EDC

chemicals. The small amounts of individual tissues available for study and the difficulty in excising these tissues from these small organisms has limited the efficacy of these techniques to determine effects during critical windows of time during ontogenesis or simultaneously in multiple tissues. Therefore, innovative, sensitive, and flexible techniques are needed that allow for the identification of multiple molecular target genes after chemical exposure in multiple tissues simultaneously at any stage of ontogeny.

One promising tool is fluorescence *in situ* hybridization (FISH) (Park et al., 2008; Tompsett et al., 2008; Zhang et al., 2008). This technique allows for the direct visualization of specific mRNA sequences in tissues, individual cells, and/or cell structures. FISH has been shown to have the potential to be a powerful tool by combining molecular biology with histology to evaluate gene expression associated with specific cell types in a tissue (Wilkinson, 1999; Hayat, 2004; Park et al., 2008). Principle underlying FISH is that molecular probes of complimentary mRNA sequences attached to a fluorescent molecule can be hybridized to mRNA in tissues or cells of fixed tissue. Measuring spatial and temporal changes in gene expression as a consequence of chemical exposure can provide information relative to modes of action within tissues as regulation of genes among cell types and tissues. Localization of specific genes at the tissue or cellular level can help to further our understanding of gene expression patterns in context with pathologies as determined by parallel histology.

In a previous study, a FISH protocol was optimized to detect spatial expression of mRNA in whole mount sections of Japanese medaka and validated (Park et al., 2008). Here I report the results of a study in which the optimized FISH method was used to evaluate effects of two model EDCs, the synthetic estrogen, ethinylestradiol (EE2) and

the synthetic androgen 17 $\beta$ -trenbolone (TB). These two compounds have known and fairly specific modes of endocrine action. EE2 is an analogue to the endogenous estrogen (17 $\beta$ -estradiol), is a strong estrogen receptor (ER) agonist (Lee et al., 2002), and represents one of the most potent xenoestrogens known to be present in the aquatic environment (Rotchell and Ostrander, 2003). The U.S. Geological survey found EE2 in several surface waters of the United States at concentrations as great as 0.831  $\mu$ g EE2/L (Kolpin et al., 2002). Trenbolone is the product of the hydrolysis of trenbolone acetate, which is a synthetic androgen that is a mammalian androgen receptor (AR) agonist and is used as a growth promoter for cattle in the USA (Blankvoort et al., 2001; Wilson et al., 2002; Durhan et al., 2006). TB has the potential to adversely affect aquatic organisms due to its relative long half-life in water and soil (Schiffer et al., 2001), and its potential to cause disorders in reproductive endocrine functions in fish including the masculinization of females (Davis et al., 2000; Ankley et al., 2003; Orns et al., 2006; Seki et al., 2006).

The Japanese medaka is a common model species in the field of endocrine disrupter research (Wittbrodt et al., 2002), and was chosen in this study because of the information available on its physiology, embryology and genetics and the fact that it is small and easy to rear and induce to reproduce under laboratory conditions.

The model genes selected for this study, vitellogenin II (*Vit II*), androgen receptor (*AR*) and gonadal aromatase (*CYP19a*) are considered important biomarkers for the exposure to EDCs, specifically androgens and estrogens, and thus were thought to be useful as examples of the capabilities of FISH in whole fish histological sections.

Vitellogenin is under strict control of estrogen, and is found at only very low

concentrations in male fish under normal physiological circumstances. It can serve as a marker for both exposures of males to estrogens and exposure of females to anti-estrogens or other maturation inhibiting compounds (Kime et al., 1998). The key enzyme responsible for the conversion of androgens to estrogens is aromatase. The products of this reaction, specifically 17 $\beta$ -estradiol (E2), are critical in ovarian development, reproductive function, and sexual differentiation, so that disruption of either activity or production of the enzyme could alter developmental or reproductive processes of an organism. Due to its key function in estrogen synthesis, aromatase has been considered an important biomarker to assess the exposure of EDCs (Rotchell and Ostrander, 2003). AR is a nuclear receptor that is activated by binding of androgens. It functions as a transcription factor to regulate androgen specific gene expression. Thus, binding of AR with xenoandrogens could interfere with processes such as normal male or female gonadal development.

The objective of these studies was to use FISH to characterize the effects of EE2 and TB on the tissue specific expression of *CYP19a*, *vitellogenin II*, and *androgen receptor  $\alpha$*  in whole mount sections of medaka. Furthermore, the changes in gene expression were compared to a series of histological, physiological, and/or organismal responses to further our understanding of the molecular mechanism of action of EE2 and TB.

## Materials and Methods

### *Test chemicals*

Chemicals used in this research were EE2 (17 $\alpha$ -ethinylestradiol; 17 $\alpha$ -Ethinyl-1,3,5(10)-estratriene-3,17 $\beta$ -diol 19-Nor-1,3,5(10),17 $\alpha$ -pregnatrien-20-yne-3,17-diol; Sigma-Aldrich, St. Louis, MO, USA) and 17 $\beta$ -trenbolone, TB (17 $\beta$ -Hydroxyestra-4,9,11-trien-3-one; Sigma-Aldrich, St. Louis, MO, USA). Dimethyl sulfoxide (DMSO) was used as a carrier solvent to deliver EE2 and TB treatments in water at a final concentration of 0.01 % (v/v).

### *Culture of Japanese medaka (O. latipes)*

Japanese medaka were obtained from the aquatic culture at the US EPA Mid-Continent Ecology Division (Duluth, MN, USA). The medaka were held in flow through systems under conditions to facilitate breeding (23-24 °C, 16:8 light/dark). Medaka were fed Aquatox flake food (Aquatic Ecosystems, Apopka, FL, USA) *ad libitum* once daily, and brine shrimp (*Artemia*) twice daily. All procedures used during all phases of this study were in accordance with protocols approved by the Michigan State University Instituted Animal Care and Use Committee (IACUC).

### *Chemical exposures*

Prior to initiation of exposures experiments, 12- to 14-wk old medaka were placed into 10-L tanks with 6-L of carbon filtered tap water and acclimated for 12 d under the same conditions as in the subsequent exposures. Each treatment group consisted of triplicate tanks, and each tank contained 5 male and 5 female medaka. After the acclimation period, medaka were exposed to 5.0, 50, or 500 ng EE2/L or 50, 500, or 5,000 ng TB/L.



Carbon filtered tap water containing equal amount of DMSO than the chemical treatment groups served as a control. Every day during the exposure phase of the study, one half of the water in each tank (3 L) was replaced with fresh carbon filtered water dosed with the appropriate amount of EE2 (5 mg/L in DMSO) or TB stock (50 mg/L in DMSO). Eggs produced during the past 24h were counted before the replacement of water. Medaka were fed Aquatox® (Aquatic Ecosystems, Apopka, FL, USA) flake food and brine shrimp once daily, and the tanks were kept at 24 °C and 16:8 light/dark. Water quality parameters (temperature, pH, hardness, dissolved oxygen, ammonia nitrogen, and nitrate nitrogen) were measured daily and values were within a normal range for water quality. After exposure for 7 d, medaka were euthanized in Tricaine S (50 mg/mL) (Western Chemical, Ferndale, WA, USA), weighted and snout length was measured. Medaka were separated into two groups; one group was for used in FISH analysis as described in this study and the second group was used in a different study utilizing Q RT PCR analysis that is described elsewhere (Zhang et al., 2008). Medaka designated for analysis by use of FISH, were fixed as described below. To determine the effects of chemicals on hepatic and gonadal growth, liver and gonads were weighted and the liver somatic index (LSI) and gonadal somatic index (GSI) were derived (Equations 1 and 2).

$$LSI = (\text{liver weight/body weight}) * 100 \quad (1)$$

$$GSI = (\text{gonad weight/body weight}) * 100 \quad (2)$$

### *ISH procedure*

#### 1. Preparation of sections

Sections were prepared for FISH by use of methods adapted from Park et al. (2008), and Kong et al. (2008). In brief, fish were dissected to remove fins, tail, skull roof, otoliths, and opercula. The body cavity was opened to improve the penetration of fixative (80% Histochoice MB (EMS, Hatfield, PA, USA), 2% paraformaldehyde, and 0.05% glutaraldehyde) for better internal organ fixation. Medaka were then immersed in the fixative, and allowed to fix over night at room temperature. Fixed medaka were washed with methanol and dehydrated through a graded methanol series, and then cleared in chloroform at 4 °C. Fixed and cleared samples were infiltrated with melted Paraplast Plus paraffin (McCormick Scientific, St. Louis, MO, USA) and the resulting paraffin blocks were stored under RNase free conditions at 4 °C until sectioning.

Medaka were sectioned on a rotary AO-820 microtome (American Optical, Buffalo, NY, USA) under RNase free conditions using absolute ethanol and RNase-Zap (Sigma-Aldrich, St. Louis, MO, USA). Serial sections were cut at 7 µm and placed on Superfrost Plus slides (Erie Scientific, Portsmouth, NH, USA). Slides were stored in RNase-free containers at room temperature until used for ISH.

## 2. Fluorescence labeled riboprobe synthesis

All procedures to synthesize fluorescence labeled riboprobes were adapted from the study of Park et al. (2008) with minor modifications. To synthesize the riboprobes, reverse-transcribed first-strand cDNA was used as a template in a conventional PCR with corresponding primers to amplify PCR products of *CYP19a*, vitellogenin II (*Vit II*), and androgen receptor- $\alpha$  (*AR*) (Table 3.1). Probes for FISH were designed using the Beacon Designer 2 (PREMIER Biosoft Int., Palo Alto, CA, USA) to have lengths of

approximately 500 bp. Probe length was chosen based on a review of Wilkinson (1999) that reported that either too short (less than 100 bp) or too long (more than 1000 bp) probes may give weaker signals possibly due to either low specificity to target transcript or low penetration efficiency into tissue, respectively. The sequence of each riboprobe to detect corresponding target mRNA was compared with all sequences of known genes in Japanese medaka, and no sequence homogeneity was found except for the target gene of interest.

Table 3.1 Probes with primers, GenBank accession number, amplicon size, and cycling condition for conventional PCR.

Probe	Primers (sense/antisense, 5'-3')	Accession number	Amplicon size	Cycling condition		
				Denaturing (°C /time, sec)	Annealing (°C /time, sec)	Extension (°C /time, sec)
CYP19a	CCTGTTAATGGTCTGGAGTCAC/ GAAGAGCCTGTTGGAGATGTC	D82968	496	94/45	55/30	72/90
Androgen receptor- $\alpha$	GTGCGAGCAAGAACGACTG/ CCATCCTAAAGCGAACACCATC	AB076399	461	94/45	55/30	72/90
Vitellogenin II	CACATCCATCAGCATTCATCTC/ TTGACTTACTCCATTGCGAACAG	AB074891	480	94/45	55/30	72/90

The method used to clone the PCR product into pGEM T-Easy vector (Promega, Madison, MI, USA) has been described previously (Park et al., 2008). In order to synthesize the sense probes, their corresponding cloned plasmids were digested with *SalI* (Invitrogen, Carlsbad, CA, USA) for *CYP19a* and *Vit II* gene, and *SpeI* (New England Biolabs, Ipswich, MA, USA) for *AR* gene. For antisense probes, cloned plasmids were digested with *NcoI* (Invitrogen, Carlsbad, CA, USA) for *CYP19a* and *Vit II*, and *SacII* (New England Biolabs, Ipswich, MA, USA) for *AR* gene. I confirmed the digestion with electrophoresis on agarose gel by observing single band with size of plasmid plus inserted PCR product (data not shown). Sense and antisense riboprobes were synthesized using in vitro transcription and labeled with fluorescence dye (Alexa Flour 488, Molecular Probes, Eugene, OR, USA), as described in the method of Park et al. (2008).

### 3. Fluorescent *in situ* hybridization

A brief summary of the steps in the ISH is provided (Fig 3.1). The procedures of ISH and washing steps were in accordance with the methods depicted in Park et al. (2008) with minor modification to improve probe specificity to the mRNA sequence of interest. Microtome sections of medaka were hybridized with the riboprobe (1.5 ng/μL for *AR* and *Vit II*, and 2 ng/μL for *CYP19a*) at 43 °C for 17 h. To evaluate the specificity of binding of antisense probe there were sections that received equal amount of sense probe. Expression of the *Vit II* gene was measured in male and female medaka exposed to EE2 and *AR* gene expression was measured in female medaka exposed to TB. *CYP19a* gene expression was measured in female medaka exposed to both EE2 and TB.

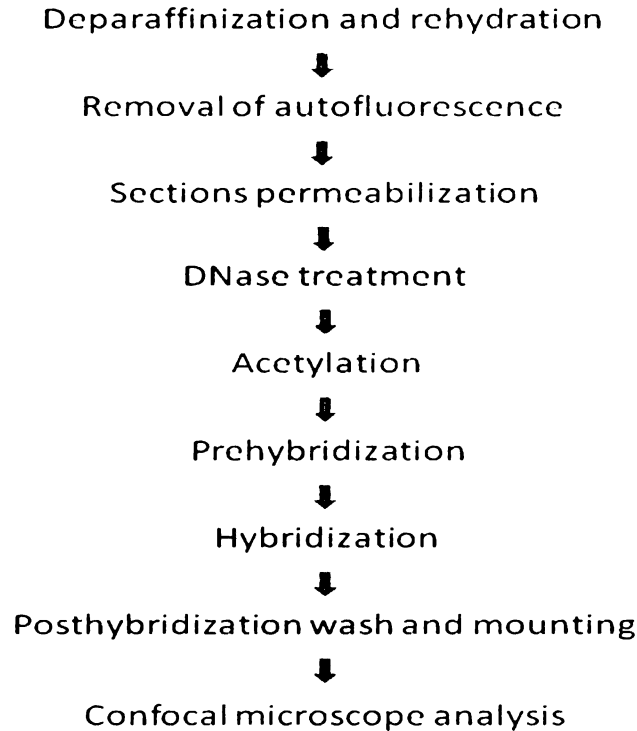


Figure 3.1 Sequence of steps of mRNA in situ hybridization with fluorescence labeled riboprobe.

#### 4. Confocal laser scanning microscopy (CLSM) image analysis

Distribution of the fluorescent probes were identified and quantified by use of confocal fluorescence microscopy. Expression of genes was detected and quantified by use of the LSM 510 Meta system (Carl Zeiss, 07740 Jena, Germany) as described by Park et al. (2008). To account for background auto-fluorescence due to tissues and/or components of the hybridization procedure, individual spectral components associated with auto-fluorescence, background, and Alexa Flore 488 dye were separated using the confocal system. Auto-fluorescence and background spectral components were obtained from the section of each tissue (ovary, testes, and liver) on the slide hybridized without probe. The

specific spectrum of Alexa Fluor 488 dye was obtained directly from dye reagent. Once defined, the number of significant and independent sources of the specific spectral components using CLSM was then subjected to linear spectral unmixing to separate the individual components and to remove auto-fluorescence signal in the recorded images to obtain the specific fluorescence signal of Alexa Fluor 488 dye. To avoid the alteration of the auto-fluorescence spectral shape by photo-bleaching that can result from consecutive laser scans, each set of ISH experiments had at least one ISH section with sense probe for antisense probe specificity and one ISH section without probe for the separation of spectral components.

Images of the tissues were collected at 10X magnification. Expression of the *CYP19a* gene was quantified by randomly selecting 3 different areas of ovary sections hybridized with *CYP19a* antisense probe and then quantifying the fluorescence in 3 early stage of oocytes (less than 100  $\mu\text{m}$  in diameter) randomly selected in each area. Based on morphological criteria developed by Iwamatsu et al. (1988), those oocytes were classified as being in the previtellogenic stage (less than 200  $\mu\text{m}$ ) of oogenesis. Previtellogenic oocytes were classified as being primary oocytes (less than 100  $\mu\text{m}$ ) or pre-vitellogenic oocytes (100 - 200  $\mu\text{m}$ ) according to their size. Fluorescence intensity was divided by the total area of the collected oocytes to compensate variation caused by the size of oocytes. Gene expression in testis and liver, was measured in a randomly selected area of tissue (approx. 1/4 of entire testis) and two areas of tissue (each approx. 1/10 of entire liver), respectively. To measure gene expression in the ovary, the same method as described for the quantification of *CYP19a* gene expression was followed. The fluorescence of testis and liver, was collected from the whole tissue in the image, and

then divided by the area across which the signal was measured. Also, due to the detection of small amounts of Alexa Flour dye specific signal in the sections hybridized with sense probe, the antisense signal was normalized to sense signal in each ISH experiment.

### *Histology*

Histological changes in medaka ovaries were evaluated using H & E stained sections (Tompsett et al., 2008). Briefly, slides were de-paraffinized in xylene and rehydrated through a descending ethanol series (100, 95, and 70%). Slides were then stained in Harris' hematoxylin (EMS, Hatfield, PA, USA) for 3 min, processed through acid alcohol, ammonia, and ethanol washes, and then stained in 1% Eosin Y (EMS, Hatfield, PA, USA) in 80% ethanol for 1 min. Slides were then dehydrated through an ethanol series (70, 95, and 100%) and cleared in xylene. Slides were preserved under glass cover slips using Entellan mounting medium (EMS, Hatfield, PA, USA) and allowed to dry. Images of the gonad and liver on each slide were recorded using a Nikon Eclipse TE300 microscope with image software (SPOT, Diagnostic Instrument, Inc). The intensity of staining of hepatocytes with hematoxylin, a measure of the amount of genetic material present in the tissue, was measured with image analysis software (Image J 1.38X, National Institute of Health, USA). Briefly, digitized images of livers were segmented to obtain the purple color on the image by setting the Hue histogram to 212 - 255, which represents the genetic materials in the cell stained with Hematoxylin. Purple stains greater than 400 pixels in size were enumerated.

### *Statistics*

Statistical analyses were conducted using SAS (SAS Institute Inc. Cary, NC, USA). Data sets were tested for normality using the Shapiro-Wilk's test, and were log-transformed if necessary to achieve normality. Statistical differences between treated groups were determined using one way analysis of variance (ANOVA), followed by the Student-Newman-Keuls test for multiple comparisons. For comparison of means of two groups, the Student's t test was applied. The relationship between the degree of staining of hepatocytes with hematoxylin and expression of *Vit II* gene as measured by FISH, was investigated by use of non-parametric 2-tailed Spearman rank correlation. The criterion for significance in all statistical tests was  $p < 0.05$ .

### **Results**

#### *Weight, length, biological indices and fecundity*

The wet weight and length of medaka exposed to either EE2 or TB were not significantly different from those of control medaka (Table 3.2). In female medaka, EE2 did not significantly affect LSI or GSI, while in male medaka exposure to all concentrations of EE2 resulted in statistically greater LSIs compared to the controls (Fig 3.2A). TB caused a statistically significant effect on LSI at concentrations greater of equal to 50 ng TB/L in females while the concentration required to cause a statistically significant effect on GSI was 500 ng. For males, the only statistically significant effect was observed for LSI after exposure to 500 ng TB/L (Fig 3.2B).

Production of eggs was approximately 48% less in medaka exposed to 5000 ng EE2/L than in the controls. However, this difference was not statistically significant (Fig



3.3A). Cumulative egg production was 60 and 79% less in medaka exposed to 500 or 5000 ng TB/L, respectively (Fig 3.3B). Egg production almost completely ceased after the second day of the exposure to 5000 ng TB/L.

Table 3.2 Body weight (g) and length (mm) of Japanese medaka used in this study.

	Solvent Control	(ng EE2/L)			(ng TB/L)		
		5	50	500	50	500	5,000
Male	0.30±0.01 (25.96±0.41)	0.32±0.02 (25.85±0.47)	0.27±0.01 (24.62±0.45)	0.34±0.02 (26.17±0.55)	0.34±0.03 (27.44±1.18)	0.30±0.02 (25.65±0.34)	0.27±0.01 (25.09±0.41)
Female	0.31±0.03 (25.07±0.93)	0.31±0.03 (24.87±0.66)	0.33±0.02 (25.94±0.12)	0.33±0.03 (25.54±0.52)	0.39±0.04 (26.82±0.33)	0.38±0.04 (26.59±0.89)	0.34±0.03 (26.69±0.51)

\* Solvent control group was treated with DMSO.

\* mean ± SEM, the number in the bracket is snout length.

\* No significant difference of weight and length of fish among treatments in both EE2 and TB ( $p > 0.05$ ).

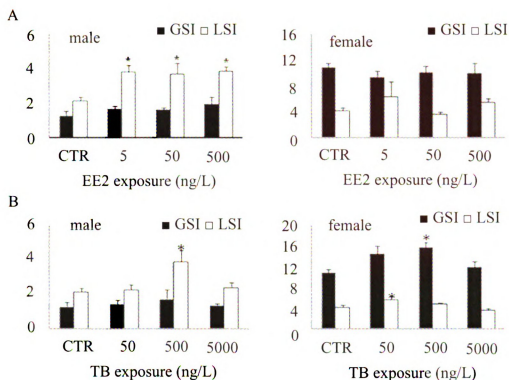


Figure 3.2 Mean values ( $\pm$  SEM) of liver somatic index (LSI) and gonado-somatic index (GSI) in Japanese medaka exposed to EE2 (A) or TB (B). Significant differences relative to the control are indicated with an asterisk ( $p < 0.05$ ,  $n = 4 \sim 6$ ).

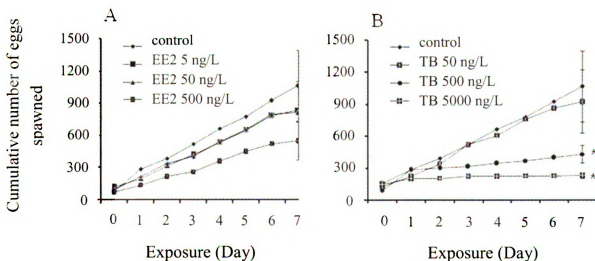


Figure 3.3 Cumulative numbers of fertilized eggs spawned by male and female Japanese medaka exposed to EE2 (A) or TB (B). Each treatment consisted of triplicate tanks, and each tank contained 6 pairs of medaka. Significant differences relative to the control are indicated with an asterisk ( $p < 0.05$ ).

### *Histology of medaka exposed to EE2 or TB*

Both testes and ovaries of control medaka exhibited complete gonadal differentiation and maturation characteristic for this species (Figs 3.4A and 3.4B). Testicular tissue was well developed and all types of germ cells were present with spermatogonia (SG) and spermatocytes (SC) located in the periphery and spermatids (ST) and spermatozoa (SZ) in the center of the testis. All stages of oocyte maturation were present in the ovary, including primary oocytes (PR), previtellogenic oocytes (PO), vitellogenic oocytes (VO), mature oocytes (MO) that had a clearly expressed yolk globule, and visible corpora lutea.

Exposure to EE2 caused changes in both the ovary and testes. All types of germ cells were present in testes of males exposed to 500 ng EE2/L, but spermatozoa were starting to degrade and there was a greater proportion of connective tissue present. Testicular ovarian follicles (perinucleus stage) were observed in the testes of only one male medaka exposed to 500 ng EE2/L (Fig 3.4C). Exposure of females to EE2 resulted in alterations of the composition of cells with different maturation stages in the ovary. There were fewer mature oocytes, more atretic oocytes, and larger volume of somatic stromal tissue (Fig 3.4D).

Exposure to TB resulted in profound effects on the ovary, but few effects on testes. The only effects of TB on the histology of testes were observed in medaka exposed to 5,000 ng TB/L. While all types of germ cells were present in the testes of medaka exposed to this concentration, there was an accelerated development of spermatozoa such that fewer spermatogonia were observed compared to the controls (Fig 3.4E). Exposure of females to 5,000 ng TB/L resulted in the predominant cell type being mature oocytes and there were fewer previtellogenic oocytes present compared to

controls (Fig 3.4F). Most of the mature oocytes exhibited signs of disruption of yolk accumulation and increased yolk vacuolization.

EE2 caused changes in the histology of livers of both males and females. Liver tissue of control males was mainly stained with eosin which stains extracellular or intracellular proteins in the cytoplasm of hepatocytes. After exposure to 500 ng EE2/L, there was a shift in the staining of hepatocytes in livers of males towards predominantly hematoxylin, which is an indicator of the presence of nucleic acids (Fig 3.5). The number of stains with hematoxylin in livers of males exposed to 500 ng EE2/L was significantly greater than in livers of unexposed males. There was no statistically significant difference in numbers of hematoxylin stains between livers of male exposed to EE2 and that of control females (Fig 3.5D). Expression of *Vit II* mRNA in liver of males, as measured by FISH, was directly proportional to the number of hematoxylin-stained stains ( $r^2 = 0.821$ ,  $n = 23$ ,  $p < 0.05$ ).

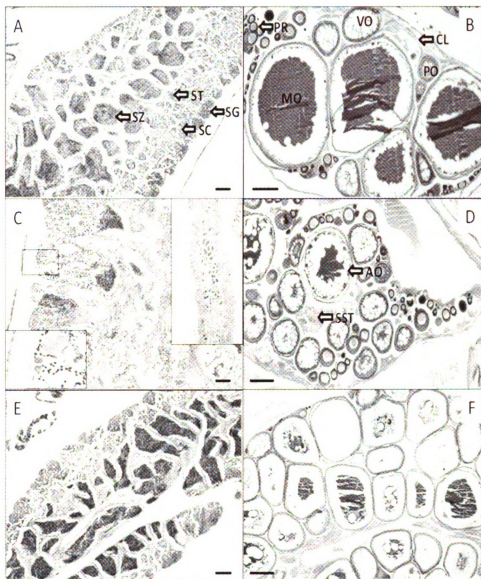


Figure 3.4 H & E stained cross section of gonads of Japanese medaka. (A) testis of control (100X, bar = 20  $\mu$ m). SZ: spermatozoa, ST: spermatid, SC: spermatocyte, and SG: spermatogonia. (B) control ovary (40X, bar = 50  $\mu$ m). PR: primary oocyte, PO: previtellogenic oocyte, VO: vitellogenic oocyte, and MO: matured oocyte. (C) testis of male exposed to 500 ng/L of EE2 (200X, (40 and 400X in the boxes) bar = 10  $\mu$ m). Testis-ova observed in the form of perinuclear stage, degrading spermatozoa and greater proportion of connective tissue were observed. (D) ovary of female exposed to 500 ng/L of EE2 (40X, bar = 50  $\mu$ m). AO: atretic oocyte, and SST: somatic stromal tissue. There were fewer mature oocytes, more atretic oocytes, and larger volume of somatic stromal tissue. (E) testis of male exposed to 5,000 ng/L of TB (100X, bar = 20  $\mu$ m). Accelerated spermatozoa development and fewer spermatogonia were observed. (F) ovary of female exposed to 5,000 ng/L of TB (40X, bar = 50  $\mu$ m). Predominant matured oocytes and fewer previtellogenic oocytes were observed.

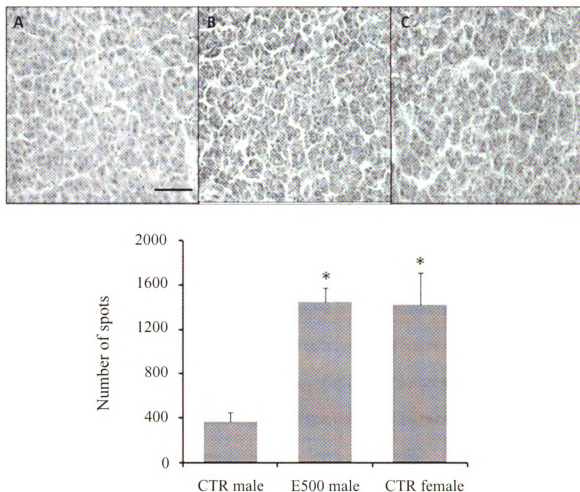


Figure 3.5 H & E stained cross section of liver of Japanese medaka. (A) control male showing eosinophilia, (B) male liver of fish exposed to 500 ng/L of EE2 and (C) female liver of control Japanese medaka showing intense staining with hematoxylin. (D) number of hematoxylin-stained stains (mean  $\pm$  SEM). Significant differences relative to the control are indicated with an asterisk ( $p < 0.05$ ). Bar = 50  $\mu$ m.

### *Chemical-induced gene expression changes by ISH*

#### *1. Vitellogenin II mRNA expression in male and female medaka exposed to EE2*

Expression of *Vit II* mRNA in livers and gonads of both male and female medaka was detected by use of optimized FISH (Fig 3.6). Exposure to EE2 caused up-regulation of *Vit II* mRNA in tissues of male and female medaka, with the exception of ovary. In sections of ovary hybridized with *Vit II* antisense probe fluorescence intensity signal was

specific to previtellogenic oocytes, rather than matured oocytes. Sections hybridized with sense probe were not fluorescent (Fig 3.6B, left panel). *Vit II* mRNA expression in ovary of control fish was not significantly different from that in ovary of medaka exposed to 500 ng EE2/L (Fig 3.8B). Although there was no significant difference in location or specific intensity of fluorescence in sections of testes between EE2-exposed and control medaka, the average fluorescence intensities of the exposed fish were approximately 2-fold greater than the controls (Fig 3.8A). *Vit II* mRNA expression was detectable in female livers, but there was no difference between livers of females exposed to EE2 and the controls (Fig 3.8C). The fluorescence intensity in livers of control males was not different from that of sections hybridized with sense probe. Fluorescence from *Vit II* antisense probe was present primarily in regions of the testes where spermatogonia were developing and rarely in the region of matured spermatozoa. Intensities of fluorescence were in the following order: spermatogonia >> spermatocytes and spermatid>>spermatozoa) (Fig 3.6A). In livers of males, expression of the *Vit II* gene was significantly greater in exposed fish, relative to that of controls (Figs 3.6C and 3.8C). Expression of the *Vit II* gene was greatest in livers of males exposed to 500 ng EE2/L and was comparable to that observed in livers of females (Figs 3.6D and 3.8C).

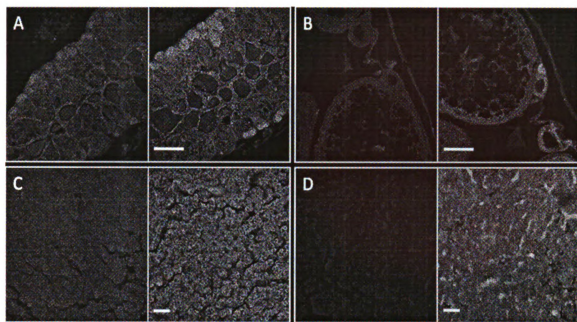


**Figure 3.6** Expression of vitellogenin II mRNA in the gonads (A and B) and liver (C and D) of Japanese medaka after hybridization of longitudinal whole mount sections with a fluorescence riboprobes using optimized ISH. Expression of Vit II mRNA was detected in the testes (A, bar = 200  $\mu$ m) exposed to EE2 and control ovary (B, bar = 100  $\mu$ m) of fish with hybridization of antisense probe, especially strongly in the region of spermatogonia in testes and primary stage of oocytes in ovary, respectively. Very weak detected fluorescence signal in the section hybridized with sense probe. Vit II expression in the male liver (C, bar = 50  $\mu$ m) of Japanese medaka exposed to EE2 (500 ng/L) was as high as that in the section of female liver (D, bar = 50  $\mu$ m) hybridized with Vit II antisense probe. Display channel was set to green for antisense probe labeled with Alexa Fluor 488 and to red for autofluorescence.

## 2. *AR* mRNA expression changes in female medaka exposed to TB

While *AR* mRNA could be detected in both ovary and liver of female medaka by use of FISH antisense probe (Figs 3.7E and 3.7F), there was no fluorescence in tissues hybridized with sense probe (data not shown). In the ovary, TB caused dose-dependent greater expression of *AR* gene expression. No significant changes in *AR* gene expression in liver tissue were observed among concentrations of TB (Figs 3.9A and 3.9B). Overall, *AR* mRNA expression in tissues of both control and exposed female medaka was low



except for *AR* mRNA gene expression in ovaries of medaka exposed to 5000 ng TB/L (Fig 3.9A).

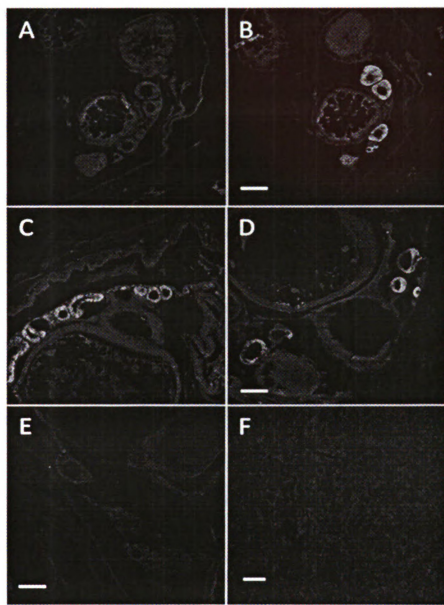


Figure 3.7 Expression of CYP19a (A – D) and AR (E and F) in the ovary and liver of female Japanese medaka using the FISH. Expression of CYP19a was very lowly detected in the ovary hybridized with sense probe (A), while it was specifically detected in the cytoplasm of primary oocytes of control ovary (B, bar = 100  $\mu$ m), ovary exposed to EE2 (C), and ovary exposed to TB (D, bar = 100  $\mu$ m). AR mRNA expression was detected, but lowly, in the ovary (E, bar = 100  $\mu$ m) and liver (F, bar = 50  $\mu$ m) exposed to TB. Display channel was set to green for antisense probe labeled with Alexa Fluor 488 and to red for autofluorescence.

### 3. *CYP19a* mRNA expression changes in female medaka exposed to EE2 or TB

Hybridization of longitudinal sections whole medaka with *CYP19a* antisense probe showed that this gene was predominantly expressed in the ovary (Fig 3.7B). The specificity of hybridization was demonstrated by ISH using sense probe, and which resulted in a very weak fluorescence signal (Fig 3.7A). The greatest fluorescence intensity was associated with premature early stages of oocytes and previtellogenic oocytes. Expression of *CYP19a* was less in vitellogenic oocytes, and matured oocytes cells expressed little or no *CYP19a* (Figs 3.7B - D). Exposure to concentrations of EE2 as great as 50 ng/L caused a significant and dose-dependent up-regulation of *CYP19a* expression in ovary. At the greatest dose, however, this trend was reversed and *CYP19a* expression was less than that in ovaries of control females.

Exposure of females to TB resulted in a dose-dependent up-regulation of *CYP19a* gene expression in the ovary that was similar to the pattern observed after exposure to EE2. The effect was dose-dependent to 500 ng TB/L, but less at 5000 ng TB/L. While these differences were observable, they were not statistically significant due to the relatively great variation that was observed among replicates (Figs 3.10A and 3.10B).

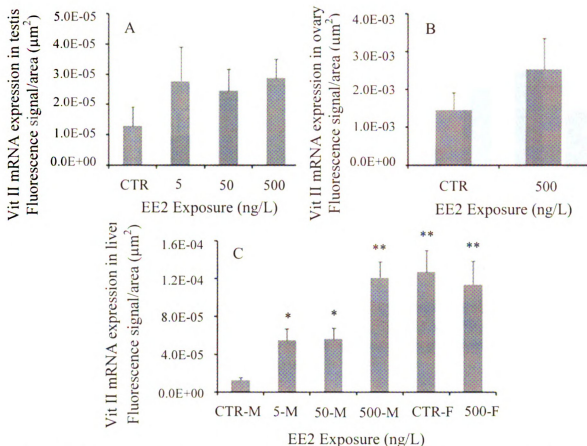


Figure 3.8 Fluorescence intensity of *Vit II* in testes (A), ovary (B), and liver (C) of Japanese medaka exposed to EE2. Each bar represents mean  $\pm$  SEM. Significant differences relative to the control are indicated with an asterisk ( $p < 0.05$ ).

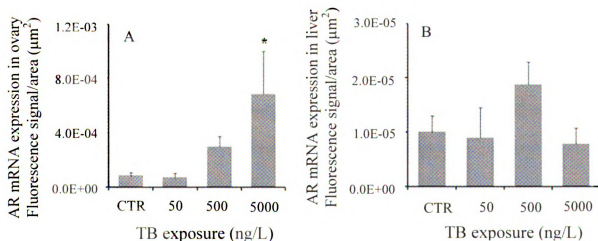


Figure 3.9 Fluorescence intensity of *AR* in ovary (A) and liver (B) of Japanese medaka exposed to TB. Each bar represents mean  $\pm$  SEM. Significant differences relative to the control are indicated with an asterisk ( $p < 0.05$ ).

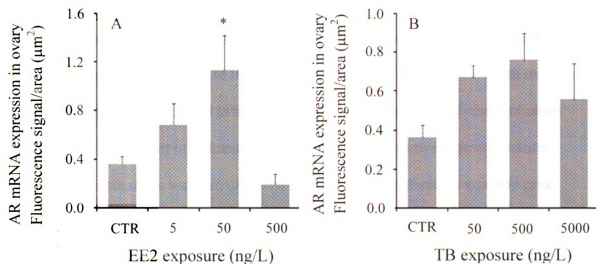


Figure 3.10 Fluorescence intensity of *CYP19a* in randomly selected three primary stage of oocytes in the ovary of Japanese medaka exposed to EE2 (A) and TB (B), and each bar represents mean  $\pm$  SEM. *CYP19a* mRNA expression was not significantly different among treatment in both EE2 and TB exposure ( $p > 0.05$ ).

## Discussion

### *Optimization of in situ hybridization analysis*

Using the optimized FISH method described previously (Park et al., 2008), it was possible to identify and to quantify expression of the *CYP19a*, *Vit II*, and *AR* genes in paraffin embedded whole mount sections of Japanese medaka. The optimized FISH method utilized spectral linear unmixing of the fluorescence signals and sodium borohydride treatment that significantly reduced background fluorescence. However, even with these adaptations, there was a weak signal detectable in sections hybridized with sense probe. Similar background fluorescence using FISH has been observed previously and has been hypothesized to be either due to incomplete removal of non-hybridized probes during post-hybridization, or to auto-fluorescence of the tissue and/or ISH components at the same wave-length than the specific probe signal (Alexa Fluor

488; Park et al., 2008). The variation in fluorescence signal limited statistical power. However, significantly greater fluorescence intensity was observed in sections hybridized with antisense probe compared to those hybridized with the sense probe, which indicates the specificity of the developed ISH protocols. This result is similar to those of other studies using fluorescent or radionuclide-based ISH where relatively great variation between replicate slides was also observed such that it was difficult to quantify gene expression by use of the ISH (Park et al., 2008; Tompsett et al., 2008). Thus, in future studies using FISH, the number of replicates would need to be optimized to demonstrate statistical significance at a specified power. While this might limit the utility of FISH as a screening tool with small numbers of replicates, the high resolution and integration into classical histological analysis renders studied FISH technique a powerful tool for mechanistic research.

*Fecundity, histology, and gene expression of medaka exposed to EE2*

Exposure to EE2 resulted in fewer eggs produced by Japanese medaka, a result that is consistent with the results of a study by Scholz and Gutzeit (2000) where exposure of Japanese medaka 10 or 100 ng EE2/L resulted in reduced egg production and a lesser GSI than in unexposed medaka. Production of fewer fertile eggs by medaka exposed to EE2 may be due to impairment of the reproductive system in females or deficient sperm and/or suppression of sexual behavior in males (Kang et al., 2002). In this study, based on histological examination, testes from medaka exposed to 500 ng EE2/L were normal, except for some degeneration of spermatozoa. However, histological examination of ovaries of female medaka exposed to EE2 revealed fewer oocytes and atrophy of the

ovary, which indicates that the reduced fecundity observed at this stage was caused by impaired oocyte development. However, exposure duration was only 7 d, and it cannot be excluded that the degenerative changes observed in the testis would have been progressed over time, and thus, also impacting fecundity due to effects in the males as well as those observed for the females.

The FISH method used in our study allowed the detection of a specific *Vit II* antisense signal in both the liver and gonads of Japanese medaka sections. In contrast, *Vit II* was rarely detected in the testis or liver of control male medaka. This is in accordance with findings of Wang et al. (2005) and Islinger et al. (2003) who did not detect vitellogenin in testes or liver of control male zebrafish using northern blotting and RT PCR analysis, respectively. In this study, exposure to EE2 caused greater expression of *Vit II* in both liver and testes of male medaka. In the testis, fluorescence specific to *Vit II* was localized in spermatogonia which are located in the peripheral region of testis. It has been previously reported that Japanese medaka exposed to exogenous estrogen accumulated vitellogenin protein, measured by immuno-histochemistry, in the cytoplasm of spermatocytes in the seminiferous tubule, but not in spermatogonia (Kobayashi et al., 2005). The fact that in this study fluorescence of the *Vit II* mRNA probe was rarely detected in the spermatocytes of testis after treatment of male medaka with EE2 (Fig 3.6A) implies that synthesis and accumulation of vitellogenin in the testis can occur at different locations.

Up-regulation of *Vit II* in testis of males exposed to EE2 is in accordance with findings in another oviparous fish, the zebrafish (Islinger et al., 2003; Wang et al., 2005). Similarly, xenoestrogens up-regulated vitellogenin mRNA expression in testes of sea

breem (*Diplodus sargus*) (Pinto et al., 2006) and resulted in greater concentrations of vitellogenin in testis of rainbow trout (Skillman et al., 2006). Vitellogenin transcription is activated through binding of an estrogen to the ER. Therefore, a greater number of ERs in the testis might explain the up-regulation of vitellogenin mRNA expression. Although the presence of ERs in testis, either at the gene or protein level, was not quantified in the current study, significant up-regulation of transcript or protein levels of estrogen receptors after estrogen treatment have been reported in other studies with medaka (Contractor et al., 2004), goldfish (*Carassius auratus*) (Nelson et al., 2007), sea bream (Pinto et al., 2006), and rainbow trout (Skillman et al., 2006). Based on results obtained using ISH, exposure of tilapia (*Oreochromis aureus*) to 17 $\beta$ -estradiol (E2) induced synthesis of vitellogenin mRNA in the testes (Ding et al., 1993). This indicates the presence of functional ER in the testes. Induction of *Vit II* mRNAs in testes of E2-treated male medaka was more evident than in ovary of E2-treated female fish. This indicates that males were more sensitive to the effects of EE2 than were females.

The ovary of teleost fish has been regarded as the destination of vitellogenin produced in the liver, while it had been believed that liver is the primary place for synthesis of vitellogenin (Wahli, 1988). As a consequence, to date most efforts have focused on the deposition and accumulation of vitellogenin in oocytes, but information on the synthesis or gene expression of vitellogenin in the gonads is rare. Based on the optimized FISH method, *Vit II* mRNA expression was detected in the cytoplasm of previtellogenic oocytes in both control fish and EE2 exposed fish, and expression of the *Vit II* gene ovary of EE2-treated medaka was greater than in control fish. This is consistent with the findings of studies with spotted ray (*Torpedo mamorata*) that revealed

active synthesis of vitellogenin in granulosa cells associated with both previtellogenic and vitellogenic oocytes. This demonstrates that these cells play a role in vitellogenesis in the ovary (Pisco et al., 2004). Vitellogenin mRNA in ovary of zebrafish, measured by use of ISH, was reported to be slightly greater in ovary after exposure to 17 $\beta$ -estradiol (Wang et al., 2005). However, these authors stated that vitellogenin mRNA was expressed in adipose tissues of ovary, not in oocytes. In the study on which I report here, fluorescence of the *Vit II* mRNA probe was localized in the cytoplasm of previtellogenic oocytes. The relevance of vitellogenesis in ovaries of fish is unclear but it may be an additional source of vitellogenin when hepatic vitellogenesis is disrupted. Another possibility is that ovarian vitellogenesis could have a supporting function in context with maturation of the previtellogenic oocyte.

The observation that *Vit II* mRNA expression was not observed in liver of control males, but once exposed to EE2, *Vit II* mRNA expression was significantly up-regulated, is consistent with previous studies, in which exogenous estrogen induced either vitellogenin mRNA expression or protein level in male liver of teleosts (Zhang et al., 2002; Islinger et al., 2003; Van der Ven et al., 2003; Scholz et al., 2004; Kobayashi et al., 2005; Wang et al., 2005; Skillman et al., 2006; Miracle et al., 2006). As observed for the gonads, there was a gender-specific difference in the sensitivity of response to EE2 exposure as measured by *Vit II* expression in the liver, with males being more sensitive than females. The level of *Vit II* expression in livers of males exposed to 500 ng EE2/L was similar or greater than that measured in livers of control and exposed females, which is in accordance with findings in zebrafish (Wang et al., 2005). Although *Vit II* mRNA expression was detected throughout the entire liver section, there appeared to be a



tendency to slightly greater gene abundance in the outer layer of the liver. This result suggests that the surface regions are primarily involved with vitellogenesis, which has also been reported in zebrafish (Wang et al., 2005).

In a previous study, it has been proposed that H & E staining can also be used to detect changes in mRNA content in cells or tissues (Van der Ven et al., 2003). The significantly greater number of stains with hematoxylin in liver of males exposed to EE2 is an indication that there was more genetic material such as mRNA in the hepatocytes, and which was assumed to be related to the greater *Vit II* mRNA production observed with FISH. The greater number of cells staining with hematoxylin in liver observed in this study was consistent with similar results in zebrafish (Van der Ven et al., 2003). The intensity of staining with hematoxylin is a function of the greater amount of genetic material. The greater staining observed in liver in this study as well as similar results obtained by ISH suggests that the greater incidence of hematoxylin-stained cells in the liver is useful as a screening method for estrogen stimulation of male fish (Van der Ven et al., 2003). This hypothesis was confirmed in the present study by the strong correlation between the two methods ( $r^2 = 0.821$ ,  $p < 0.05$ ).

As observed in a previous study (Park et al., 2008), *CYP19a* mRNA expression as measured by FISH was most prominent in the cytoplasm of early stage of oocytes, which is consistent with findings in other teleost species, such as killifish (*Fundulus heteroclitus*) (Dong and Willett, 2008), zebrafish (Goto-Kazeto et al., 2004; Wang and Orban, 2007), and Atlantic croaker (*Micropogonias undulatus*) (Nunez and Applebaum, 2006). Although not statistically significant, expression of *CYP19a* mRNA was directly proportional to EE2 concentration, except for the greatest concentration where it was less

than the controls. The mechanism of EE2 interaction with *CYP19a* gene expression, induction at low doses and reduction at high dose, is unknown. There have been studies that have found that EE2 at relatively low concentrations increased expression of *CYP19a* in ovary. In fathead minnows, exposure to 10 ng EE2/L caused up-regulation of *CYP19a* gene expression (Filby et al., 2007), and exposure to 100 ng EE2/L resulted in up-regulation of *CYP19a* gene expression in Japanese medaka (Scholz and Gutzeit, 2000). Other studies have found that exposure to relatively great concentrations of estrogens resulted in down-regulation of *CYP19a* gene expression in adult zebrafish (5 µg EE2/L; Ortiz-Zarragoitia et al., 2006), juvenile zebrafish (~ 30 µg EE2/L; Kazeto et al., 2004), and embryo zebrafish (~ 270 µg E2/L; Kishida and Callard, 2001). It has been suggested that the down-regulation of *CYP19a* mRNA was not controlled by transcription due to the lack of the ERE on its 5'-flanking region, but that this inhibiting effect was more likely due to a direct effect of EE2 on gametogenesis (Kazeto et al., 2004).

#### *Fecundity, histology, and gene expression of medaka exposed to TB*

Effects of TB on reproductive and related functions were more pronounced than those observed for EE2, with the two greatest concentrations completely inhibiting egg production shortly after initiation of the exposure experiments. Similar results have also been observed in other teleost species such as channel catfish (*Ictalurus punctatus*) (Davis et al., 2000) and fathead minnow (Ankley et al., 2003). Histological observations of the gonads revealed that the lesser fecundity was caused by impairment of gonadal development in both males and females. Males and females exhibited an increase in the proportion of spermatozoa and stimulated spermatogenesis, and impairments of

vitellogenesis and oocyte development, respectively. Disruption of vitellogenin accumulation in the ovary was most likely due to TB causing lesser plasma vitellogenin concentrations, as has been demonstrated for fathead minnows (Ankley et al., 2003). Other studies have also found similar histological changes in the testis as were observed in our study (Ankley et al., 2003; Orn et al., 2006).

The optimized FISH method revealed that *AR* mRNA expression was induced in a dose-dependent manner in the ovary but no significant changes were observed in the liver. This observation is in agreement with those of a previous study in which expression of *AR* mRNA in liver, measured by means of Q RT PCR, was not altered (Zhang et al., 2008). While in our study, a dose-dependent increase in *AR* mRNA abundance was observed in the ovary, no comparable effects were observed when *AR* was measured using RT-PCR (Zhang et al., 2008). The reasons for this difference are not clear. Exposure of mosquitofish (*Gambusia affinis affinis*) to TB resulted in a rapid increase in the expression of the *AR-α* and *AR-β* in the anal fin of females (Sone et al., 2005). That result confirmed that TB has the potential to up-regulate *AR* gene expression.

The results of the FISH revealed tissue specific detection of *CYP19a* mRNA that was specific to the cytoplasm of early stage of oocytes. No expression of *CYP19a* was observed in brain or liver, which is consistent with the results of a previous study (Park et al., 2008). This indicates that the ovary is the predominant tissue of estrogen synthesis by gonadal aromatase. *CYP19a* mRNA expression in the ovary of fish exposed to TB was not significantly different from the control fish, but there appeared to be a trend towards increased abundance *CYP19a* mRNA in fish from all TB treatment groups when compared to the controls. This trend was confirmed by a parallel study utilizing Q RT

PCR analysis, which also showed a clear dose-dependent increase of *CYP19a* gene expression in fish from the same experiment (Zhang et al., 2008). It has been shown in a different study that exposure to androgens such as TB can up- and down-regulate CYP19 gene expression depending on the tissues fish (Filby et al., 2007). Thus, due to its tissue- and/or species-specificity, the mode of action of TB on *CYP19a* gene expression still remains unclear. However, induction of *CYP19a* mRNA expression in ovary exposed to TB in this study might be a compensatory response to the decreased levels of plasma estrogen caused by this chemical (Ankley et al., 2003; Jensen et al., 2006). A comparable increase in ovarian *CYP19a* expression has also been observed after the exposure of medaka to an aromatase inhibitor, fadrozole, a result which suggests a similar compensatory mechanism in response to decreased endogenous estrogen (Park et al., 2008; Tompsett et al., 2008).

In summary, the optimized FISH method used in this study was able to detect and quantify changes in *Vit II*, *AR*, and *CYP19a* mRNA transcripts in tissues of Japanese medaka exposed to two common endocrine disruptors, the xenoestrogen, EE2 and the androgen, TB. The primary strength of the FISH approach was its ability to localize changes in the expression of target genes at the cellular and/or tissue level that provided useful information on spatial changes in gene expression that can be used to further our understanding of molecular changes at the histological level. However, due to the semi-quantitative nature of this method and the variability observed in the measured signal, additional work is needed to optimize these methods. Specifically, additional effort is needed relative to further reduce background fluorescence that in some instances made it difficult to evaluate gene expression at the cellular level for low expressed genes.

Additional efforts should focus on developing more precise approaches to quantifying fluorescence signals with tissues or cell types within tissues such that some of the variability observed in this study is reduced. Regardless of these rather minor uncertainties, the use of FISH methodology represents a valuable tool to further our understanding of the molecular mechanisms of action of chemicals and to aid in linking effects at the molecular level to pathologies.

### **Acknowledgement**

This study was supported by a grant from the US Environmental Protection Agency Strategic to Achieve Results (STAR) to J.P. Giesy, M. Hecker, and P.D. Jones (Project no. R-831846), an Area of Excellence grant from the University Grants Committee of the Hong Kong Special Administrative Region, China (Project no. AoE/P-04/04) and a grant from the Hong Kong University Grants Council (Project no. 7002234) to D. Au and J.P. Giesy. Prof. Giesy was supported by an at large Chair Professorship at the Department of Biology and Chemistry and Research Centre for Coastal Pollution and Conservation, City University of Hong Kong.

## References

- Ankley G.T., Jensen, K.M., Makynen E.A., Kahl, M.D., Korte, J.J., Hornung, M.W., Henry T.R., Denny, J.S., Leino, R.L., Wilson, V.S., Cardon, M.C., Hartig P.C., and Gray L.E. 2003. Effects of the androgenic growth promoter 17- $\beta$ -trenbolone on fecundity and reproductive endocrinology of the fathead minnow. *Environmental Toxicology and Chemistry*, 22: 1350-1360.
- Blankvoort, B.M., de Groene, E.M., van Meeteren-Kreikamp, A.P., Witkamp, R.F., Rodenburg, R.J., and Aarts, J.M. 2001. Development of an androgen reporter gene assay (AR-LUX) utilizing a human cell line with an endogenously regulated androgen receptor. *Analytical Biochemistry*, 298: 93-102.
- Contractor, R.G., Foran, C.M., Li, S., and Willett, K.L. 2004. Evidence of gender- and tissue-specific promoter methylation and the potential for ethinylestradiol-induced changes in Japanese medaka (*Oryzias latipes*) estrogen receptor and aromatase genes. *Journal of Toxicology and Environmental Health, Part A*, 67: 1-22.
- Davis, K.B., Morrison, J., and Galvez, J.I. 2000. Reproductive characteristics of adult channel catfish treated with trenbolone acetate during the phenocritical period of sex differentiation. *Aquaculture*, 189: 351-360.
- Ding, J.L., Ng, W.K., Lim, E.H., and Lam, T.J. 1993. *In situ* hybridization shows the tissue distribution of vitellogenin gene expression in *Oreochromis aureus*. *Cytobios*, 73: 197-208.
- Dong, W., and Willet, K.L. 2008. Local expression of CYP19A1 and CYP19A2 in developing and adult killifish (*Fundulus heteroclitus*), *General and Comparative Endocrinology*, 155: 307-317.
- Durhan, E.J., Lambright, C.S., Makynen, E.A., Lazorchak, J., Hartig, P.C., Wilson, V.S., Gray, L.E., and Ankley, G.T. 2006. Identification of metabolites of trenbolone acetate in androgenic runoff from a beef feedlot. *Environmental Health Perspective*, 114: 65-68.
- Filby, A.L., Thorpe, K.L., Maack, G., and Tyler, C.R. 2007. Gene expression profiles revealing the mechanism of anti-androgen and estrogen-induced feminization in fish. *Aquatic Toxicology*, 81: 219-231.

- Goto-Kazeto, R., Kight, KE., Zohar, Y., Place, AR., and Trant, JM. 2004. Localization and expression of aromatase mRNA in adult zebrafish. *General and Comparative Endocrinology*, 139: 72-84.
- Hayat, M.A., 2004. Comparison of immunochemistry, *in situ* hybridization, fluorescence *in situ* hybridization, and chromogenic *in situ* hybridization, p. 3-11. *In* Hayat, M.A. (ed.), *Handbook of immunochemistry and in situ hybridization of human carcinomas* (Vol. 1). Elsevier Academic Press, Burlington, MA.
- Islinger, M., Willimski, D., Volkl, A., and Braunbeck, T. 2003. Effects of 17 $\alpha$ -ethinylestradiol on the expression of three estrogen-responsive genes and cellular ultrastructure of liver and testes in male zebrafish. *Aquatic Toxicology*, 62: 85-103.
- Iwamatsu, T., Ohta, T., Oshima, E., and Sakai, N. 1988. Oogenesis in the medaka *Oryzias latipes*-stages of oocytes development. *Zoological Sciences*, 5: 353-373.
- Jensen, KM., Makynen, EA., Kahl, MD., and Ankley, GT. 2006. Effects of the feedlot contaminant 17 $\alpha$ -trenbolone on reproductive endocrinology of the Fathead minnow. *Environmental Science and Technology*, 40: 3112-3117.
- Kang, IJ., Yokota, H., Oshima, Y., Tsuruda, Y., Yamaguchi, T., Maeda, M., Imada, N., Tadokoro, H., and Honjo, T. 2002. Effect of 17 $\beta$ -estradiol on the reproduction of Japanese medaka (*Oryzias latipes*). *Chemosphere*, 47: 71-80.
- Kazeto, Y., Place, AR., and Trant, JM. 2004. Effects of endocrine disrupting chemicals on the expression of CYP19 genes in zebrafish (*Danio rerio*) juveniles. *Aquatic Toxicology*, 69: 25-34.
- Kime, DE. 1998. Introduction to fish reproduction, p. 81-101. *In* *Endocrine disruption in fish*. Kluwer Academic Publishers, Massachusetts, MA.
- Kishida, M., and Callard, GV. 2001. Distinct cytochrome P450 aromatase isoforms in zebrafish (*Danio rerio*) brain and ovary are differentially programmed and estrogen regulated during early development. *Endocrinology*, 142: 740-750.
- Kobayashi, K., Tamotsu, S., Yasuda, K., and Oishi, T. 2005. Vitellogenin-

immunohistochemistry in the liver and the testis of the medaka, *Oryzias latipes*, exposed to 17 $\beta$ -estradiol and p-nonylphenol. *Zoological Science*, 22: 453-461.

Kolpin, DW., Furlong, ET., Meyer, MT., Thurman, EM., Zaugg, SD., Barber, LB., and Buxton, HT. 2002. Pharmaceuticals, hormones, and other organic wastewater contaminants in U.S. streams, 1999-2000: A national reconnaissance. *Environmental Science and Technology*, 36: 1202-1211.

Kong, RYC., Giesy, JP., Wu, RSS., Chen, EXH., Chiang, MWL., Lim, PL., Yuen, BBH., Yip, BWP., Mok, HOL., and Au, DWT. 2008. Development of a marine fish model for studying in vivo molecular responses in ecotoxicology. *Aquatic Toxicology*, 86: 131-141.

Lee, C., Jeon, S.H., Na, J.G., Choi, Y.J. and Park, K. 2002. Sensitivities of mRNA expression of vitellogenin, chriogenin, and estrogen receptor by estrogenic chemicals in medaka, *Oryzias latipes*. *Journal of Health Science*, 48:441-445.

Miracle, A., Ankley, G., and Lattier, D. 2006. Expression of two vitellogenin genes (vg1 and vg3) in fathead minnow (*Pimephales promelas*) liver in response to exposure to steroidal estrogens and androgens. *Ecotoxicology and Environmental Safety*, 63: 337-342.

Nelson, ER., Wiehler, WB., Cole, WC., and Habibi, HR. 2007. Homologous regulation of estrogen receptor subtypes in goldfish (*Carassius auratus*). *Molecular reproduction and development*, 74: 1105-1112.

Nunez, BS., and Applebaum, SL. 2006. Tissue- and sex-specific regulation of CYP19a1 expression in the Atlantic croaker (*Micropogonias undulates*). *General and Comparative Endocrinology*, 149: 205-216.

Orn, S., Yamani, S., and Norrgren, L. 2006. Comparison of vitellogenin induction, sex ratio, and gonad morphology between zebrafish and Japanese medaka after exposure to 17 $\alpha$ -ethinylestradiol and 17 $\beta$ -trenbolone. *Archives of Environmental Contamination and Toxicology*, 51: 237-243.

Ortiz-Zarragoitia, M., Trant, JM., and Caaraville, MP. 2006. Effects of dibutylphthalate and ethinylestradiol on liver peroxisomes, reproduction, and development of zebrafish (*Danio rerio*). *Environmental Toxicology and Chemistry*, 25: 2394-



- Park, JW., Hecker, M., Zhang, X., Tompsett, AR., Newsted, JL., Jones, PD., Au, DWT., Kong, RYC., Wu, RSS., and Giesy, JP. 2008. Fluorescence *in situ* hybridization techniques (FISH) to detect changes in CYP19a gene expression of Japanese medaka (*Oryzias latipes*). Toxicology and Applied Pharmacology, (Submitted).
- Pinto, PIS., Singh, PB., Condeca, JB., Teodosio, HR., Power, DM., and Canario, AVM. 2006. ICI 182,780 has agonistic effects and synergizes with estradiol-17 $\beta$  in fish liver, but not in testes. Reproductive Biology and Endocrinology, 27: 4:67.
- Pisco, M., Valiante, S., Romano, M., Ricchiare, L., Liguoro, A., Laforgia, V., Limatola, E., and Andereuccetti, P. 2004. Ovarian follicle cells in *Torepedo marmorata* synthesize vitellogenin. Molecular reproduction and development, 67: 424-429.
- Rotchell, J.M. and Ostrander, G.K. 2003. Molecular markers of endocrine disruption in aquatic organisms. Journal of Toxicology and Environmental Health Part B: Critical Reviews, 6: 453-495.
- Schiffer, B., Daxenberger, A., Meyer, K., and Meyer, HHD. 2001. The fate of trenbolone acetate and melengestrol acetate after application as growth promoters in cattle: Environmental studies. Environmental Health Perspectives, 109: 1145-1151.
- Scholz, S., and Gutzeit, HO. 2000. 17- $\alpha$ -ethinylestradiol affects reproduction, sexual differentiation and aromatase gene expression of the medaka (*Oryzias latipes*). Aquatic Toxicology, 50: 363-373.
- Scholz, S., Kordes, C., Hamann, J., and Gutzeit, HO. 2004. Induction of vitellogenin in vivo and in vitro in the model teleost medaka (*Oryzias latipes*): comparison of gene expression and protein levels. Marine Environmental Research, 57: 235-244.
- Seki, M., Fujishima, S., Nozaka, T., Maeda, M., and Kobayashi, K. 2006. Comparison of response to 17 $\beta$ -estradiol and 17 $\beta$ -trenbolone among three small fish species. Environmental Toxicology and Chemistry, 25: 2742-2752.
- Skillman, AD., Nagler, JJ., Hook, SE., Small, JA., and Schultz, IR. 2006. Dynamics of 17 $\alpha$ -ethinylestradiol exposure in rainbow trout (*Oncorhynchus mykiss*):

absorption, tissue distribution, and hepatic gene expression pattern. *Environmental Toxicology and Chemistry*, 25: 2997-3005.

Sone, K., Hinago, M., Itamoto, M., Katsu, Y., Watanabe, H., Urushitani, H., Tooi, O., Guillette Jr., L.J., and Iguchi, T. 2005. Effects of an androgenic growth promoter 17 $\beta$ -trenbolone on masculinization of mosquitofish (*Gambusia affinis affinis*). *General and Comparative Endocrinology*, 143: 151-160.

Tompsett, AR., Park, JW., Zhang, X., Jones, PD., Newsted, JL., Au, DWT., Chen, EXH., Wu, RSS., Kong, RYC., Giesy, JP., and Hecker, M. 2008. Development of validation of an *in situ* hybridization system to detect gene expression along the HPG-axis in Japanese medaka, *Oryzias latipes*. *Achieves of Environmental Contamination and Toxicology*, (Submitted).

Van der Ven, LTM., Holbech, H., Fenske, M., Van den Brandhof, EJ., Gielis-Proper, FK., and Wester, PW. 2003. Vitellogenin expression in zebrafish *Danio rerio*: evaluation by histochemistry, immunohistochemistry, and *in situ* mRNA hybridization. *Aquatic Toxicology*, 65: 1-11.

Wahli, W. 1988. Evolution and expression of vitellogenin genes. *Trends in Genetics*, 4: 227-232.

Wang, H., Tan, JTT., Emelyanov, A., Korzh, V., and Gong, Z. 2005. Hepatic and extrahepatic expression of vitellogenin genes in the zebrafish, *Danio rerio*. *Gene*, 356: 91-100.

Wang, XG., and Orban, L. 2007. Anti-mullerian hormone and 11 beta-hydroxylase show reciprocal expression to that of aromatase in the transforming gonad of zebrafish males. *Developmental Dynamics*, 236: 1329-1338.

Wilkinson, D.G., 1999. The theory and practice of *in situ* hybridization, p. 1-21. *In* Wilkinson, D.G. (ed.), *In situ* hybridization: A practical approach (2<sup>nd</sup> Ed). IRL Press, Oxford, NY.

Wilson, VS., Lambright, C., Ostby, J., and Gray, LE. 2002. In vitro and in vivo effects of 17 $\beta$ -trenbolone: a feedlot effluent contaminant. *Toxicological Sciences*, 70: 202-211.

- Wittbrodt, T., Shima, A., and Scharl, M., 2002. Medaka-a model organism from the Far East. *Nature Reviews Genetics*, 3: 53-64.
- Zhang, L., Khan, IA, and Foran, CM. 2002. Characterization of the estrogenic response in genistein in Japanese medaka (*Oryzias latipes*). *Comparative Biochemistry and Physiology, Part C* 132: 203-211.
- Zhang, X., Hecker, M., Park, JW., Tompsett, AR., Newsted, JL., Nakayama, K., Jones, PD., Au, DWT., Kong, RYC., Wu, RSS., and Giesy, JP. 2008. Real time PCR array to study effects of chemicals on the Hypothalamic-Pituitary-Gonadal axis of the Japanese medaka. *Aquatic Toxicology*, (Submitted).

## CONCLUSION

The aim of my dissertation research was to develop and validate sensitive and reliable molecular techniques that can be used to elucidate the endocrine modes of chemical action in vertebrates. The focus of my research was on wildlife species such as amphibians and fish. The developed and validated methods were utilized for the integrated examination of chemical effects at the molecular, histological, and organismal level by measuring the amount of mRNA, assessing tissue morphology, and by evaluating how changes in gene expression and tissue morphology relate to effects on reproductive functions in the test organism. The techniques developed allowed for the determination of mechanisms of toxic action of single chemicals.

In phase I, the Q RT PCR method developed to quantify *CYP19a* gene expression in testicular tissues of male *X. laevis* was sufficiently sensitive, rapid, and reproducible to allow the measurement of single digit copies of total RNA. This sensitive and precise assay could be a useful tool that allows for quantifying specific types of mRNA that are expressed at low levels in certain tissues such as *CYP19a* in testes of male frogs and that allows for direct comparison of gene expression levels between samples. In fact, the Q RT PCR technique developed in this study has been successfully applied in a parallel studies to demonstrate that atrazine does not interact with aromatase gene expression in either male or female *X. laevis* (Hecker et al., 2005a in introduction). Furthermore, the Q RT PCR method developed for *X. laevis* during these studies was further optimized to aid as a validation tool in the subsequent FISH studies of spatial changes in gene expression using medaka as a whole animal model. The methods were used to test the hypothesis

that atrazine, a commonly used herbicide, was up-regulating CYP19a activity in the testes of male frogs and thus causing feminization that could contribute to population declines. It was found that atrazine did not affect expression of *CYP19a* in the gonads of frogs. This information was critical to a decision of the Science Advisory Panel of the US EPA when they made a decision to support registration of this important agricultural chemical. Thus, my published work had impacts on the science and on national policy decisions.

The optimized FISH method developed was sufficiently sensitive to detect and quantify changes of gene expression in tissues of Japanese medaka after exposure to certain types of EDCs. Also, FISH allowed for the determination of tissue-and/or gender-specific differences in gene expression as well as how different tissues interact in response to chemical exposure. This method not only provided useful information relative to spatial changes in gene expression at the cellular and/or tissue level, but also could help in the understanding of molecular changes at the level of histological observation with the ultimate goal of being able to link histological changes to potential pathologies. However, it should be mentioned here that there are still some limitations regarding the use of FISH for routine chemical characterization. These limitations are primarily related to issues regarding auto-fluorescence of tissues or components of the ISH procedure, the semi-quantitative nature due to the variability observed in the measured signal among sections for some genes, and the labor intensity of this method. While complete removal of auto-fluorescence still poses a challenge, once removed, it might allow detecting and quantifying gene expression at the cellular level with a resolution and sensitivity that would even allow the quantification of very lowly expressed genes. Furthermore, FISH has the potential to be further optimized using

multiple riboprobes with different emission spectra simultaneously with the same section allowing for the simultaneous detection of multiple genes. The potential to such improvements in combination with the here demonstrated capacity of FISH to detect modes of chemical action and to relate these to pathologies renders this technique a powerful future tool for chemical risk assessment.

MICHIGAN STATE UNIVERSITY LIBRARIES



3 1293 02956 5664